



# Murdoch

## UNIVERSITY

### Green tea extract and its metabolites induce biochemical changes linked to hepatotoxicity in HepG2 cells

Emily Claire Davies

BSc in Biomedical Science and Clinical Laboratory Science

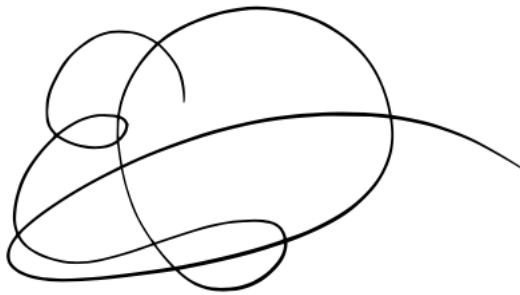
This thesis is presented for the Honours degree in Molecular Biology at Murdoch  
University, Discipline of Medical, Molecular and Forensic Sciences

Perth, Western Australia

October 2019

## Declaration

I declare that this thesis is my own account of my research and contains as its main content work which has not been previously submitted for a degree at any tertiary institution.

A handwritten signature in black ink, consisting of several overlapping loops and a long horizontal stroke extending to the right.

---

Emily Claire Davies

Thesis word count: 19859 words

## Abstract

Green tea has been consumed for thousands of years and its concentrated extract is now a popular herbal supplement frequently consumed in isolation or as part of a multi-ingredient product. Green tea extract (GTE) is commonly used for its wide range of purported health benefits and, as with most herbal supplements, its sale on the Australian market is regulated by the Therapeutic Goods Administration without requiring pre-market safety or efficacy analysis. Unfortunately, GTE has been implicated in over 50 cases of liver damage in the last 20 years, a number of which resulted in transplantation as the only option for patient survival. Despite the clear link between this supplement and liver injury in these individuals, little is currently known in regards to which biochemical pathways are affected during GTE-induced hepatotoxicity and the extent to which this is mediated by metabolic products of GTE.

In this study, GTE and individual catechins were metabolised with S9 human liver fraction and subsequently analysed using untargeted metabolomics. The results confirmed that some metabolism of the GTE had occurred, with the production of at least 17 GTE metabolites. Of these suspected metabolites, 10 were also found in the metabolised catechins, suggesting that more than half of these compounds were metabolites of the catechins in GTE.

To assess hepatotoxicity, HepG2 cells were exposed to either unmetabolised or metabolised GTE at doses equivalent to 1 mg/mL. Additionally, to assess the impact of GTE on drug-induced liver injury, another group of cells were exposed to 15 mM paracetamol, 1 mg/mL GTE or a combination of both treatments. The exposure

period for all treatments was 24 h, after which small molecule metabolites were extracted from harvested cells and analysed using untargeted metabolomics. Changes were observed in amino acids, carbohydrates and fatty acids in all treatment groups, and the same biochemical pathways appeared to be affected in all GTE treatment variations. Cell treatment with GTE metabolites appeared to yield less cytotoxicity than those treated with unmetabolised GTE. It was unable to be determined whether GTE exacerbated paracetamol-induced hepatotoxicity from the results obtained in this study.

Overall, the findings from this study suggested that GTE causes disruption to cellular lipids, proteins, nucleic acids and the mitochondria, potentially as a result of oxidative stress. Given the popularity and ready availability of GTE, regulation of herbal supplements containing this product must be improved to ensure consumer safety and ultimately prevent further cases of liver damage.

# Table of contents

Declaration .....	ii
Abstract .....	iii
List of figures .....	ix
List of tables .....	xii
List of units .....	xiii
Abbreviations .....	xiv
Acknowledgements .....	xvii
1. Introduction .....	1
1.1 Herbal complementary and alternative medicines .....	2
1.1.1 Background .....	2
1.1.2 Regulation of HCAMs.....	2
1.1.3 Safety issues with HCAMs.....	4
1.2 Hepatotoxicity.....	5
1.2.1 Xenobiotic metabolism in the liver .....	5
1.2.2 Herb-induced liver injury .....	7
1.3 Green tea extract .....	10
1.3.1 Composition.....	10
1.3.1.1 Catechins.....	11
1.3.2 Catechin metabolism.....	14
1.3.2.1 Methylation.....	16

1.3.2.2	Glucuronidation.....	17
1.3.2.3	Sulfation .....	17
1.3.3	Uses of GTE .....	18
1.3.4	Hepatotoxicity of GTE.....	19
1.3.4.1	Cases of GTE-induced liver injury.....	21
1.3.4.2	Mechanisms of GTE-induced hepatotoxicity .....	23
1.4	Analytical techniques .....	26
1.4.1	Metabolomic analysis of hepatotoxicity .....	26
1.4.2	Chromatography .....	27
1.4.3	Mass spectrometry.....	30
1.5	Concluding statements and aims.....	37
2.	Materials and methods .....	39
2.1	Green tea extract and chemicals.....	39
2.2	Cell preparation .....	40
2.2.1	Cell culture.....	40
2.2.2	Cell counts.....	41
2.3	GTE effect on cell viability .....	42
2.3.1	Extraction of GTE.....	42
2.3.2	MTT cytotoxicity assay .....	42
2.4	Hepatotoxicity of GTE constituents and metabolites.....	47
2.4.1	Metabolism of GTE.....	47
2.4.2	Cell treatment .....	48

2.4.3 Extraction of small molecule metabolites.....	49
2.4.4 Metabolomic analysis.....	49
2.4.4.1 Derivatisation .....	49
2.4.4.2 Instrumentation .....	50
2.4.4.3 Data analysis .....	51
2.4.5 Characterisation of GTE metabolites .....	53
2.4.5.1 Metabolomic analysis.....	55
2.5 GTE and paracetamol-induced hepatotoxicity.....	57
2.5.1 Rifampicin-induced CYP450 activity.....	57
2.5.2 Cell treatment .....	57
2.5.3 Metabolomic analysis.....	58
3. Results and discussion .....	60
3.1 MTT cytotoxicity assay .....	60
3.2 Hepatotoxicity of GTE and its metabolites.....	66
3.2.1 Cell density.....	66
3.2.2 Metabolomic analysis.....	70
3.3 Identification of GTE metabolites .....	78
3.4 The effect of GTE on paracetamol-induced hepatotoxicity.....	79
3.4.1 Cell density.....	79
3.4.2 Metabolomic analysis.....	83
4. General discussion .....	94
4.1. GTE-induced oxidative stress.....	94

4.2 GTE metabolites.....	98
4.3 Future considerations .....	100
4.4 Conclusion .....	103
5. References.....	105
6. Supplementary information .....	125



## List of figures

Figure 1.1 Chemical structure of the four main catechins found in green tea.....	13
Figure 1.2. Pathway of EGCG metabolism .....	15
Figure 1.3. The fate of sample molecules following a) split and b) splitless injection .....	29
Figure 1.4. Overview of electron ionisation; where “e-“ represents energised electrons, “N” represents neutral molecules and “+” represents charged molecules .....	32
Figure 1.5. Single quadrupole mass analyser.....	34
Figure 1.6. Triple quadrupole mass analyser .....	36
Figure 2.1. Overview of the workflow followed for the analysis of HepG2 cell viability using the MTT cytotoxicity assay.....	46
Figure 2.2. Overview of workflow followed for the analysis of hepatotoxicity induced by GTE constituents and metabolites using GC-MS.....	53
Figure 2.3. Overview of GTE metabolite preparation and characterisation using GC- MS analysis.....	56
Figure 2.4. Overview of workflow followed to determine effect of GTE on paracetamol-induced hepatotoxicity using GC-MS analysis .....	59
Figure 3.1. Change in HepG2 cell viability following exposure to increasing concentrations of APAP as measured by MTT assay.....	61
Figure 3.2. Change in HepG2 cell viability following exposure to increasing concentrations of EGCG, EGC, EC or CH as measured by MTT assay.....	62

Figure 3.3. Change in HepG2 cell viability following exposure to increasing concentrations of GTE as measured by MTT assay.....	63
Figure 3.4. Change in HepG2 cell viability measured by MTT assay following exposure to increasing concentrations of GTE with spent medium replaced prior to addition of MTT dye solution.....	65
Figure 3.5. Light microscope images at 100x magnification comparing a) untreated HepG2 cells with those exposed to b) 1 mg/mL GTE or c) 1 mg/mL GTEM for 24 h	67
Figure 3.6. HepG2 cell concentration following exposure to 1 mg/mL GTE or 1 mg/mL GTEM for 24 h compared to untreated controls .....	69
Figure 3.7. PCA scores plots comparing HepG2 cell metabolites from a) control (blue), GTE (green) and GTEM (red) sample groups and b) GTE and GTEM sample groups, as measured by GC-MS analysis .....	71
Figure 3.8. PLS-DA scores plot comparing HepG2 cell metabolites following exposure to GTE (green) or GTEM (red) for 24 h, as measured by GC-MS analysis .....	72
Figure 3.9. Light microscope images at 100x magnification comparing a) untreated HepG2 cells with those exposed to b) 1 mg/mL GTE, c) 15 mM APAP and 1 mg/mL GTE or d) 15 mM APAP for 24 h .....	81
Figure 3.10. HepG2 cell concentration following exposure to GTE, APAP/GTE and APAP for 24 h compared to untreated controls .....	82
Figure 3.11. PCA scores plot comparing HepG2 cell metabolites from controls (blue) to metabolites from cells exposed to GTE (green), APAP/GTE (purple) or APAP (red) for 24 h, measured by GC-MS analysis .....	83

Figure 3.12. PLS-DA scores plots comparing HepG2 cell metabolites from controls (blue to cells treated with a) GTE (green), b) APAP/GTE (purple), and c) APAP (red), measured by GC-MS analysis .....	85
Figure 3.13. PLS-DA scores plots comparing metabolites from HepG2 cells treated with a) GTE (green) vs. APAP (red), b) GTE vs. APAP/GTE (purple), and c) APAP vs. APAP/GTE, measured by GC-MS analysis .....	87
Figure 4.1. Summary of cellular disturbances suspected to occur during GTE-induced hepatotoxicity based on the data from this study .....	98
Figure S1. X- and Y-loadings plot from which X-loadings were derived for analysis of metabolites contributing most to variance between a) untreated controls and GTE-treated cells, b) untreated controls and GTEM-treated cells, and c) GTE-treated and GTEM-treated cells, measured by GC-MS. ....	125
Figure S2. Kruskal-Wallis pairwise comparisons of sample groups: 1) untreated controls, 2) GTE treatment group, and 3) GTEM treatment group. ....	126
Figure S3. X- and Y-loadings plot from which X-loadings were derived for analysis of metabolites contributing most to variance between untreated HepG2 cells and a) GTE-treated cells, b) APAP/GTE-treated cells, and c) APAP -treated cells, measured by GC-MS.....	136
Figure S4. X- and Y-loadings plot from which X-loadings were derived for analysis of metabolites contributing most to variance between cells treated with a) GTE vs APAP b) GTE vs APAP/GTE, and c) APAP vs APAP/GTE, measured by GC-MS .....	137
Figure S5. Kruskal-Wallis pairwise comparisons of sample groups: 1) untreated controls, 2) GTE-treated cells, 3) APAP-treated cells, and 4) APAP/GTE combined treatment group .....	138

## List of tables

Table 2.1 Concentrations of catechins ( $\mu\text{M}$ ), GTE ( $\text{mg/mL}$ ) and APAP ( $\text{mM}$ ) and corresponding well designations used for the analysis of HepG2 cell viability with the MTT cytotoxicity assay.....	43
Table 3.1. Fold change observed in metabolites of HepG2 cells post-exposure to GTE or GTEM compared to untreated controls .....	74
Table 3.2. Suspected metabolites of GTE following metabolism with S9 human liver fraction and frequency of detection using GC-MS analysis.....	79
Table 3.3. Fold change observed in metabolites of HepG2 cells post-exposure to GTE, APAP/GTE or APAP compared to untreated controls .....	90
Table S1. Unidentified metabolites of purified catechin hydrate following metabolism with S9 human liver fraction and GC-MS analysis.....	127
Table S2. Unidentified metabolites of purified epicatechin following metabolism with S9 human liver fraction and GC-MS analysis .....	129
Table S3. Unidentified metabolites of purified epigallocatechin following metabolism with S9 human liver fraction and GC-MS analysis.....	131
Table S4. Unidentified metabolites of purified epigallocatechin-3-gallate following metabolism with S9 human liver fraction and GC-MS analysis .....	133

## List of units

°C	Degrees Celsius
eV	Electron volts
h	Hours
m	Metre
µg	Microgram
µL	Microlitre
µm	Micrometre
µM	Micromolar
mg	Milligram
mL	Millilitre
mm	Millimetre
mM	Millimolar
min	Minute
nm	Nanometre
rcf	Relative centrifugal force
rpm	Revolutions per minute
s	Seconds

## Abbreviations

5MS	5% diphenyl/95% dimethylsiloxane
APAP	Paracetamol/acetaminophen
ARTG	Australian Register of Therapeutic Goods
CAM	Complementary and alternative medicine
CH	Catechin hydrate
CI	Chemical ionisation
CO <sub>2</sub>	Carbon dioxide
COMT	Catechol-O-methyltransferase
CYP450	Cytochrome P450
DC	Direct current
DCFDA	Dichlorodihydrofluorescein diacetate
DILI	Drug-induced liver injury
DMEM	Dulbecco's Modified Eagle Medium
DMSO	Dimethyl sulfoxide
EC	Epicatechin
ECG	Epicatechin gallate
EDTA	Ethylenediaminetetraacetic acid
EGC	Epigallocatechin
EGCG	Epigallocatechin gallate
EI	Electron ionisation
FCS	Foetal calf serum
FID	Flame ionisation detector

GC	Gas chromatography
GSH	Glutathione
GTC	Green tea catechin
GTE	Green tea extract
GTEM	Green tea extract metabolites
HCAM	Herbal complementary and alternative medicine
HILI	Herb-induced liver injury
HPLC	High-performance liquid chromatography
InsP3 R-I	Type I inositol 1,4,5-triphosphate receptor
IRE1 $\alpha$	Inositol-requiring enzyme-1 $\alpha$
LC	Liquid chromatography
<i>m/z</i>	Mass-to-charge ratio
MDA	Malondialdehyde
MgCl <sub>2</sub>	Magnesium chloride
MHC	Major histocompatibility complex
MS	Mass spectrometry
MS/MS	Tandem mass spectrometry
MSTFA	<i>n</i> -methyl- <i>n</i> -(trimethylsilyl) trifluoroacetamide
MTT	3-(4,5-dimethylthiazol-2-yl)-2,5-diphenyltetrazolium bromide
NADPH	Nicotinamide adenine dinucleotide phosphate (reduced form)
NIST	National Institute of Standards and Technology
NMR	Nuclear magnetic resonance
NAPQI	<i>N</i> -acetyl- <i>p</i> -benzoquinone imine
NQO1	NADPH:quinone oxidoreductase 1

PAPS	3'-phosphoadenosine 5'-phosphosulphate
PBS	Phosphate buffered saline
PCA	Principal component analysis
PLS-DA	Partial least squares-discriminant analysis
Q	Single quadrupole
QC	Quality control
QQQ	Triple quadrupole
QTOF	Quadrupole time-of-flight
RF	Radiofrequency
RNS	Reactive nitrogen species
ROS	Reactive oxygen species
RSD	Relative standard deviation
RT	Retention time
STAT3	Signal transducer and activator of transcription 3
SULT	Sulfotransferase
TBARS	Thiobarbituric acid-reactive substances
TCA	Tricarboxylic acid
TGA	Therapeutic Goods Administration
UDPGA	Uridine diphosphate glucuronic acid
UGT	Uridine diphosphate-glucuronosyltransferase



## Acknowledgements

I have found my honours year to be extremely fulfilling and have thoroughly enjoyed the continual opportunity to learn and grow intellectually. I have been fortunate enough to work with a number of great minds throughout this project and as such I am not only grateful for the learning opportunities I have had this year, but the people I have gotten to know along the way as well.

To my supervisor, Dr. Garth Maker – thank you for your ongoing advice and encouragement, and for continuing to answer my never-ending questions with a smile. It has been a real privilege to work with and learn from you this year, an experience I am extremely grateful for. Thank you also to my co-supervisor, A/Prof. Robert Trengove, for sharing your knowledge and enthusiasm for all things mass spectrometry.

To Dr. Hayley Abbiss – thank you for your help with determining the right statistical tests for my data, and repairing my relationship with AnalyzerPro (and technology in general) on more than one occasion.

I'd like to thank my fellow students Xue Dong, Martin Mead, Natasha Morrison, Jayden Roberts, Monique Ryan and Wei San Wong, for the moral support and laughs shared throughout the year. Thank you also to my friend, Soraya Haynes, for making as many mistakes as I did this year, thus making me feel less incompetent!

Finally, I'd like to thank my family for their unwavering support and encouragement. If it weren't for you, I would never have reached this point – every success I have is because of you.

## 1. Introduction

Herbal complementary and alternative medicines (HCAMs) are becoming an increasingly popular therapeutic choice amongst consumers, largely due to the perception that their natural origin indicates they are a safer option compared to conventional medicines.<sup>1</sup> Green tea extract is a herbal medicine that has a wide range of purported benefits, such as its ability to aid in weight loss and the prevention and management of certain chronic diseases, believed to be due to its high catechin content.<sup>2</sup>

Over the last 20 years there have been more than 50 cases of liver injury in which green tea extract has been implicated, with the most severe cases requiring liver transplantation.<sup>3, 4</sup> The idiosyncratic, acute onset has made it difficult to predict which individuals may be predisposed to a hepatotoxic response to this HCAM.<sup>3, 4</sup> It is currently unknown which green tea extract constituents or metabolites are responsible for this liver damage, although the catechins are suspected due to their presence in high concentrations. Additionally, the mechanisms by which the hepatotoxicity occurs are also poorly understood.

Using metabolomics for hepatotoxicity analysis is a novel approach which may provide insight into both of these unknowns by providing a snapshot of the metabolome following exposure to green tea extract and its metabolites, enabling conclusions to be drawn about the biochemical responses to these compounds.<sup>5</sup>

## **1.1 Herbal complementary and alternative medicines**

### **1.1.1 Background**

Complementary and alternative medicines (CAMs) have become an increasingly popular therapeutic option around the world in recent years, with an estimated two-thirds of the Australian population using these medicinal products.<sup>1, 6, 7</sup> This popularity led CAM revenue in Australia to reach \$4.9 billion in 2018.<sup>1, 8</sup>

HCAMs make up a large portion of CAM sales and are typically taken in a bid to maintain or enhance the consumer's health.<sup>8</sup> They contain ingredients derived from plants, parts of plants (e.g. leaves, flowers, seeds and roots) or other organisms which the International Code of Botanical Nomenclature regards as plants (e.g. yeast, fungi and algae).<sup>9</sup> HCAMs are typically complex multicomponent substances, however, due to their natural origins they are generally perceived by consumers to be safer than conventional medicines.<sup>1, 10</sup> This, however, is a misconception as HCAMs, like pharmaceuticals, contain active ingredients capable of causing adverse effects in the consumer.<sup>6</sup> For this reason, they are required to be evaluated by the Therapeutic Goods Administration (TGA) prior to going on the Australian market.<sup>9</sup>

### **1.1.2 Regulation of HCAMs**

The TGA requires that all medicinal products, including HCAMs, be either registered or listed with the Australian Register of Therapeutic Goods (ARTG) in order to be marketed.<sup>9</sup> Whether a medicine is registered or listed is based on whether the product's ingredients are deemed high- or low-risk, respectively, along with its indication.<sup>9</sup> For a medicine to be registered, the TGA assesses the product to ensure its safety, efficacy and quality before approving its addition to the ARTG.<sup>9</sup> The

evaluation of a medicinal product is carried out based on an extensive report provided to the TGA by the manufacturer, which should include data to support the efficacy, safety and quality of the substance.<sup>9</sup>

Medicines may instead be listed if they are composed of low-risk ingredients at appropriate concentrations, manufactured in compliance with Good Manufacturing Practice and are only indicated for certain “non-serious, self-limiting conditions” or health maintenance and enhancement.<sup>9</sup> The TGA does not assess the indications on medicines applying for listing on the ARTG.<sup>9</sup> Instead, manufacturers must only claim to have recorded evidence for their product’s efficacy.<sup>9</sup> Whilst they must make this information available to the TGA should they request it, it is not a requirement to prove they have the documentation in order to be listed.<sup>9</sup>

The TGA carries out annual compliance reviews on listed medicines; however, due to the sheer number of listed products it is impossible to evaluate all of them.<sup>9</sup> Instead, random or targeted reviews for noncompliance are undertaken, based on a risk management approach employed to identify priority substances.<sup>9</sup> Random compliance reviews are carried out on a proportion of newly listed medicinal products, chosen using a computer-based mathematical model.<sup>9</sup> Targeted compliance reviews are also carried out on listed products which have been highlighted as being potentially noncompliant.<sup>9</sup>

The vast majority of HCAMs are listed on the ARTG, meaning they face less stringent regulation than mainstream medicines.<sup>11</sup> This enables them to reach the Australian market with relative ease.<sup>6, 9</sup> This in turn is associated with a greater risk to the consumer, and leaves many questions surrounding the efficacy, quality and safety of

HCAMs.<sup>6, 7, 12, 13</sup> To date, a number of safety concerns in relation to HCAM usage have been identified, including from research carried out at Murdoch University.<sup>7, 12</sup>

### **1.1.3 Safety issues with HCAMs**

The consumption of HCAMs is associated with a number of safety issues which pose a considerable risk to the consumer; for example, batch and product variation, contamination, adulteration and the ability of consumers to self-prescribe without medical supervision.<sup>12-17</sup>

The chemical composition of a given HCAM is subject to variability.<sup>7, 14, 15</sup> This variation may be due to differences between plant species and variety, growth conditions, time and season of harvest, the geographical origin of the herbal materials and the harvesting and handling processes involved.<sup>7, 15</sup> These factors alone can result in significant variation among batches of the same herbal medicine, and also between different products containing the same ingredients.<sup>7, 14</sup>

A number of HCAMs have been found to be contaminated or adulterated.<sup>7, 12, 13</sup> An example of a chemical contaminant found in HCAMs is heavy metals.<sup>12</sup> A 2015 study found arsenic levels well over 10 times the recommended daily limit in one particular traditional Chinese medicine.<sup>12</sup> This is of particular concern given that arsenic is a highly toxic metal which has the potential to cause serious adverse reactions in the consumer, or even death.<sup>12</sup> Perhaps more concerning is the fact that some HCAMs have been found to have been intentionally adulterated, with parts of exotic animals and pharmaceutical medications, such as anti-inflammatory drugs.<sup>12, 13</sup> A 2018 paper found that a number of St John's Wort samples contained food dye, which was

suggested to be a method used by some manufacturers to pass spectroscopic analysis with a product that is of inadequate quality.<sup>13</sup>

Additionally, the ability of the consumer to self-prescribe poses another risk, particularly as many individuals do not disclose their herbal remedy regime to their medical practitioners.<sup>16, 17</sup> This opens up the potential for herb-herb interactions, if the individual is taking multiple herbal remedies, and drug-herb interactions, if they are prescribed a pharmaceutical by a doctor who is unaware of the other substances being consumed by their patient.<sup>16, 17</sup>

HCAMs, like other xenobiotics, are metabolised in the liver.<sup>18, 19</sup> For this reason, the liver is the main target of toxicity should an ingested substance contain toxic compounds, heavy metals or undisclosed pharmaceuticals.<sup>18, 20, 21</sup> Additionally, herbal compounds may be metabolised into toxic products during hepatic metabolism, increasing the risk of hepatotoxicity.<sup>18</sup> Thus, HCAMs are becoming increasingly implicated in cases of liver damage.<sup>22</sup>

## **1.2 Hepatotoxicity**

### **1.2.1 Xenobiotic metabolism in the liver**

The liver is the major site of xenobiotic metabolism, where molecules are converted into a more hydrophilic form with decreased biological activity in order to enable excretion via the kidneys.<sup>18, 19</sup> There are two main phases involved in the biotransformation process and, depending on the type, xenobiotics may go through one or both of these phases prior to being eliminated from the body.<sup>18, 19</sup>

Phase I involves the modification of a molecule via oxidation, reduction and hydrolytic reactions to make the xenobiotic more polar, enhancing its water solubility.<sup>19</sup> This changes the biological activity of the xenobiotic and can be a crucial step in the activation of prodrugs.<sup>18</sup> The most important enzymes in Phase I metabolism are those of the cytochrome P450 (CYP450) superfamily.<sup>19</sup> It is predominantly the CYP 1-4 families that are involved in xenobiotic metabolism and, of these, CYP3A4 is the most abundant.<sup>18, 19</sup>

In Phase II, xenobiotics or their metabolites from Phase I are conjugated with endogenous compounds via the action of transferase enzymes.<sup>18</sup> This process generally renders biologically active metabolites inactive and the resulting metabolic products are more readily excreted.<sup>18</sup> Examples of reactions involved in Phase II metabolism are glucuronidation, sulfation and glutathione conjugation.<sup>18, 19</sup> The majority of these reactions occur in the cytosol, excluding glucuronidation, which is carried out in microsomes and mediated by the uridine diphosphate-glucuronosyltransferase (UGT) enzymes.<sup>18</sup>

A third phase was first suggested in 1992, accounting for the efflux of metabolic products produced during the biotransformation phases.<sup>23</sup> Phase III is considered a detoxification reaction, as it is responsible for the final transport of drug molecules out of the liver for excretion.<sup>23</sup> Whilst no metabolic processes occur during this phase, it is important to consider as it has been found that polymorphisms in these transporters or inhibition of their activity may predispose certain individuals to herb or drug-induced liver injury.<sup>24, 25</sup>

Whilst hepatic metabolism plays an important role in preparing xenobiotics for elimination, it can also be responsible for the production of toxic metabolites.<sup>18</sup> The accumulation of toxic compounds in the liver or metabolic activation of such substances may cause hepatotoxicity.<sup>18, 24</sup> For example, whilst the majority of paracetamol (APAP) is metabolised via Phase II metabolism, approximately 5-15% is oxidised by CYP450 enzymes into the highly reactive metabolite *N*-acetyl-*p*-benzoquinone imine (NAPQI).<sup>26</sup> At therapeutic doses, glutathione-mediated detoxification prevents the accumulation of this toxic metabolite.<sup>26</sup> In the event of an overdose glutathione becomes depleted, leading to NAPQI build-up and ultimately hepatotoxicity.<sup>26</sup>

### **1.2.2 Herb-induced liver injury**

Drug-induced liver injury (DILI) is a major cause of acute liver failure worldwide.<sup>27</sup> The proportion of these cases that result from herbal medicines has been difficult to determine, given the widespread use of HCAMs and underreporting of this usage to healthcare professionals.<sup>1, 16</sup> However, a recent review found that herbs were implicated in approximately 25% of all DILI cases.<sup>22</sup>

The majority of herb-induced liver injury (HILI) cases are idiosyncratic, in which the cause of damage is dose-independent and unpredictable.<sup>22</sup> The pattern of injury observed in HILI cases is predominantly hepatocellular, which is associated with cellular necrosis and inflammation.<sup>4, 22, 28</sup> Cholestatic and a mixed type of injury have also been observed to a lesser extent.<sup>4, 22, 28</sup> Cholestatic injury occurs when bile flow from the liver reduces or ceases due to damage to the bile ducts, resulting in its



accumulation in the hepatocytes, while the mixed pattern of injury includes both hepatocellular and cholestatic characteristics.<sup>2</sup>

Due to the unpredictable nature of HILI, the mechanisms of hepatotoxicity are better understood for DILI.<sup>29</sup> There are a number of processes involved in DILI that have been identified, and it is often a combination of these that contributes to the development of liver damage.<sup>29,30</sup> Death of hepatocytes via apoptosis or necrosis can occur as a result of exposure to toxic metabolites formed during the biotransformation of medicinal compounds.<sup>18, 29</sup> Reactive metabolites can act on a range of cellular molecules, resulting in loss or change in protein function, lipid peroxidation or damage to DNA.<sup>29</sup> These metabolites may also induce an immune response or stress in the mitochondria and endoplasmic reticulum.<sup>29, 30</sup> The activation of immune cells results in inflammation, which may exacerbate tissue damage in the liver.<sup>29</sup>

Herbs contain multiple compounds and even single-ingredient HCAMs are chemically complex.<sup>10</sup> This is worsened by individuals taking additional herbal or conventional medicines, increasing the risk of herb-herb or herb-drug interactions, which could also trigger liver injury.<sup>16,17</sup> Whilst HILI cases have been observed in individuals taking a single-component herbal medicine, those taking multicomponent HCAMs or concurrently taking multiple herbs or medicines have been found to be at an increased risk of liver damage.<sup>4</sup> Liver injury in these individuals tends to be more severe than that observed in individuals taking a single herbal medicine, and females have been found to be more susceptible to HILI than males.<sup>4, 22, 28, 31</sup>

It has been suggested that factors such as administration conditions and polymorphisms in certain genes may influence an individual's predisposition to developing HILI or DILI.<sup>32-34</sup> Fasting may affect the bioavailability or systemic clearance of some biologically active compounds, thus individuals who take HCAMs in a fasted state may be at an increased risk.<sup>32, 33</sup> Significant genetic variation occurs in important biological molecules such as the CYP450 enzymes and major histocompatibility complex (MHC) classes I and II.<sup>34, 35</sup> Polymorphisms such as these may predispose certain individuals to a heightened susceptibility to hepatotoxicity, although a clear link is yet to be established.<sup>34, 36</sup> Specific polymorphisms suspected to influence the susceptibility of an individual to DILI or HILI have been found to occur at higher frequencies in certain ethnic groups.<sup>34</sup> For example, a CYP2B6 polymorphism is associated with increased susceptibility to ticlopidine DILI and occurs more frequently in Asian populations than European.<sup>34, 36</sup> It is theorised that polymorphisms such as this may partly explain why DILI/HILI is more prevalent in individuals of certain ethnicities.<sup>35</sup>

There are additional risk factors associated with DILI which may also influence the likelihood of HILI.<sup>37</sup> It is unclear whether elderly individuals have an increased susceptibility to DILI, however it has been observed that the pattern of injury tends to be cholestatic as opposed to the predominance of hepatocellular injury in those who are younger.<sup>37</sup> The reason for this is not yet fully understood, however it may be phenotypic or dependent on the type of drug consumed.<sup>37</sup> Additionally, whilst there is currently no data suggesting that individuals with an underlying liver condition are at a higher risk for developing DILI, there appears to be an increased

likelihood that they will suffer more severe reactions when liver damage does occur.<sup>37</sup>

Dosage must also be taken into consideration as it has been suggested that, in the belief that HCAMs are harmless, some individuals may take more than the recommended daily dose in order to achieve their desired results sooner.<sup>4</sup> For example, some athletes may turn to supplements rich in antioxidants in order to combat the oxidative stress induced by exercise.<sup>38, 39</sup> Those that choose to take additional supplements may end up with liver damage, as studies have shown that an excessive intake of antioxidants may have a pro-oxidative effect.<sup>40, 41</sup>

Alarming, certain HCAMs that are marketed as being hepatoprotective have been implicated in cases of HILI.<sup>42, 43</sup> One such herbal medicine which has been gaining attention for its implication in hepatotoxicity is green tea extract (GTE).<sup>4, 43-45</sup> In addition to potentially causing hepatotoxicity in its own right, it has been found that GTE may exacerbate liver injury caused by other drugs or herbs.<sup>46</sup> For example, numerous studies have demonstrated that GTE exacerbates paracetamol-induced liver injury, even when consumed at therapeutic doses.<sup>46-48</sup>

### **1.3 Green tea extract**

#### **1.3.1 Composition**

Green tea has been consumed for thousands of years and has a reputation for having numerous health-promoting properties, resulting in its popularity continuing to increase.<sup>49</sup> GTE is a concentrated form of the tea derived from the leaves of the *Camellia sinensis* (L.) plant.<sup>2</sup> Unlike other teas, green tea is not fermented prior to drying and thus the high concentration of polyphenols found in the leaves is

retained.<sup>50</sup> For example, it has been found that green tea has a polyphenol content up to 100 times higher than black tea.<sup>50</sup> In addition to the polyphenols, GTE also contains methylxanthine alkaloids and phenolic acids, such as gallic acid.<sup>51</sup> Other constituents commonly found in dried green tea leaves include proteins; amino acids, approximately 50% of which is theanine, an N-methylated derivative of glutamine; carbohydrates, such as glucose; vitamins, such as vitamin C; minerals and trace elements, such as potassium and aluminium; pigments, such as chlorophyll; and volatile compounds, such as aldehydes.<sup>50, 51</sup>

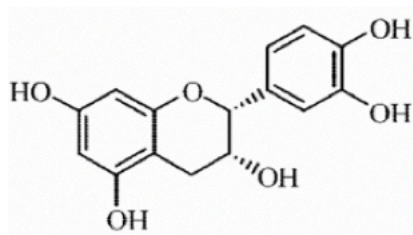
Of its many constituents, the major pharmacologically active compounds of green tea are the polyphenols and methylxanthine alkaloids.<sup>51</sup> The main methylxanthine alkaloid found in green tea is caffeine, although some GTE supplements may be decaffeinated.<sup>51, 52</sup> Other examples of these compounds include theophylline and theobromine, although the quantities present in tea leaves are believed to be minimal, with levels as low as 0.02 and 0.1% reported in the literature, respectively.<sup>51</sup> Whilst the methylxanthine alkaloids, particularly caffeine, are biologically active, it is the polyphenols that are believed to be responsible for the broad range of health benefits claimed to be associated with GTE consumption.<sup>51, 53</sup>

#### *1.3.1.1 Catechins*

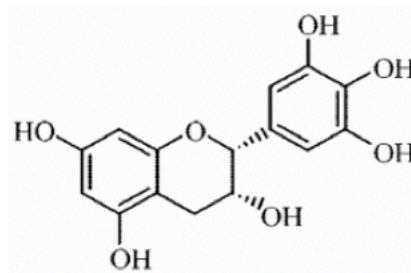
The most important polyphenols are the catechins, which are secondary plant metabolites that readily scavenge free radicals, an important property responsible for the antioxidant role of green tea.<sup>51</sup> The main catechins found in green tea are (-)-epigallocatechin-3-gallate (EGCG), (-)-epigallocatechin (EGC), (-)-epicatechin gallate (ECG), (-)-epicatechin (EC), with (-)-catechin and other isomers present to a lesser

extent (Figure 1).<sup>50, 54</sup> The general consensus appears to be that EGCG is the most abundant green tea catechin (GTC) and primarily responsible for the various health-promoting properties associated with its consumption.<sup>55</sup> Some studies have found other catechins to be present in a higher concentration than EGCG, however this may be due to catechin concentration being highly dependent upon the age of the leaf from which the tea is derived, with first leaves and buds having been found to contain the highest EGCG concentrations.<sup>50, 51</sup> In addition to the catechins, there are other polyphenols found in green tea, such as quercetin, however these are present in significantly lower concentrations.<sup>51, 55</sup>

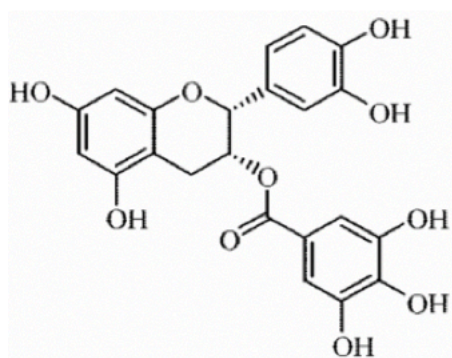
The catechins share a chemical structure composed of one dihydropyran heterocyclic ring and two benzene rings, but differ based on the presence or absence of additional functional groups (Figure 1).<sup>51</sup> The gallocatechins, such as EGC, have an additional hydroxyl group on the B-ring; the catechin gallates, such as ECG, have a gallic acid group esterified to the hydroxyl group on the pyran ring (Figure 1.1).<sup>51</sup>



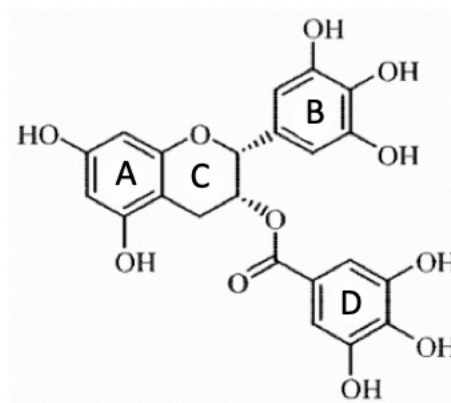
**(-)-epicatechin  
(EC)**



**(-)-epigallocatechin  
(EGC)**



**(-)-epicatechin-3-gallate  
(ECG)**



**(-)-epigallocatechin-3-gallate  
(EGCG)**

Figure 1.1 Chemical structure of the four main catechins found in green tea.<sup>56</sup> The catechins each contain two benzene rings (A, B) and one dihydropyran heterocyclic ring (C).<sup>51</sup> EGC and EGCG are classified as gallocatechins due to the addition of a third hydroxyl group on the B-ring.<sup>51</sup> EGCG is also classified as a catechin gallate, along with ECG, due to the esterification of a gallic acid group (D) to the hydroxyl group on the dihydropyran ring.<sup>51</sup>

### 1.3.2 Catechin metabolism

As with other GTE components, GTCs undergo biotransformation in the liver prior to being excreted.<sup>57-59</sup> Phase I metabolism of GTCs has not yet been observed in *in vitro* or *in vivo* studies, however, it does appear that they may inhibit the activity of certain CYP450 enzymes.<sup>60, 61</sup> For example, GTE and EGCG have been found to noncompetitively inhibit CYP3A4 and competitively inhibit CYP2B6 and CYP2C8.<sup>60</sup> This inhibition of CYP450 enzymes appears to be clinically relevant, and may impact the Phase I metabolism of other drugs co-administered with GTE supplementation.<sup>60</sup> Catechins are predominantly metabolised via Phase II processes, with glucuronidation, sulphation and methylation appearing to be the major reactions involved in the biotransformation of these compounds.<sup>54, 57-59</sup> The extensive Phase II metabolism of GTCs yields a wide range of metabolites; this is demonstrated by the full metabolic profile of EGCG, comprising 22 metabolites, shown in Figure 1.2.<sup>61</sup>

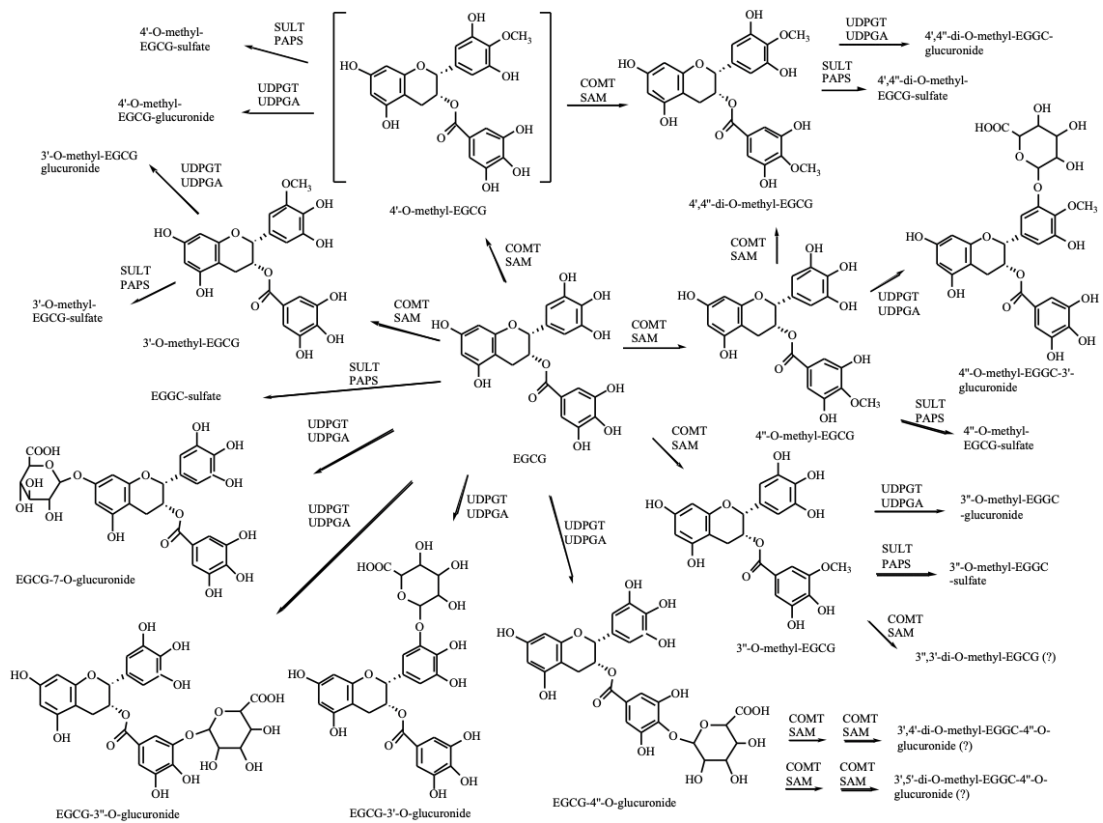


Figure 1.2. Overview of the pathways involved in EGCG metabolism.<sup>61</sup> Catechins are metabolised via Phase II reactions such as glucuronidation, sulfation and methylation.<sup>61</sup> These compounds may undergo several Phase II reactions, leading to the production of a large variety of catechin metabolites.<sup>61</sup> The metabolic profile of EGCG depicted here demonstrates that at least 22 different metabolites can be produced from this catechin alone.<sup>61</sup>



It is important to note that GTCs may be metabolised at other sites in the body, including the small intestine or via microbial metabolism in the colon.<sup>59, 62</sup> For example, a 2000 study that used rats to understand the metabolism of catechin and EC in the small intestine found that, depending on the location of absorption, GTCs may undergo methylation, glucuronidation and/or O-methyl-glucuronidation via various enzymes during their transfer through enterocytes.<sup>62</sup> This has been found to occur with catechins absorbed in the jejunum, resulting in a significant proportion of these compounds entering the portal vein already partially metabolised.<sup>62</sup> In contrast, this does not appear to occur with catechins absorbed in the ileum, with these compounds being transferred to the portal vein unmetabolised.<sup>62</sup> Additionally, it was found that the total percentage of catechins that reach the portal vein via the ileum was approximately 5-fold greater than those absorbed in the jejunum.<sup>62</sup>

#### *1.3.2.1 Methylation*

GTCs undergo methylation by cytosolic catechol-O-methyl-transferase (COMT), with all four of the main catechins having been demonstrated to undergo this process.<sup>57</sup> In COMT-mediated methylation, a methyl group from S-adenosylmethionine is transferred to the compound being metabolised.<sup>19</sup> Compared with EGC and EC, lower O-methylation rates have been demonstrated with EGCG and ECG; however, it has been found that glucuronidation on the B- or D-ring of EGCG inhibits methylation of the same ring, which may explain this observation (Figure 1).<sup>57</sup> At high concentrations of EGCG, monomethylated EGCG metabolites are the most prevalent, whilst at low concentrations the majority of EGCG metabolic products are dimethylated.<sup>57</sup> In addition to being methylated by COMT, EGCG has also been observed to

noncompetitively inhibit its activities by binding to a different site instead of the catechol binding site.<sup>57</sup>

### *1.3.2.2 Glucuronidation*

Glucuronidation involves the production of uridine 5'-diphosphoglucuronic acid (UDPGA) in the cytoplasm, which is subsequently transported into the endoplasmic reticulum where UGT can catalyse its conjugation to the compound being metabolised.<sup>19</sup> EGCG and EGC have been demonstrated to undergo glucuronidation in the liver, with UGT1A1, UGT1A8 and UGT1A9 being the main enzymes responsible for these reactions, although UGT1A8 has been shown to have low activity with EGC.<sup>58</sup> A 2003 study found that the major EGCG glucuronide formed is EGCG-4''-O-glucuronide.<sup>58</sup>

### *1.3.2.3 Sulfation*

Sulfotransferases (SULTs) are Phase II enzymes which are responsible for the sulfation of compounds, a process which is essential for the metabolism of many exogenous substances.<sup>19</sup> There are two forms of SULT, one found in the cytosol and one which is membrane-bound; it is the cytosolic SULTs which are metabolically important.<sup>19</sup> These enzymes conjugate 3'-phosphoadenosine 5'-phosphosulphate (PAPS) to sulfur, nitrogen or oxygen atoms in the compound being metabolised.<sup>19</sup> Sulfation of EC has been found to occur primarily through the action of SULT1A1, the SULT responsible for metabolising phenols, amines and alcohols.<sup>19, 56, 59</sup> Sulfation of EGCG has also been demonstrated, although in this case it appears to be concentration- and time-dependent.<sup>56, 59</sup>

### 1.3.3 Uses of GTE

GTE is widely used for its abundant antioxidants and claimed health benefits, including weight management, anti-inflammatory properties and protection against a number of chronic diseases.<sup>2, 63</sup> For example, GTE is supposedly able to protect against, or alleviate the symptoms of, cardiovascular and liver diseases, Diabetes mellitus, Alzheimer's disease and even cancer.<sup>43, 55, 64-66</sup> These benefits of green tea have been extensively researched, with many studies yielding promising results, however it is worth noting that there have also been conflicting reports in the literature.<sup>67, 68</sup> For this reason, further research is required in order to confidently establish whether GTE is capable of preventing or treating these diseases in a clinically significant manner.

One of the most popular applications of GTE is for its purported ability to stimulate weight loss, a claim which has been researched extensively using mouse models and human studies.<sup>2, 69-72</sup> The literature is inconclusive as to whether GTE supplementation leads to weight loss, although it seems that it may yield a modest reduction in weight, but only when administered at high doses.<sup>72</sup> It appears that a catechin-caffeine combination is required for this weight loss to occur, with studies using decaffeinated GTE yielding no significant reduction in weight.<sup>52, 73</sup> Furthermore, this weight loss is often clinically insignificant, therefore supplementation with GTE for this purpose is unlikely to yield substantial results in the consumer.<sup>74</sup>

Whilst most individuals appear to be able to consume GTE regularly without ill effect, there are a number of cases of hepatotoxicity that have been associated with this supplement.<sup>4</sup> The majority of these GTE-induced liver damage cases appear to occur

in individuals taking the supplement for weight loss purposes.<sup>4</sup> As outlined above, the dosage required to achieve significant weight loss is likely to be higher than the recommended daily limit and, in the belief that the supplements are harmless due to their natural origin, consumers may be inclined to take extra doses to obtain the results they are looking for.<sup>74</sup> In addition to this, it is currently unknown whether long-term consumption of GTE is safe, thus individuals using it for extended periods of time, regardless of the purpose, could also be at an increased risk.<sup>2</sup>

### **1.3.4 Hepatotoxicity of GTE**

In June 2018, the TGA issued a safety advisory for consumers and healthcare professionals to alert them to the potential for GTE-induced liver damage.<sup>44</sup> At that time, 20 cases of hepatotoxicity associated with GTE consumption had been reported to the TGA, and three of these cases involved products containing only *C. sinensis* as the active ingredient.<sup>44</sup> Hepatotoxicity associated with GTE is generally seen in individuals using the supplement for weight loss purposes.<sup>45, 75-81</sup> The predominant pattern of liver injury is hepatocellular, with the acute onset of liver damage at times so severe that liver transplantation is the only treatment option.<sup>45, 75, 79, 81-85</sup> In cases where the hepatotoxicity is caught early, the liver injury was resolved simply by discontinuing consumption of GTE.<sup>75, 76, 83, 85</sup> In instances where these patients have rechallenged their system with GTE, recurrence of hepatotoxicity has been observed.<sup>3, 4</sup>

Despite the bioavailability of GTCs being low following an oral dose, it can be enhanced under certain conditions, such as supplementing in a fasted state or repeat administration.<sup>33</sup> Other HILI risk factors which have been suggested as contributors

to GTE hepatotoxicity include individuals taking concomitant medications, consumption of high doses, and gender, with females developing liver damage from this supplement more frequently than males.<sup>3,4</sup> Additionally, with growing evidence that certain polymorphisms in genes encoding CYP450, UGT and reactive oxygen species (ROS)-detoxifying enzymes increase the risk of HILI, along with particular MHC class I and II genotypes, the possibility of a genetic basis for the development of GTE-induced liver damage in certain individuals cannot be ruled out.<sup>86</sup>

A number of weight loss products containing GTE have been associated with hepatotoxicity and liver failure, examples of which include Hydroxycut, Exolise and SlimQuick.<sup>78, 79, 87-89</sup> Hydroxycut has a long history of being associated with hepatotoxicity, with more recent events believed to be due to its GTE content; since this was uncovered, Hydroxycut products no longer contain GTE as an ingredient.<sup>2, 77, 87</sup> Exolise and SlimQuick are weight loss products containing GTE which have also been implicated in cases of liver damage.<sup>78, 79, 88, 89</sup> The sale of Exolise was banned in France and Spain in 2003 due to its association with 13 adverse reactions since 1999, one of which resulted in an individual requiring a liver transplant, which prompted the manufacturer Arkopharma to withdraw the product from the market worldwide.<sup>88</sup> In both Exolise- and SlimQuick-induced liver damage, GTE was determined to be the most likely cause.<sup>78, 79, 88, 89</sup> The acute liver injury associated with these products typically manifests in a hepatocellular manner, which is consistent with GTE-induced hepatotoxicity.<sup>78, 79, 89</sup>

Over 50 cases of hepatotoxicity believed to be linked to the consumption of green tea or GTE have been reported in the literature over the last 20 years.<sup>3,4</sup> Whilst some

of these cases were due to weight loss products such as those outlined above, others were the result of other supplements which either contained GTE as one of a number of constituents or from the consumption of green tea or GTE in isolation.<sup>3, 4</sup>

#### *1.3.4.1 Cases of GTE-induced liver injury*

In England, 2015, it was reported that a 16-year-old girl suffered acute liver damage in response to Chinese green tea purchased via the internet.<sup>90</sup> It was concluded that green tea was the culprit after ruling out all other possibilities, such as pregnancy, alcohol, “over-the-counter” medications and illicit drugs, nor had she recently received a blood transfusion.<sup>90</sup> Acute hepatitis, viral hepatitis, autoimmune hepatitis, Wilson’s disease, haemochromatosis,  $\alpha$ -1-antitrypsin deficiency and rare portal vein disturbances, such as Budd-Chiari syndrome, were also excluded.<sup>90</sup> The patient did not immediately divulge her consumption of the green tea, which was purchased in a bid to lose weight.<sup>90</sup> With intravenous fluids and treatment with *N*-acetylcysteine, the observed hepatitis completely resolved soon after discontinuing green tea consumption.<sup>90</sup>

In Italy, 2007, a 51-year-old woman presented with a long-term history of abnormal liver function tests, specifically elevated serum aminotransferases,  $\gamma$ -glutamyl-transpeptidase and alkaline phosphatase, with histological examination showing mild cholestasis.<sup>91</sup> Cessation of oestrogen and progestogen treatment following a hysterectomy did not rectify her liver function results, and tests for viral hepatitis, sclerosing cholangitis and primary biliary cirrhosis were negative.<sup>91</sup> It was uncovered that, for at least 5 years, the patient had been consuming green tea every day and, when green tea consumption was ceased, the patient’s liver function tests began to

normalise within two months.<sup>91</sup> The individual rechallenged her system with green tea six months later and there was a marked increase in serum aminotransferases,  $\gamma$ -glutamyl-transpeptidase and alkaline phosphatase in response; again, these liver function tests returned to normal following cessation of green tea consumption.<sup>91</sup> Interestingly, the patient's 20-year-old daughter also had abnormal liver function tests which normalised after she discontinued drinking green tea, suggesting that there may be a genetic element in determining the susceptibility of an individual to green tea-induced liver injury.<sup>91</sup>

A third example from 2017 involves a 50-year-old woman who presented at a hospital in the USA with abnormal liver parameters and symptoms of liver damage.<sup>82</sup> A liver biopsy demonstrated severe hepatic necrosis, however laboratory tests were negative for autoimmune hepatitis, hepatitis A, B, C and E, human immunodeficiency virus, herpes simplex virus, Wilson's disease and  $\alpha$ -1-antitrypsin deficiency.<sup>82</sup> When questioned further by the medical practitioner, the patient disclosed that she had been consuming Vital Stem, an over-the-counter nutritional supplement containing GTE, for the last month.<sup>82</sup> Having ruled out all other likely causes, it was determined that GTE was the ingredient most likely to be the cause of the observed acute liver injury.<sup>82</sup> Following treatment with prednisone and cessation of Vital Stem supplementation, the patient's condition improved over time.<sup>82</sup>

In 2016 it was reported that a 26-year-old man from Western Australia presented with liver damage so severe that he was given two weeks to live without a transplant.<sup>45, 92</sup> The ABC reported that the only compatible liver that became available during this time was infected with hepatitis B, thus, in order to survive the

man must now live the rest of his life with this disease.<sup>92</sup> This is not the only instance in which GTE-induced hepatotoxicity has been reported in the media; in 2014 the BBC reported that when a 50-year-old man from England took GTE as part of an effort to lose weight, he was admitted to hospital approximately two to three months after commencing the supplementation and diagnosed with acute liver damage so severe he was given only days to live, thus also requiring a transplant.<sup>93</sup>

Despite the differences between products consumed in the cases outlined, a process of elimination was employed by which GTE was determined to be the most probable cause in each.<sup>45, 82, 90-93</sup> The idiosyncratic, acute onset characterised by a hepatocellular pattern of injury is typical of GTE-induced liver damage, and is observed repeatedly throughout the case reports in the literature.<sup>3,4</sup> It appears to be predominantly females who are affected and most, but not all, cases are associated with individuals endeavouring to lose weight.<sup>3,4</sup>

#### *1.3.4.2 Mechanisms of GTE-induced hepatotoxicity*

GTE products may differ depending on the preparation procedure: aqueous extracts tend to contain predominantly hydrophilic components, whereas hydroalcoholic extracts contain both hydrophilic and hydrophobic compounds.<sup>94</sup> Given that catechins are polar compounds, they are retained in both types of extract, however it has been found that they are present in higher concentrations in hydroalcoholic preparations.<sup>94</sup> This could indicate that it is the catechins, particularly EGCG due to its abundance, that are responsible for GTE-induced liver damage.<sup>3</sup> So far, the majority of research into GTE hepatotoxicity has been carried out using animal



models, predominantly with mice and rats, with many primarily focusing on EGCG.<sup>40, 46, 95, 96</sup>

It has been found that, at toxic doses, EGCG is metabolised to EGCG-2''-cysteine and EGCG-2'-cysteine in mice.<sup>97</sup> There is speculation that this may be due to EGCG being oxidised to a quinone or semiquinone, which goes on to react with the sulfhydryl group of cysteine and potentially other cysteine-containing molecules such as glutathione (GSH).<sup>97</sup>

A 2006 study found that GTE-induced cytotoxicity is associated with GSH depletion and the formation of ROS, with GSH-depleted hepatocytes exhibiting greater susceptibility to EGCG toxicity.<sup>98</sup> The same study also demonstrated that inhibition of NADPH:quinone oxidoreductase 1 (NQO1) is linked to increased ECG cytotoxicity and inhibition of COMT is associated with increased EGCG cytotoxicity and ROS formation.<sup>98</sup> It has also been determined that polyphenols may have pro-oxidant properties, believed to be associated with the gallic acid component, with EGCG having been demonstrated to be the most cytotoxic and EC the least.<sup>98, 99</sup> The production of ROS in response to EGCG and its metabolites has been suggested to lead to oxidative stress in liver cells, which may be responsible for the hepatocellular necrosis observed in certain individuals consuming GTE.<sup>3</sup> Aside from ROS formation, collapse of the mitochondrial membrane and the subsequent dysfunction of hepatocyte mitochondria has also been suggested as a major mechanism of EGCG-induced cytotoxicity.<sup>40</sup>

GTE may also impact cellular respiration, with a 2015 study finding that EGCG reduces anaerobic glycolysis, glycolytic rate, glucose consumption and lactate production in

pancreatic carcinoma cells.<sup>100</sup> This was followed by a 2016 study which reported similar findings using both *in vitro* and *in vivo* methods, with the results leading to the suggestion that EGCG promotes a shift from glycolysis in hepatocellular carcinoma cells by directly suppressing the activity of phosphofructokinase, and ultimately results in apoptosis due to metabolic stress.<sup>101</sup>

In 2017, a number of biochemical changes were found to occur in rats following GTE treatment for one month, including increased levels of alanine aminotransferase, aspartate aminotransferase and malondialdehyde (MDA) and decreased GSH levels and hepatic catalase activity.<sup>46</sup> Increased MDA and aminotransferases are indicative of oxidative stress and liver damage, respectively; decreased GSH levels and hepatic catalase activity, antioxidants involved in detoxifying ROS, likely exacerbate these hepatotoxic processes.<sup>46</sup> The observations made in the histological examination were consistent with the biochemical results, demonstrating that GTE had induced moderate centrilobular hepatic necrosis with interstitial haemorrhage and infiltration of inflammatory cells; findings consistent with previous research into GTE toxicity using rat and mouse models.<sup>46, 102</sup>

Whilst there is a clear link between GTE consumption and the subsequent development of liver damage in certain individuals, the causative compounds and mechanisms of injury remain speculative. GTE is composed of many potentially-hepatotoxic compounds, and this is further complicated when the different metabolites formed from these constituents *in vivo* are considered.<sup>50, 51, 61</sup> Given the accessibility and widespread use of GTE, a better understanding of how this

supplement induces hepatotoxicity is vital; metabolomics is one advanced technique which has shown promise in this field.<sup>5</sup>

## **1.4 Analytical techniques**

### **1.4.1 Metabolomic analysis of hepatotoxicity**

Whilst traditional methods of toxicological analysis provide end-point results in assessing the toxicity of a given substance, they are unable to provide details on the mechanisms involved and any alterations in biochemical processes that occur.<sup>5</sup> For example, a popular method of analysing *in vitro* toxicity involves the bioconversion of 3-(4,5-dimethylthiazol-2-yl)-2,5-diphenyltetrazolium bromide (MTT), resulting in the production of NADPH which yields a colour change proportionate to the number of viable cells, known as the MTT assay.<sup>5, 103, 104</sup> This provides information on the effect a substance has on cell viability, but no details about the mechanisms involved in any changes observed.<sup>5, 103, 104</sup> Through the use of 'omics' techniques, which generate complex data representing cellular changes in response to a given trigger, it is possible to hypothesise the mechanisms by which a substance induces toxicity in the cell.<sup>5, 105</sup> Metabolomics, a technique that provides insights into the biochemical profile of an organism, is a novel method for analysing *in vitro* hepatotoxicity.<sup>5, 105</sup> Given that changes in small molecules at the biochemical level of an organism represent the most downstream response to a stimulus, the metabolomic fingerprint allows for characterisation of the mechanisms involved in the toxicity of a substance in addition to the overall toxicological outcome.<sup>105</sup>

For the *in vitro* metabolomic analysis of hepatotoxicity, HepG2 cells are the most commonly used cell model, likely due to their low variability and ready availability;

the primary setback associated with this cell line is their limited biotransformation capacity.<sup>5</sup> The typical exposure timeframe used in *in vitro* metabolomic studies is 24 h, and it is generally accepted that using five or more replicates provides the most reliable results, however as little as three can be adequate.<sup>5</sup> The most common method of metabolomic analysis is chromatography coupled to mass spectrometry (MS), a hyphenated technique that has broad metabolite coverage and is highly sensitive and versatile.<sup>5</sup>

Whilst liquid chromatography-MS (LC-MS) has been the most commonly used method for the *in vitro* metabolomic analysis of cytotoxicity, gas chromatography-MS (GC-MS) is also capable of providing highly reproducible data in this field.<sup>5, 106, 107</sup> In addition to this, the libraries available for the identification of compounds by GC-MS are comprehensive and easier to navigate than those used for LC-MS.<sup>108</sup> This results in the more efficient and straightforward analysis of data generated via GC-MS than for that produced via LC-MS.

### **1.4.2 Chromatography**

Chromatography is a separation technique in which a sample is added to a mobile phase that is then passed through a stationary phase, with different analytes within the sample eluting from the stationary phase at different rates.<sup>106, 107, 109</sup> There are two main types chromatography: liquid and gas, named after the state of the mobile phase.<sup>106, 107, 109</sup>

In gas chromatography (GC), the mobile phase is an inert gas, such as helium; the role of the carrier gas, or eluant, is to aid in the movement of analytes from the inlet, through the column containing the stationary phase and into the detector.<sup>107</sup> In order

for GC analysis to be effective, sample molecules must be volatile and stable enough to withstand the high temperatures in the GC oven; to ensure this, samples can be derivatised prior to injection in order to enhance the volatility and thermal stability of the compounds.<sup>110</sup> Examples of compounds which require derivatisation include amino acids, saccharides and drugs.<sup>110</sup>

There are a number of different ways in which a sample can be introduced into the GC inlet, and the application determines which type is best suited.<sup>107</sup> Typically, injection involves the vaporisation of the sample in the inlet into a stream of carrier gas. For split injection, only a portion of the sample/carrier gas mixture is directed onto the GC column and the rest is expelled (Figure 1.3a).<sup>107</sup> Alternatively, during splitless injection, the splitter vent is closed and thus the entire sample is directed onto the column (Figure 1.3b).<sup>107</sup> This allows for concentration of the sample on the column for a period of time before the splitter vent is opened and the majority of the solvent is purged.<sup>107</sup> The inlet is kept at a high temperature to ensure instantaneous vaporisation of the sample as it is introduced.<sup>106</sup>

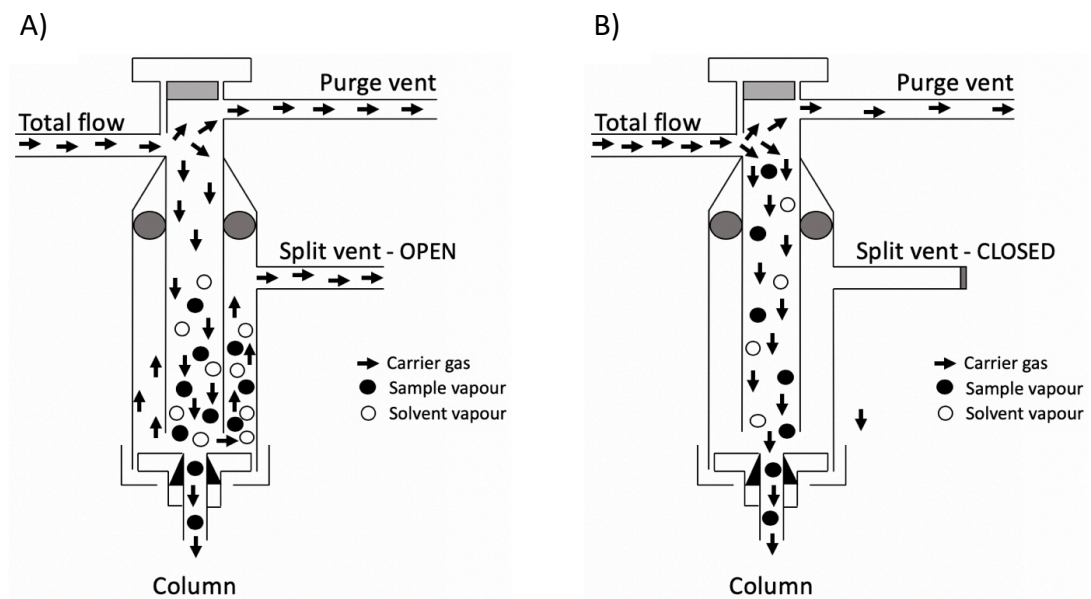


Figure 1.3. The fate of sample molecules following split (A) and splitless injection (B).<sup>106</sup> During a split injection the split vent is open, resulting in only part of the mixture of sample and carrier gas being directed onto the column.<sup>106</sup> Alternatively, the split vent is closed during a splitless injection.<sup>106</sup> This results in the sample being concentrated on the column for a set period of time prior to the split vent being opened to purge the majority of the solvent.<sup>106</sup>

The column, found inside the GC oven, is where separation of the sample molecules takes place.<sup>106</sup> The column is typically composed of polysiloxane with a 5% diphenyl/95% dimethylsiloxane (5MS) stationary phase adhered to the inside surface.<sup>107</sup> Sample molecules are carried onto the column by the eluant and become delayed by the stationary phase.<sup>107</sup> The temperature inside the GC oven is gradually increased (4-20°C/minute), thus, sample molecules elute from the stationary phase at different times, depending on their boiling points.<sup>107</sup>

As with methods of sample introduction, there are a wide variety of detectors available for GC analysis which may be universal, such as the flame ionisation detector (FID), or selective, such as the thermionic specific detector.<sup>107</sup> In an FID, the sample compounds combust as they pass through a hydrogen flame, generating ions and electrons that cause a current flow, producing a signal which is recorded as a peak on the chromatogram.<sup>107</sup>

### **1.4.3 Mass spectrometry**

MS is a technique used to separate charged particles within a sample based on their mass-to-charge ratio ( $m/z$ ).<sup>109, 111</sup> In order for this to occur, sample molecules must carry a charge, thus prior to entering the mass analyser the sample passes through an ionisation source which ionises the particles via methods such as chemical (CI) or electron ionisation (EI).<sup>112</sup> CI is considered a soft ionisation technique as particles leave the source charged but intact; EI is considered a hard ionisation technique as particles within the sample become fragmented during the process (Figure 1.4).<sup>112,</sup>

In EI, electrons are released from a metal filament following sufficient electrical heating and accelerated to 70 eV through an electric field.<sup>112, 113</sup> The electrons are attracted to an anode on the opposite side of the ionisation source, creating an electron beam that travels perpendicular to the sample path.<sup>113</sup> As the sample is introduced into the ionisation source it passes through this electron beam and the electrons transfer some of their energy to the molecules, generating charged product ions mostly via electron ejection.<sup>112, 113</sup> An excess internal energy of 6 eV in the sample molecules is sufficient to cause reproducible fragmentation; this fragmentation pattern can be beneficial in the identification of compounds.<sup>112, 113</sup> Once formed, the product ions leave the ionisation source and are directed into the mass analyser.<sup>113</sup>



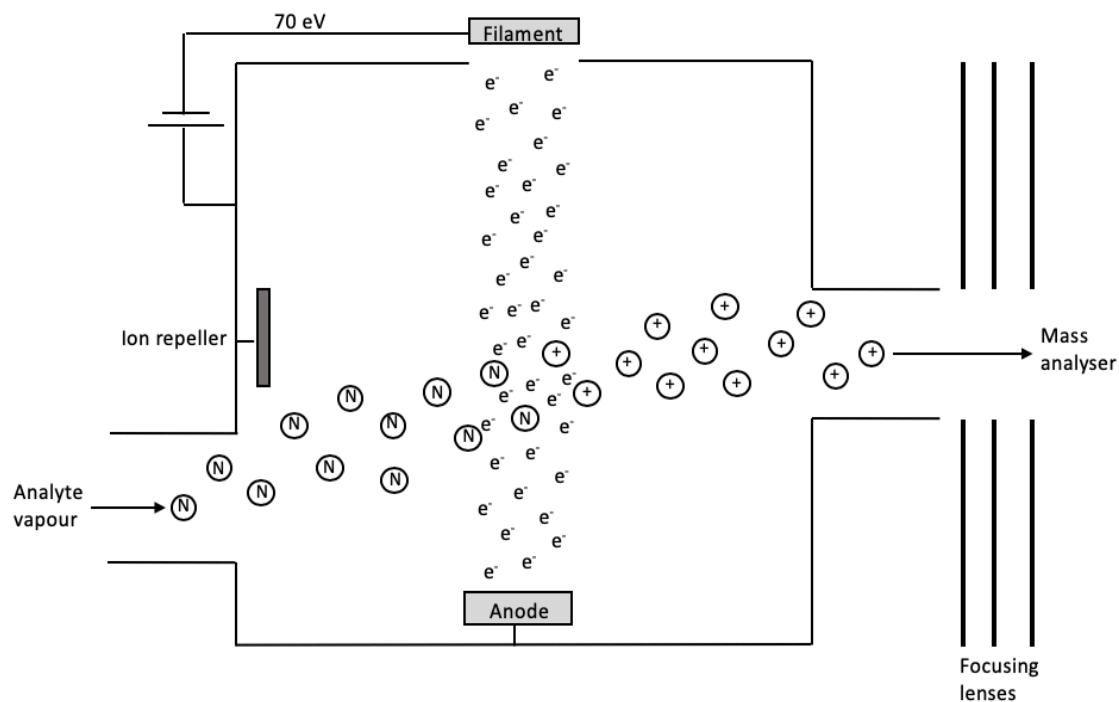


Figure 1.4. Overview of electron ionisation; where “e<sup>-</sup>” represents energised electrons, “N” represents neutral molecules and “+” represents charged molecules.<sup>109, 111</sup> Samples must pass through an ionisation source to ensure the analyte particles carry a charge prior to entering the mass analyser.<sup>109, 111</sup> During electron ionisation, electrons are released from a metal filament, accelerated to 70 eV and attracted to an anode on the opposite side of the ionisation chamber, creating an electron beam that travels perpendicular to the sample path.<sup>109, 111</sup> As the analyte vapour is introduced into the ionisation source, electrons transfer energy to the molecules as they pass through the electron beam, generating charged product ions.<sup>109, 111</sup> These product ions then leave the ionisation source and directed onto the mass analyser.<sup>109, 111</sup>

The mass analyser is responsible for the separation of molecules according to their  $m/z$ . Here, product ions are held until the appropriate  $m/z$  is scanned, allowing them to move through to the ion detector and be recorded.<sup>109</sup> There are a number of different mass spectrometers, which differ in their method of separation and robustness. Examples include single quadrupole (Q), ion trap, triple quadrupole (QQQ) and quadrupole time-of-flight (QTOF) mass analysers.<sup>111</sup>

Prior to entering the high-vacuum environment of a Q analyser, product ions are condensed into a stream by a series of lenses which use varying voltages to draw out and direct the ion beam to the quadrupole.<sup>109</sup> The Q analyser uses direct-current (DC) and radiofrequency (RF) fields to individually screen the various  $m/z$  in a given sample.<sup>109,111</sup> The quadrupole itself consists of four longitudinally parallel quartz rods clamped in a pair of ceramic collars, with a hyperbolic cross-section between diagonally-opposed rods that is crucial for the operation of the mass analyser (Figure 1.5).<sup>109</sup> The DC and RF signals are applied across the rods, with adjacent rods having opposite charges.<sup>109, 111</sup> Each set of DC and RF voltages is specific for ions of a particular  $m/z$ , which then follow a stable path through the centre of the quadrupole to the detector; all other ions of different  $m/z$  collide with the rods and cannot traverse the length of the quadrupole.<sup>109, 111</sup> Typically, minimum and maximum  $m/z$  are established prior to analysis, and the entire mass spectrum within this range is scanned by changing the voltages applied to the rods.<sup>111</sup>

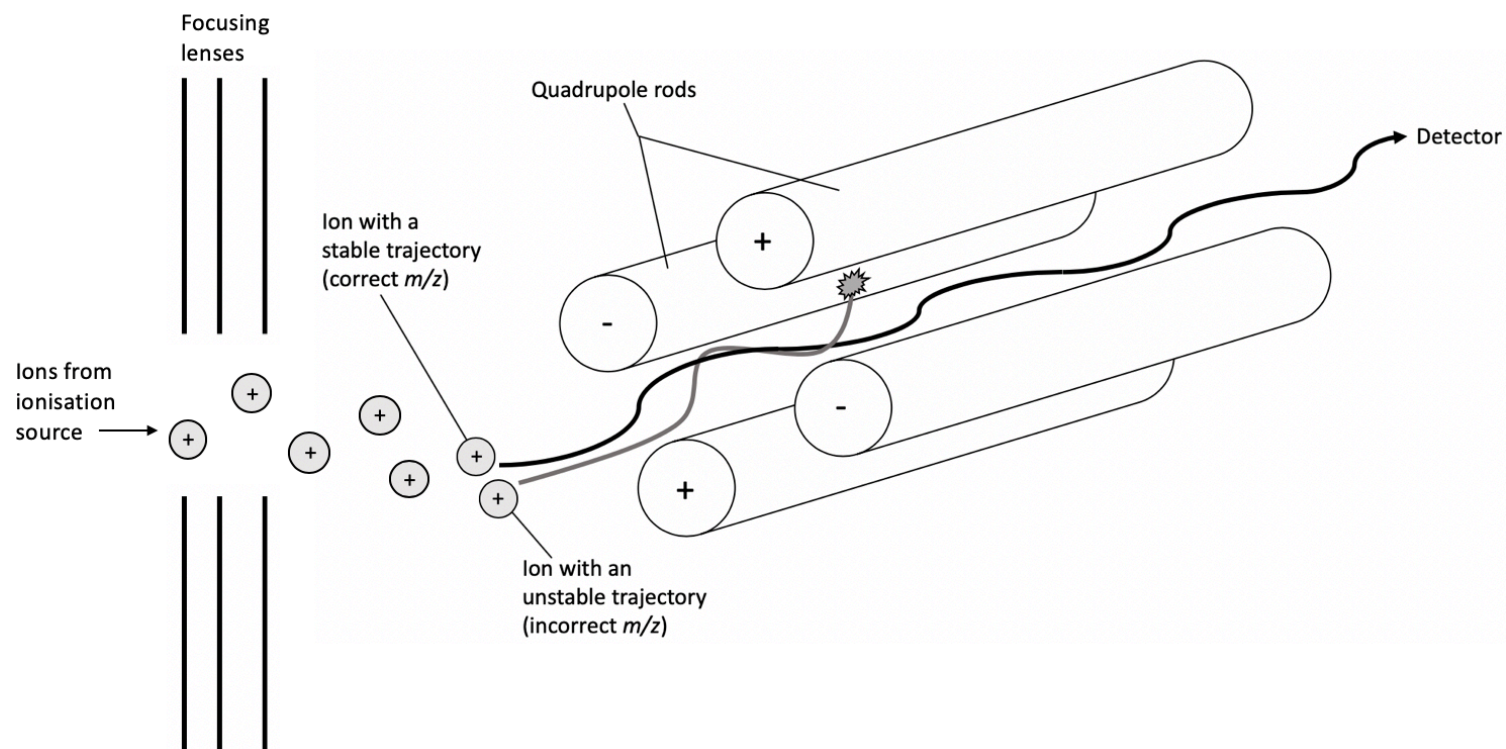


Figure 1.5. Overview of a single quadrupole mass analyser.<sup>111, 112</sup> A series of focusing lenses direct the sample ions to the quadrupole mass analyser, which consists of four longitudinally parallel rods and has a hyperbolic cross-section between the diagonally opposing rods that is crucial for its operation.<sup>111, 112</sup> The mass analyser uses oscillating direct-current (DC) and radiofrequency (RF) fields to individually screen the various mass to charge ratios ( $m/z$ ) in a given sample.<sup>111, 112</sup> Each set of DC and RF frequencies are specific to ions of a particular  $m/z$ , resulting in only one  $m/z$  species being able to follow a stable trajectory through the quadrupole at a given point in time.<sup>111, 112</sup> Mismatched  $m/z$  species collide with the rods and are unable to traverse the length of the quadrupole.<sup>111, 112</sup>

A variation of the quadrupole mass analyser is the QQQ, which comprises three consecutive quadrupoles: the first ( $Q_1$ ) is used to select for a precursor  $m/z$  corresponding to the ion of interest, the second ( $Q_2$ ) uses a collision gas such as argon to dissociate that species into fragments, and the third ( $Q_3$ ) scans a pre-set  $m/z$  range to produce a product ion spectrum (Figure 1.6).<sup>112</sup> QQQ is a form of tandem mass spectrometry (MS/MS), however it can also operate in full scan mode, in which  $Q_1$  scans the sample and the subsequent quadrupoles merely direct the ions to the detector.<sup>112</sup> A voltage gradient lines the QQQ, generating a negative bias in order to draw positive ions into the analyser and through to the detector.<sup>111</sup>

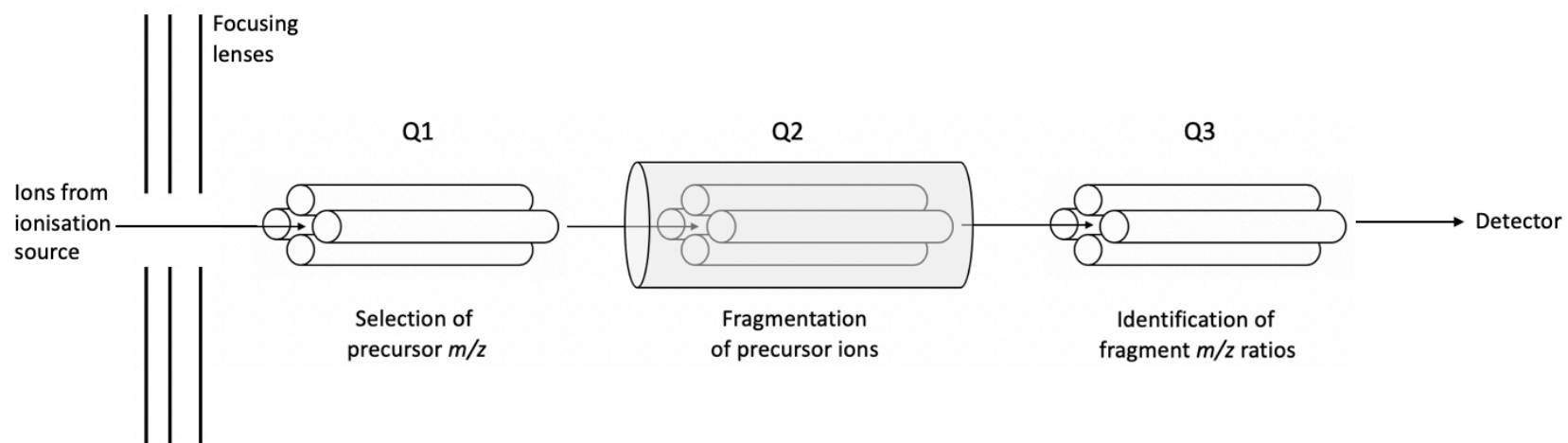


Figure 1.6. Overview of a triple quadrupole mass analyser.<sup>111, 112</sup> The triple quadrupole is a variation of the quadrupole mass analyser which comprises three consecutive quadrupoles (Q1, Q2 and Q3) and can function as a form of tandem mass spectrometry or set to full scan mode.<sup>111, 112</sup> For tandem mass spectrometry, Q1 is used to select for a precursor mass-to-charge ratio ( $m/z$ ) corresponding to the sample ion of interest, which then pass into Q2 where a collision gas is introduced that dissociates the sample ions into fragments.<sup>111, 112</sup> Finally, the resulting product ions enter Q3 where they are scanned over a  $m/z$  range to produce a product ion spectrum.<sup>111, 112</sup> When set to full scan mode, Q1 scans the sample over a pre-set  $m/z$  range and the subsequent quadrupoles simply direct the sample ions to the detector.<sup>111, 112</sup>

## **1.5 Concluding statements and aims**

Due to the complex composition of GTE, toxicological assays are unable to provide sufficient information in regards to which components may be responsible for the hepatotoxicity certain individuals experience in response to this supplement, nor do they aid in establishing the mechanisms by which the toxic compounds act. Currently, the role metabolites of GTE play in the development of hepatotoxicity in certain individuals is also poorly understood. By using untargeted metabolomic analysis, it will be possible to characterise the metabolites of GTE, as well as identify any biochemical changes in hepatocytes following exposure to these compounds. If cytotoxicity occurs, the biochemical changes observed could provide valuable insight into the mechanisms of toxicity associated with GTE consumption. Identifying these pathways will enable future studies to further identify which metabolites, if any, contribute to the manifestation of liver damage in certain individuals following consumption of GTE.

The primary aim of this study is to identify the biochemical changes in liver cells caused by exposure to GTE and its metabolites. This will be done by:

- Exposing HepG2 cells to GTE, paracetamol and isolated catechins for 24 h and analysing cell viability with the MTT cytotoxicity assay.
- Metabolising GTE with S9 human liver fraction and characterising the resulting metabolites using untargeted GC-MS analysis.
- Exposing HepG2 cells to GTE and its metabolites for 24 h and harvesting cells post-exposure to identify biochemical changes that have occurred via untargeted GC-MS analysis.
- Exposing HepG2 cells to GTE and paracetamol for 24 h and harvesting cells post-exposure to identify biochemical changes that have occurred via untargeted GC-MS analysis.

## 2. Materials and methods

### 2.1 Green tea extract and chemicals

Green tea extract (GTE) was purchased online in powdered form. The catechin standards catechin hydrate (CH), epicatechin (EC), epigallocatechin (EGC) and epigallocatechin-3-gallate (EGCG) were purchased from Sigma-Aldrich (Sydney, Australia) at the highest available purity, as were glutathione (GSH), paracetamol (APAP), 3'-phosphoadenosine-5'-phosphosulfate (PAPS), magnesium chloride (MgCl<sub>2</sub>), reduced nicotinamide adenine dinucleotide phosphate (NADPH), phosphate buffered saline (PBS), S9 pooled human liver fraction and uridine 5'-diphosphoglucuronic acid (UDPGA). Dulbecco's Modified Eagle Medium (DMEM), L-glutamine, heptane, methoxyamine hydrochloride, *n*-alkanes (C<sub>10</sub>, C<sub>12</sub>, C<sub>15</sub>, C<sub>19</sub>, C<sub>22</sub>, C<sub>28</sub>, C<sub>32</sub> and C<sub>36</sub>), *n*-methyl-*n*-(trimethylsilyl) trifluoroacetamide (MSTFA), penicillin/streptomycin solution, 0.25% trypsin-ethylenediaminetetraacetic acid (EDTA) solution and pyridine were also purchased in the purest forms available from Sigma-Aldrich. Carbon dioxide (CO<sub>2</sub>) and helium were sourced from BOC (Sydney, Australia). Foetal calf serum (FCS), used to supplement the cell culture medium, was sourced from Serana (Bunbury, Australia). Methanol (> 99.9%), LC-MS grade acetonitrile (99.9%) and LC-MS grade water were sourced from Fisher Scientific (Fair Lawn, USA). Dimethyl sulfoxide (DMSO) was purchased from VWR Chemicals (Pennsylvania, USA). Corning Costar 6- and 96-well plates were sourced from Sigma-Aldrich.



## 2.2 Cell preparation

### 2.2.1 Cell culture

HepG2 human hepatocarcinoma cells were purchased through Sigma-Aldrich from the European Collection of Cell Cultures. HepG2 cells were cultured in 75 cm<sup>2</sup> flasks with Dulbecco's Modified Eagle Medium (DMEM) which was supplemented with 1% L-glutamine, 1% penicillin and streptomycin and 10% FCS. Cells were incubated at 37°C and 5% CO<sub>2</sub> in a humidified Thermo Scientific Heraeus BB15 Function Line incubator and the medium was changed every 48 h. All cell culture work was carried out in an aseptic environment with equipment and surfaces being treated with ethanol and UV light. Cultures were grown to 80-90% confluence prior before being passaged or used for experimentation. The passaging of cells involved removal of the media, followed by the addition of 5 mL of PBS to wash the cells. PBS was removed and 2 mL of 0.25% trypsin-EDTA solution was added to dislodge the cells from the flask. Cells were incubated with the trypsin solution for 5 min, after which they were dislodged by gently tapping the flask. To inactivate the trypsin, 8 mL of fresh supplemented DMEM was added, in which the cells were resuspended until evenly distributed. For each new flask, 1 mL of this cell suspension was aliquoted and made up to 10 ml with fresh supplemented DMEM in order to yield a 1:10 passage. Passages 30, 31, 34 and. 36 were used in this study.

An Olympus IMT-2 inverted microscope (Tokyo, Japan) was used to check the cells approximately every 48 h. To compare differences in growth and morphology of treated cells to untreated controls, cell photographs were taken using an Olympus

CKX41 microscope linked to a Moticam 2300 camera (Motic Instruments Inc., Hong Kong) using Motic Images Plus v2.0.

### 2.2.2 Cell counts

Cell counts were carried out to determine the concentration of cells; these were performed using the Trypan blue exclusion method both manually and using a NanoEnTek EVE automatic cell counter (Seoul, Korea). Non-viable cells take up the Trypan blue dye due to a loss of membrane integrity and thus have a blue appearance; viable cells appear white as they do not take up the dye.<sup>114</sup> In addition to providing the concentration of total, live and dead cells, the EVE automatic cell counter also determines percentage cell viability. To perform a cell count using a 6-well plate, the medium was removed from each counting well and replaced with 1 mL of PBS to wash the cells. This PBS was subsequently removed and the wash step was repeated. Cells were then pre-treated with 500  $\mu$ L of 0.25% trypsin-EDTA solution for 10 s, following which the trypsin was removed and 500  $\mu$ L of fresh trypsin was added to the well and distributed evenly across the cells. The plate was then incubated at 37°C and 5% CO<sub>2</sub> for 5-8 min to encourage trypsin activity. Once the cells were dislodged from the bottom surface of the well, 1.5 mL of fresh medium was added to neutralise the trypsin and cells were resuspended by pipetting until evenly distributed. 100  $\mu$ L of this cell suspension was transferred into a new microcentrifuge tube and mixed with an equal volume of 0.4% Trypan blue. The concentration of cells was calculated by adding 10  $\mu$ L of this cell suspension/Trypan blue solution to an EVE cell counting slide for analysis with the EVE automatic cell counter and a Hausser Scientific Bright-Line Haemocytometer for manual cell counts.

Cell counts determined manually were found to be more accurate for high cell concentrations and thus were used to determine the volume required for seeding 6- and 96-well plates. Cells were counted using the centre square, subdivided into 4 x 4 smaller squares, with cells bordering the left and upper sides included, and those on the lower and right borders excluded. Counts were used to determine the concentration as cells/mL. Conversely, cell counts obtained using the EVE automated cell counter were found to be more reliable at determining lower cell concentrations, so were therefore used for well counts following cell exposures. Despite their difference in use, both methods were performed for every cell count in order to validate any changes observed in cell number.

## 2.3 GTE effect on cell viability

### 2.3.1 Extraction of GTE

GTE, CH, EC, EGC, EGCG and APAP were extracted in serum-free DMEM. These solutions were then diluted with additional serum-free DMEM to obtain the concentrations outlined in the following section.

### 2.3.2 MTT cytotoxicity assay

At confluence, HepG2 cells at passage 34 were seeded at a density of  $1.2 \times 10^5$  cells/well in six 96-well plates with supplemented DMEM added to a total volume of 200  $\mu$ L, with the wells around the perimeter of each plate being excluded, along with wells B2-G2 and B11-G11. The plate allocated to the APAP treatment group received 100  $\mu$ L of DMEM + rifampicin prepared as outlined in section 2.4.1 to stimulate CYP450 activity. Finally, all empty wells around the perimeter of the plates received 200  $\mu$ L of DMEM in order to limit the possibility of edge effect impacting the sample

wells. All six plates were subsequently incubated at 37°C and 5% CO<sub>2</sub> for 48 h to settle and adhere to the bottom surface of the wells. At the conclusion of the incubation period, spent medium was removed from the wells containing cells and replaced with 100 µL of treated serum-free DMEM, with each concentration prepared in 12 replicates. Each plate was allocated one of the following treatments: GTE, CH, EC, EGC, EGCG or APAP. Table 2.1 shows the concentrations used for each treatment type and their corresponding well numbers.

Table 2.1 Concentrations of catechins (µM), GTE (mg/mL) and APAP (mM) and corresponding well designations used for the analysis of HepG2 cell viability with the MTT cytotoxicity assay.

	Concentration			
	B3-G3 B4-G4	B5-G5 B6-G6	B7-G7 B8-G8	B9-G9 B10-G10
CH	0	25	50	100
EC	0	25	50	100
EGC	0	25	50	100
EGCG	0	25	50	100
GTE	0	0.1	0.5	1.0
APAP	0	7.5	15	30

Following cell treatment and a 24-h exposure period, cell viability was measured using the Promega CellTiter 96 Non-Radioactive Cell Proliferation Assay. This colorimetric assay provides a measure of cell viability by the addition of a dye solution containing 3-(4,5-dimethylthiazol-2-yl)-2,5-diphenyltetrazolium bromide (MTT) to culture wells which viable cells reduce, forming an insoluble blue formazan

product.<sup>103, 104</sup> The subsequent addition of a solubilising stop solution containing an organic solvent, which stops the conversion of the tetrazolium salt and solubilises the formazan product, creates an evenly coloured solution of which the absorbance may be measured to determine cell viability.<sup>103, 104</sup> The colour intensity is proportional to the number of live cells, with a decrease in absorbance corresponding to a decrease in cell viability.<sup>103, 104</sup>

15  $\mu$ L of Promega dye solution was added to each well and plates were subsequently returned to the incubator for 4 h. Following incubation, 100  $\mu$ L of Promega solubilisation solution/stop mix was added to each well and plates were left overnight at room temperature in a humid environment. A Tecan Spark 10M 96-well plate reader (Männedorf, Switzerland) was used to measure absorbance, with the device set to shake the plates for 5 s prior to reading in order to form an evenly coloured solution. The absorbance was read at 570 nm for each well, with the reference wavelength set to 660 nm to reduce background interference caused by inconsistencies such as cell debris or fingerprints. An overview of the procedure followed to prepare for and carry out the MTT assays is depicted in Figure 2.1.

The MTT assay was repeated for the GTE treatment using cells at passage 36, with spent medium removed from wells and replaced with fresh serum-free DMEM prior to the addition of the dye solution. Additionally, six control wells were prepared by adding 100  $\mu$ L serum-free DMEM to wells B2-G2, which did not contain cells, followed by the addition of 15  $\mu$ L dye solution and incubation for the same 4 h period as the sample wells. 100  $\mu$ L solubilisation solution/stop mix was then added to all six wells, which were also left overnight at room temperature. The absorbance of the

cell-free controls was read at 570 nm, with the mean subsequently calculated and subtracted from the values obtained for the sample wells in order to remove background absorbance caused by components in the medium and Promega solutions.

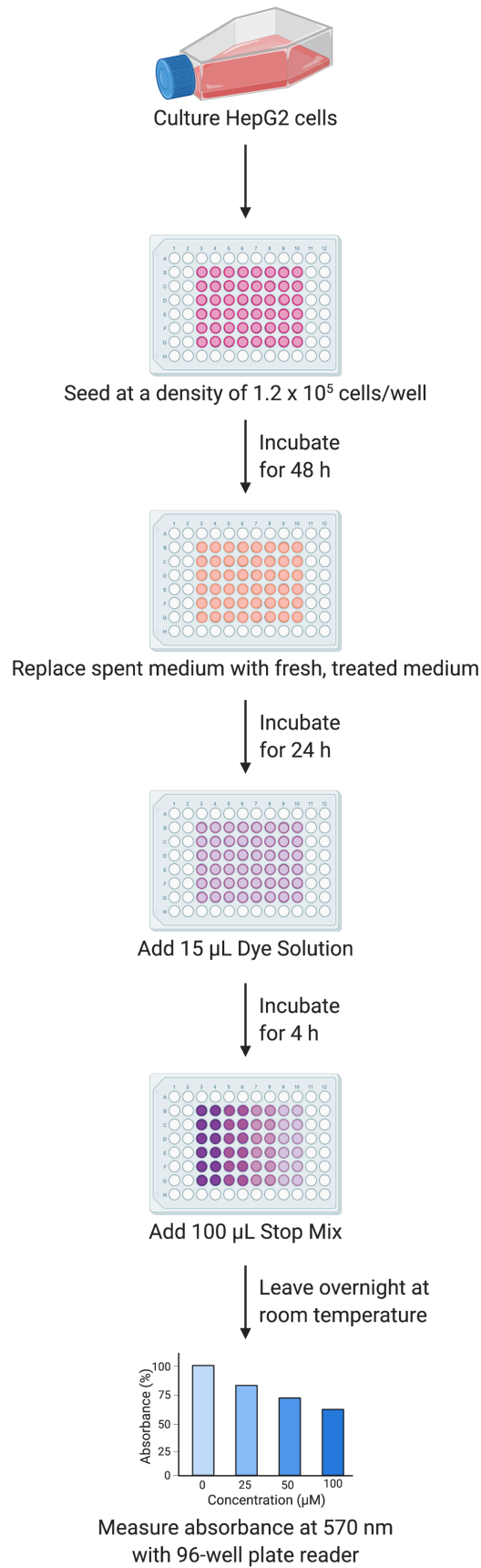


Figure 2.1. Overview of the workflow followed for the analysis of HepG2 cell viability using the MTT cytotoxicity assay. Created with BioRender.com.

## 2.4 Hepatotoxicity of GTE constituents and metabolites

### 2.4.1 Metabolism of GTE

GTE was metabolised using pooled human liver S9 fraction, which contains Phase I and Phase II enzymes, following the method outlined by Richardson et al.<sup>115</sup> NADPH was used as a cofactor to activate Phase I metabolism and GSH, UDPGA and PAPS were used to stimulate Phase II enzymes. Individual stock solutions of NADPH, GSH, UDPGA and PAPS were prepared at concentrations of 34, 31, 13 and 1.6 mg/mL, respectively.<sup>115</sup> These cofactor solutions were mixed in a 1:1:1:1 ratio to yield a solution with final concentrations of 0.85, 0.78, 0.33 and 0.04 mg/mL, respectively.<sup>115</sup> GTE was extracted with sterile water at a concentration of 100 mg/mL.

PBS was prepared as a solution containing 2 mM MgCl<sub>2</sub>; the PBS maintains the reaction pH at 7.4 and the magnesium ions stimulate cytochrome P450 (CYP450) activity.<sup>115</sup> 140 µL of the 2 mM MgCl<sub>2</sub>/PBS solution was then aliquoted into 1.5 mL tubes, followed by the addition 20 µL of S9 liver fraction and 20 µL of GTE extraction.<sup>115, 116</sup> In total, 15 replicates were prepared and preincubated at 37°C for 5 min. Reactions were initiated by the addition of 20 µL of the cofactor mixture, yielding a final reaction volume of 200 µL and a GTE concentration of 10 mg/mL.<sup>115</sup> Samples were subsequently incubated at 37°C for 60 min, after which they were put on ice to quench the reactions. All samples were centrifuged for 10 min at 4.0 x 10<sup>3</sup> rcf to remove the proteins, with centrifugation being carried out at 4°C in order to provide further quenching of metabolic reactions. Supernatant containing the GTE metabolites from each tube was subsequently pooled in a new 10 mL tube and stored at -80°C until required for cell exposures.



## 2.4.2 Cell treatment

At confluence, HepG2 cells at passage 30 were seeded at a density of  $1.0 \times 10^6$  cells/well in 6-well plates with supplemented DMEM added to reach a total volume of 2 mL. The plates were subsequently incubated at 37°C and 5% CO<sub>2</sub> for 48 h to allow cells to settle and adhere to the bottom surface of the wells.

Six plates were prepared for the exposures: 2 x GTE metabolites (GTEM), 2 x unmetabolised GTE (GTE) and 2 x controls. The GTE metabolites produced in section 2.4.1 were used to treat the cells in the GTEM plates. GTE was extracted with sterile PBS at a concentration of 10 mg/mL to treat the GTE plates.

Following the 48-h incubation period, spent medium was removed from all wells and replaced with 1.8 ml serum-free DMEM. 200 µL of the appropriate treatment (GTEM or GTE) was then added to each well. The final concentration of GTE metabolites in the GTEM plates was equivalent to 1 mg/mL unmetabolised GTE. The GTE plates contained a final GTE concentration of 1 mg/mL, as this concentration was recently shown to induce significant toxicity in HepG2 cells.<sup>117</sup> Cells in the control plates received 200 µL of sterile PBS. Plates were then returned to the incubator for a 24-h exposure period.

At the conclusion of the exposure period, all 6-well plates were put on ice. A counting well was set aside on each plate to determine cell viability following the exposures, yielding 2 replicates of each sample type for cell counts, which were performed as outlined in section 2.2.2. The cells from the remaining 5 wells were harvested using a rubber cell scraper into 500 µL methanol containing <sup>13</sup>C<sub>6</sub>-sorbitol internal standard at a concentration of 2.6 µg/mL. The contents of each well were transferred into 1.5

mL microcentrifuge tubes and put on ice in preparation for extraction of small molecule metabolites. In total, this yielded 10 replicates of each sample type for analysis via gas chromatography-mass spectrometry (GC-MS).

An additional two plates were prepared in order to be pooled and used as quality controls (QCs) for GC-MS analysis. QC plates were seeded in the same manner as the sample plates and incubated at 37°C and 5% CO<sub>2</sub> for 48 h. At the conclusion of this incubation period, cells were harvested from all wells as outlined above.

### 2.4.3 Extraction of small molecule metabolites

In order to release the small molecule metabolites for GC-MS analysis, it is essential to lyse the cell membrane and isolate them from the cellular material.<sup>118</sup> Metabolites were extracted with a Bertin Technologies Precellys 24 Lysis and Homogenisation tissue lyser (Aix-en-Provence, France) at 6500 rpm for 2 x 20 s. The tubes were then centrifuged at  $16.1 \times 10^4$  rcf for 5 min in an Eppendorf 5415R centrifuge (Sydney, Australia) to remove the cellular material, leaving the small molecule metabolites in the supernatant. 300 µL of supernatant from each sample was then transferred into new microcentrifuge tubes. Supernatant obtained from the QC samples was pooled in a 10 mL centrifuge tube prior to being aliquoted into new microcentrifuge tubes in 300 µL aliquots. All tubes were then spun in an Eppendorf Concentrator Plus rotary vacuum concentrator (Sydney, Australia) on the V-AL setting to remove the solvent.

### 2.4.4 Metabolomic analysis

#### 2.4.4.1 Derivatisation

Derivatisation was performed to chemically transform the compounds in the samples in order to ensure they were thermally stable and sufficiently volatile, thus increasing

the number of compounds able to be detected via GC-MS analysis.<sup>118</sup> Methoxyamine hydrochloride was dissolved in pyridine at a concentration of 20 mg/mL, and 20 µL of this solution was added to each dried sample. Samples were incubated at 30 °C using an Eppendorf Thermomixer Comfort (North Ryde, Australia) with agitation at 1200 rpm for 90 min. Methoxyamine prepares the compounds for derivatisation by reacting with their carbonyl groups to form oxime derivatives that stabilise the compounds for derivatisation with MSTFA.<sup>110</sup> Following incubation, 40 µL of MSTFA was added to each tube and the samples were incubated at 37°C with agitation at 300 rpm for 30 min. During this incubation period, the MSTFA adds silyl groups to functional groups on the compounds in each sample, yielding a trimethylsilyl derivative.<sup>110</sup> Due to the nature of these reactions, multiple derivatisation products for a given compound are possible.<sup>110</sup> 50 µL of each sample was transferred to 2 mL brown glass GC vials with 100 µL inserts. 5 µL of *n*-alkanes in heptane was added to each sample and the vials were capped. All sample vials were then loaded onto the GC-MS and left to react for 1 h prior to analysis.

#### ***2.4.4.2 Instrumentation***

A Shimadzu GC-2010 Plus gas chromatograph coupled to a Shimadzu GCMS-QP2010 single quadrupole mass analyser was used to perform untargeted metabolomic analysis following derivatisation. Samples were injected via a Shimadzu AOC-20i Auto Injector following 5 pre-injection methanol wash steps. The needle was rinsed with sample once prior to the 1 µL injection of the sample in splitless mode. This was followed by 5 post-injection wash steps with methanol. The temperature of the GC inlet was set to 250°C and lined with an SGE inlet liner (Trajan Scientific and Medical,

Melbourne, Australia). The carrier gas used was high purity helium, which was set to a total flow rate of 1 mL/min with the retention time locked to elute the C<sub>19</sub> *n*-alkane at 30.34 min. The GC column was an Agilent VF-5MS column (length 39.5 m + 10 m EZ-Guard; internal diameter 0.25 mm; film thickness 0.25 µm). Initial oven temperature was set to 70°C and held for 1 min between samples to stabilise, then programmed to increase at a rate of 1°C/min for the first 6 min, after which this increased to 5.63°C/min until the final temperature of 330°C was reached and held for 10 min to allow time for the remaining analytes to elute from the column. The GC-MS interface was maintained at a temperature of 300°C and, following an 8-min solvent delay, eluting analytes entered the ionisation source which was set to 250°C. Within the ion source, analytes were ionised via electron ionisation with electrons energised to 70 eV. The quadrupole mass analyser had a scan range of *m/z* 50-1000 and a scan rate of 10 scans/s.

#### **2.4.4.3 Data analysis**

GC-MS data was imported to AnalyzerPro v5.5.1 (SpectralWorks, Runcorn UK) and deconvoluted. The mass spectrum and retention index of individual spectra were searched and matched against the National Institute of Standards and Technology (NIST) Mass Spectral Library v2.3 to putatively identify unknown metabolites. Three match criteria were set for metabolite identification: 1) forward match score  $\geq 650$ , 2) reverse match score  $\geq 650$ , and 3) probability  $\geq 20\%$ .<sup>119</sup> To be considered a match, a given metabolite must have met a minimum of 2 of these 3 criteria.

Raw data was exported to Microsoft Office Excel 2016 and normalised to the <sup>13</sup>C<sub>6</sub>-sorbitol internal standard and the average cell count for each sample type.

Compounds that were present in <70% of all samples were excluded from further analysis. The remaining normalised data was then imported to The Unscrambler X v10.3 (CAMO Software, Oslo, Norway) and transformed logarithmically using the formula  $x = \log(x + 1)$ . Unsupervised analysis was carried out using principal component analysis (PCA), followed by partial least squares – discriminant analysis (PLS-DA) as a form of supervised analysis to identify variation between the sample groups. PLS-DA X-loadings were used to identify which metabolites most contributed to the variance observed between sample groups, using a threshold of +/- 0.05.

IBM SPSS Statistics v24 was used to carry out statistical analysis on the data which, following a test for normality, was determined to be non-parametric. The Mann-Whitney U test was used as a non-parametric equivalent to an independent t test for comparing results from the MTT assays. For analysing the GC-MS results obtained from cell exposures, the Kruskal-Wallis test was used as a one-way ANOVA to establish whether the metabolites differed significantly between the samples, and the pairwise output from this test was used to determine whether there was a significant difference between the overall metabolite profiles of the sample groups.<sup>120</sup> A significance level of 5% was used for each test, along with a confidence interval of 95%.<sup>120</sup>

Once the data analysis was complete, the metabolites were then mapped to biochemical pathways using the HMDB, SMPDB, MetaboAnalyst and KEGG databases in an effort to interpret the biological relevance of the observed changes in the treated cells.<sup>121-124</sup>

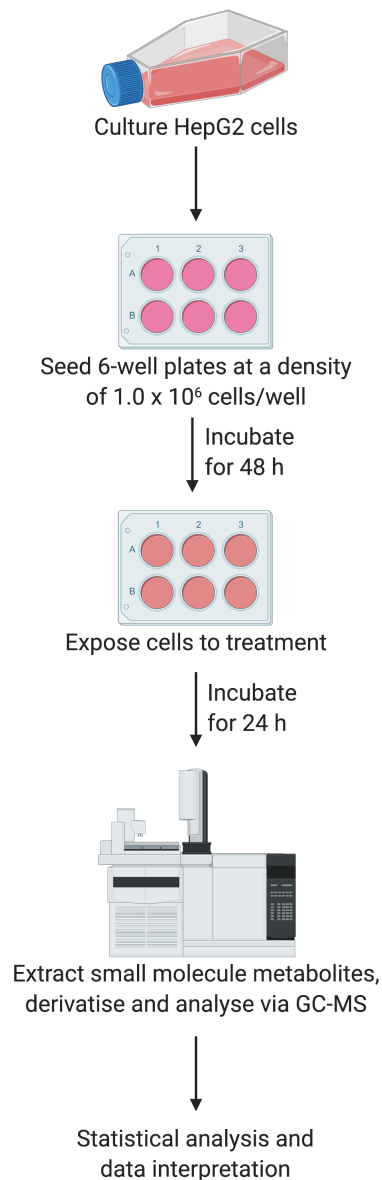


Figure 2.2. Overview of workflow followed for the analysis of hepatotoxicity following cell exposure to 1 mg/mL of GTE or GTE metabolites using GC-MS. Created with BioRender.com.

#### 2.4.5 Characterisation of GTE metabolites

GTE was extracted with LC-MS grade water at two concentrations: 10 and 50 mg/mL. Isolated CH, EC, EGC and EGCG standards were individually prepared in LC-MS grade methanol, each at a concentration of 1 mg/mL.

GTE was metabolised in the same manner as outlined in section 2.4.1, except reactions were quenched by adding 200  $\mu\text{L}$  of ice cold 50:50 methanol/acetonitrile to each tube.<sup>115</sup> Catechin standards were also metabolised following the procedure in section 2.4.1, with the only difference being that 20  $\mu\text{L}$  of a given standard was added instead of GTE. In total, 10 replicates were prepared for each of the two GTE concentrations and 3 replicates for each of the four catechin standards. The final reaction concentrations were 1 and 5 mg/mL for GTE and 0.1 mg/ml for each of the catechin standards. As in section 2.4.1, all GTE samples were centrifuged immediately after the reactions were quenched to remove the precipitated proteins, however the catechin samples were instead centrifuged following derivatisation. Supernatant was transferred into new microcentrifuge tubes, with samples kept separate. These tubes were then spun in an Eppendorf Concentrator Plus rotary vacuum concentrator on the V-AQ setting to evaporate the solvent.

Two sets of controls were also prepared for this analysis: unmetabolised GTE extracts at two concentrations (0.1 and 0.5 mg/mL) and S9 reaction blanks. GTE was extracted with LC-MS grade water and 300  $\mu\text{L}$  was aliquoted into new tubes in 3 replicates of each concentration. 10 replicates of S9 reaction blanks were prepared in the sequence outlined in section 2.4.1 and contained all constituents used for the metabolism except for the extracts of GTE or catechin standards. All controls were spun in an Eppendorf Concentrator Plus rotary vacuum concentrator on the V-AQ setting until the solvent was removed.

#### *2.4.5.1 Metabolomic analysis*

All samples were derivatised following the procedure outlined in section 2.4.4.1 and GC-MS analysis was carried out using a Shimadzu GC-2010 Plus gas chromatograph coupled to a Shimadzu GCMS-QP2010 single quadrupole mass analyser with the parameters outlined in section 2.4.4.2, however the S9 controls and metabolised GTE samples were analysed in split mode with a split ratio of 20:1, due to their high concentrations. The GTE controls and metabolised catechin standards were subsequently analysed in splitless mode to account for their lower concentrations.

GC-MS data was imported to AnalyzerPro v5.5.1 and deconvoluted. Raw peak areas for the identified compounds were exported as an Excel spreadsheet. The matrix was assessed manually and all components identified in the S9 and GTE controls, including catechins, were removed in order to isolate the GTE metabolites. Following this, compounds were retained if they were present in  $\geq 70\%$  of all samples to ensure reproducibility. In order to identify unknown metabolites, the spectra were matched to the National Institute of Standards and Technology (NIST) 2005 Mass Spectral library using the same criteria as outlined in section 2.4.4.3. Additionally, data obtained from the metabolised catechin standards were matched to the compounds in the metabolised GTE samples to tentatively confirm the presence of catechin metabolites.



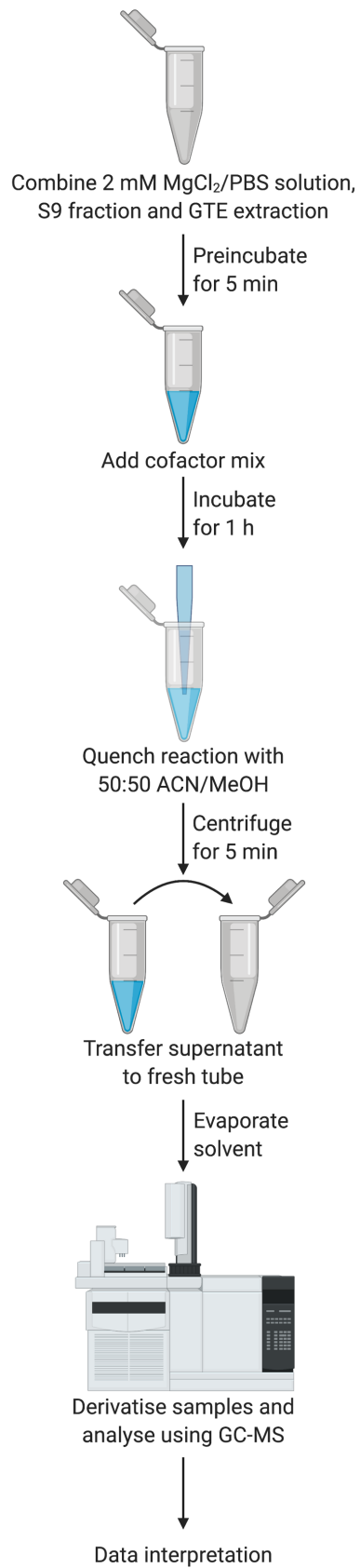


Figure 2.3. Overview of GTE metabolite preparation and characterisation using GC-MS analysis.

Created with BioRender.com.

## 2.5 GTE and paracetamol-induced hepatotoxicity

### 2.5.1 Rifampicin-induced CYP450 activity

It has been demonstrated that rifampicin can induce CYP450 activity in HepG2 cells.<sup>125</sup> A 10 mM stock solution containing rifampicin dissolved in DMSO was diluted 1:5 with PBS to yield a 2 mM working solution, which was subsequently filtered using a 0.2 µm filter to ensure sterility. 909 µL of this working solution was diluted in 49.091 mL of supplemented DMEM containing 10% FCS, yielding a 36 µM DMEM + rifampicin solution for cell exposures.

### 2.5.2 Cell treatment

At confluence, HepG2 cells at passage 31 were seeded at a density of  $1.0 \times 10^6$  cells/well in 6-well plates with 1 mL DMEM + rifampicin and topped up with additional supplemented DMEM to reach a total volume of 2 mL/well. A total of 10 plates were seeded and then incubated at 37°C and 5% CO<sub>2</sub> for 48 h to allow cells to settle and adhere to the bottom surface of the wells. Following this incubation period, spent medium was removed from the wells and the treatment solutions were added to the appropriate plates as follows: 2 mL of serum-free DMEM containing 15 mM APAP was added to the paracetamol (APAP) plates, 2 mL of serum-free DMEM containing 15 mM APAP and 1 mg/ml GTE was added to the APAP/GTE plates and 2 mL of serum-free DMEM containing 1 mg/mL GTE was added to the GTE plates. These concentrations were chosen as 15 mM APAP has been demonstrated to reduce HepG2 cell viability by approximately 20%, and 1 mg/mL GTE was consistent with other exposure concentrations used in this project.<sup>26</sup> Two plates were allocated to each treatment type and two were allocated to controls, in which the spent DMEM

+ rifampicin was replaced with fresh serum-free DMEM. These eight plates were then incubated at 37°C and 5% CO<sub>2</sub> for 24 h. The remaining two plates were harvested at the conclusion of the initial 48 h incubation period in order to be pooled and used QCs for GC-MS analysis.

At the conclusion of the exposure period, all 6-well plates were put on ice. A counting well was set aside on each plate to determine cell viability following exposure, yielding 2 replicates of each sample type for cell counts which were carried out following the method outlined in section 2.2.2. A rubber cell scraper was used to harvest the cells from the remaining 5 wells into 500 µL methanol containing <sup>13</sup>C<sub>6</sub>-sorbitol internal standard at a concentration of 2.6 µg/mL. The contents of each well were transferred into 1.5 mL microcentrifuge tubes and the small molecule metabolites were extracted following the procedure outlined in section 2.4.3. This yielded a total of 10 replicates of each sample type for GC-MS analysis.

### 2.5.3 Metabolomic analysis

Samples were derivatised following the procedure outlined in section 2.4.4.1, GC-MS analysis was carried out using a Shimadzu GC-2010 Plus gas chromatograph coupled to a Shimadzu GCMS-QP2010 single quadrupole mass analyser with the parameters outlined in section 2.4.4.2 and the data was analysed following the procedure outlined in section 2.4.4.3.

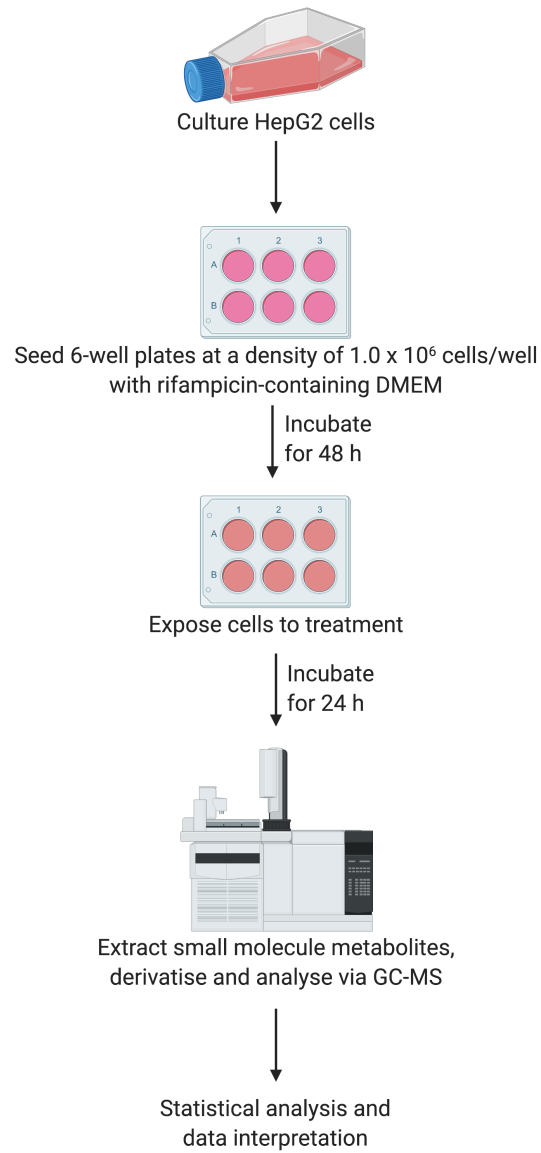


Figure 2.4. Overview of workflow followed to determine effect of GTE on paracetamol-induced hepatotoxicity using GC-MS analysis. Created with BioRender.com.

### 3. Results and discussion

#### 3.1 MTT cytotoxicity assay

A decrease in cell viability was observed as paracetamol concentration increased (Figure 3.1). Cells treated with 15 and 30 mM APAP had lower mean absorbance than was observed in untreated cells, demonstrating a 12.92% ( $\pm$  13.29%) and 19.1% ( $\pm$  23.67) decrease, respectively. These results suggest a decrease in cell viability as APAP concentration was increased. An ED<sub>50</sub> was unable to be calculated as it was not possible to determine the maximal response from the concentrations used in this study. Untreated controls had a relative standard deviation (RSD) of 17.08%, compared to 19.30%, 13.29% and 23.67% observed within the 7.5, 15 and 30 mM treatment groups. An RSD of <20% is generally an acceptable level of variation, and thus results within this range were considered reliable; only the 30 mM APAP sample group exceeded this limit. No significant difference in cell viability was observed between any of the treatment concentrations compared to untreated controls ( $p>.05$ ).

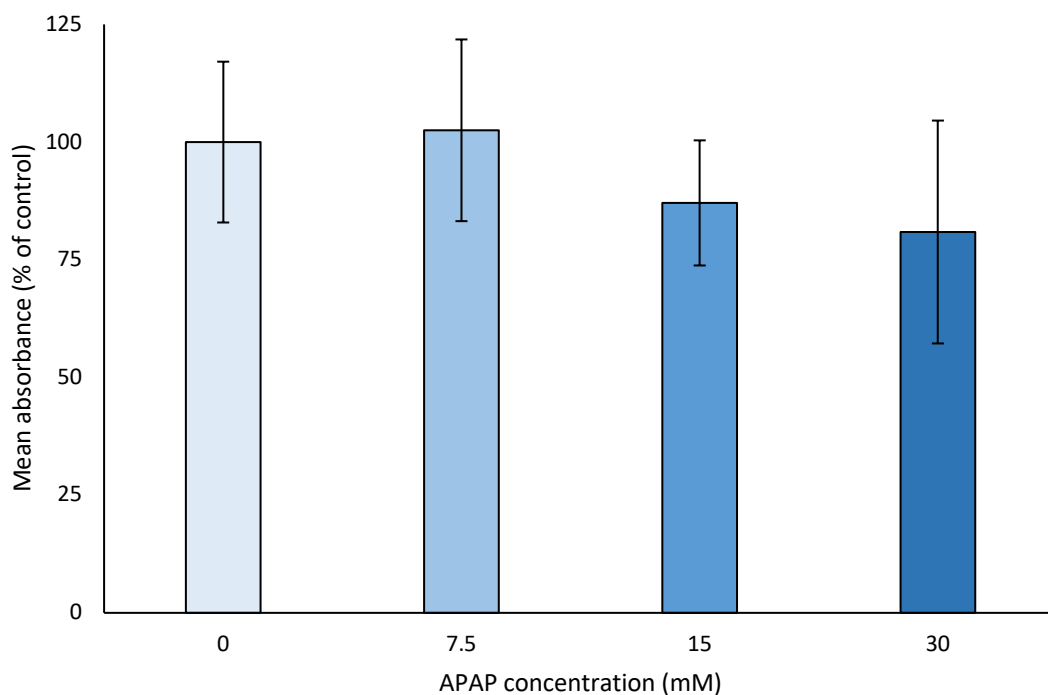


Figure 3.1. Change in HepG2 cell viability following exposure to 0, 7.5, 15 and 30 mM APAP as measured by MTT assay (n = 12 for each concentration). Error bars indicate relative standard deviation.

Absorbance appeared to increase with EGCG concentration, with 100  $\mu$ M EGCG being 76.78% ( $\pm$  13.05) higher than untreated controls (Figure 3.2). This pattern was also observed to varying degrees with the other catechins analysed, with the increase in mean absorbance most pronounced in cells treated with CH and EGCG. The least change was observed in cells treated with EGC, with 100  $\mu$ M of this catechin having an absorbance that was 11.52% ( $\pm$  18.69) higher than untreated controls. The majority of samples had an RSD <20%, except cells treated with 25  $\mu$ M EGCG (26.61%) and untreated cells in the CH MTT assay (28.04%).

The results for the catechin MTT assays are suspected to be abnormal as it was expected that cell viability, and therefore absorbance, would decrease as catechin

concentration increased. Spent DMEM and HepG2 cells had a dark brown appearance following catechin exposure, thus it is possible that this pigment may have interfered with the absorbance measurements obtained for the catechin exposures.

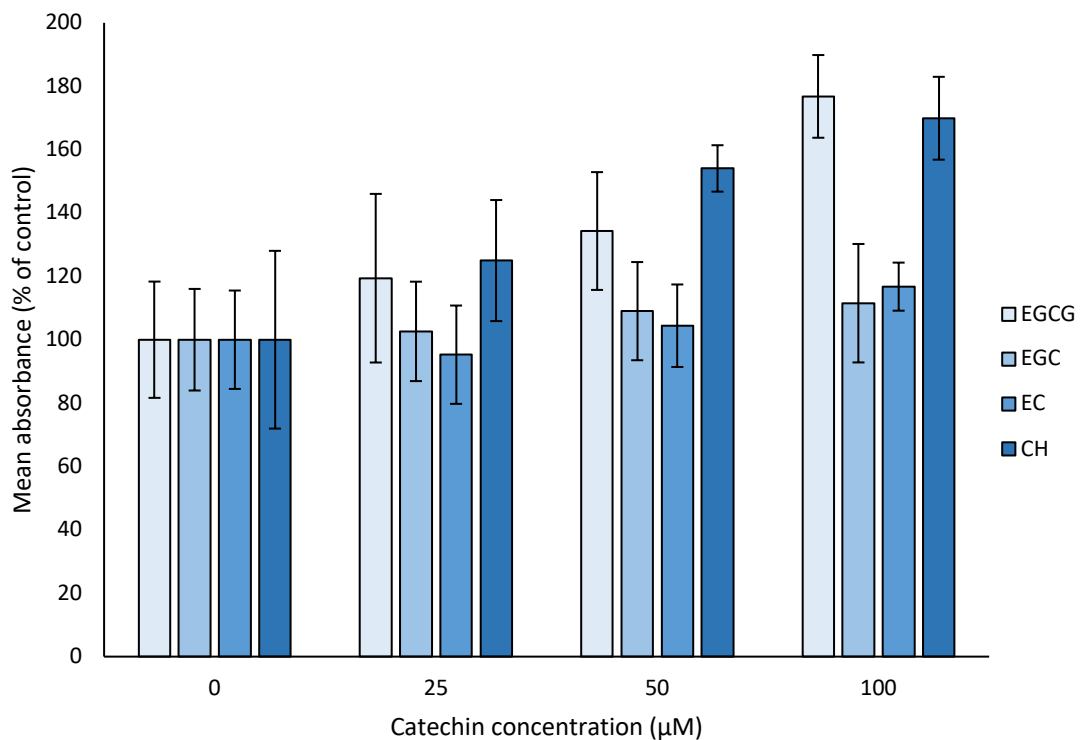


Figure 3.2. Change in HepG2 cell viability following exposure to 0, 25, 50 and 100 µM EGCG, EGC, EC or CH as measured by MTT assay (n = 12 for each concentration). Error bars indicate relative standard deviation.

An increase in mean absorbance was also observed with increasing GTE concentration (Figure 3.3). Cells treated with 1 mg/mL GTE had an absorbance 118.01% ( $\pm 1.86$ ) greater than that observed in untreated cells. As was observed in the catechin MTT assays, GTE-treated DMEM and cells had a darker appearance at

the conclusion of the exposure period; it is therefore likely that the absorbance values obtained here were also inaccurate. The RSD for untreated controls (20.31%) was higher than those observed in all three GTE treatment groups, with 0.1, 0.5 and 1.0 mg/mL samples having 12.92%, 13.18% and 1.86% RSD, respectively. It is worth noting that due to the intensity of the colour change observed in 1 mg/mL GTE treatment wells, the plate reader was only able to record absorbance values for 3 of the 12 samples. This may explain the low RSD obtained for this treatment concentration compared to the others tested in this assay.

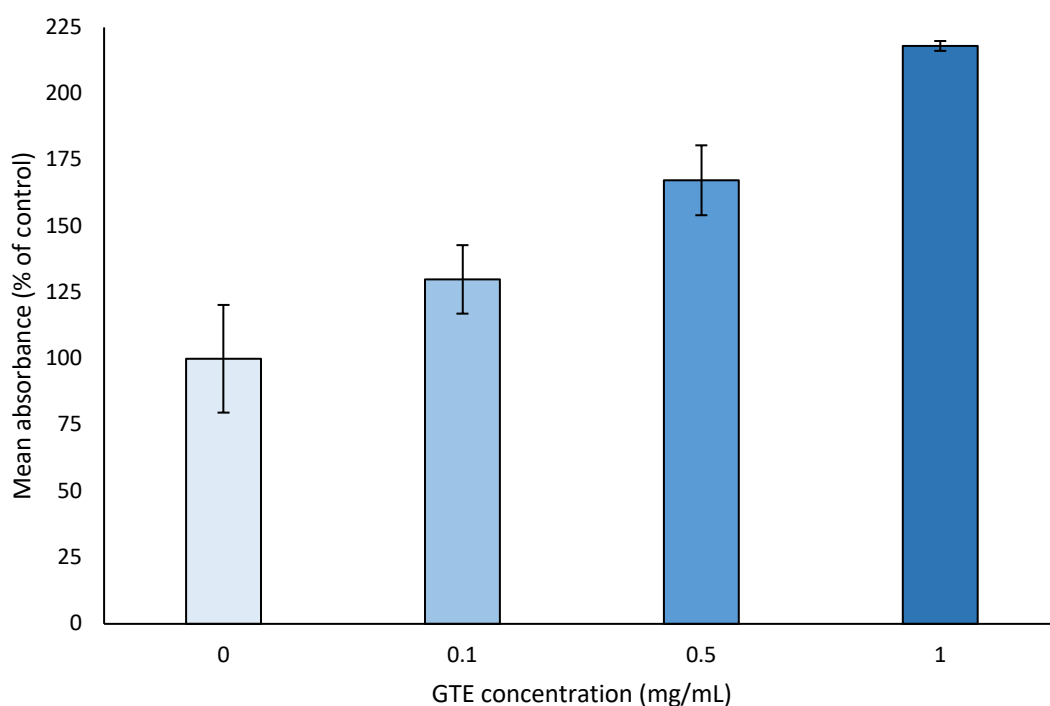


Figure 3.3. Change in HepG2 cell viability following exposure to 0, 0.1, 0.5 and 1.0 mg/mL GTE as measured by MTT assay (n = 12 for each concentration except 1 mg/mL, for which n = 3). Error bars indicate relative standard deviation.



The GTE MTT assay was repeated with the same concentrations, however spent medium was replaced with fresh serum-free DMEM prior to the addition of the dye solution in an effort to limit background interference. A decrease in the overall trend was observed, although absorbance still appeared to increase with increasing GTE concentration, with cells exposed to 1 mg/mL GTE having an absorbance 25.43% ( $\pm 7.55$ ) higher than that observed in untreated cells (Figure 3.4). This difference was markedly less than the increase of 118.01% observed between the same sample types in the original GTE MTT assay, and similar reductions were observed across the other GTE concentrations, suggesting that replacement of treated medium with fresh DMEM helped to reduce background absorbance. This assay had less variation within the untreated controls, 0.1 and 0.5 mg/mL sample groups than in the first GTE MTT assay, with RSDs of 5.23, 6.30 and 4.76%, respectively. Cells treated with 1 mg/mL GTE demonstrated greater variance compared to the first GTE MTT assay, although still within the acceptable range, with an RSD of 7.55%. The 0.5 and 1.0 mg/mL GTE had a mean absorbance significantly lower than the same concentrations in the original GTE MTT assay ( $p < .001$ ).

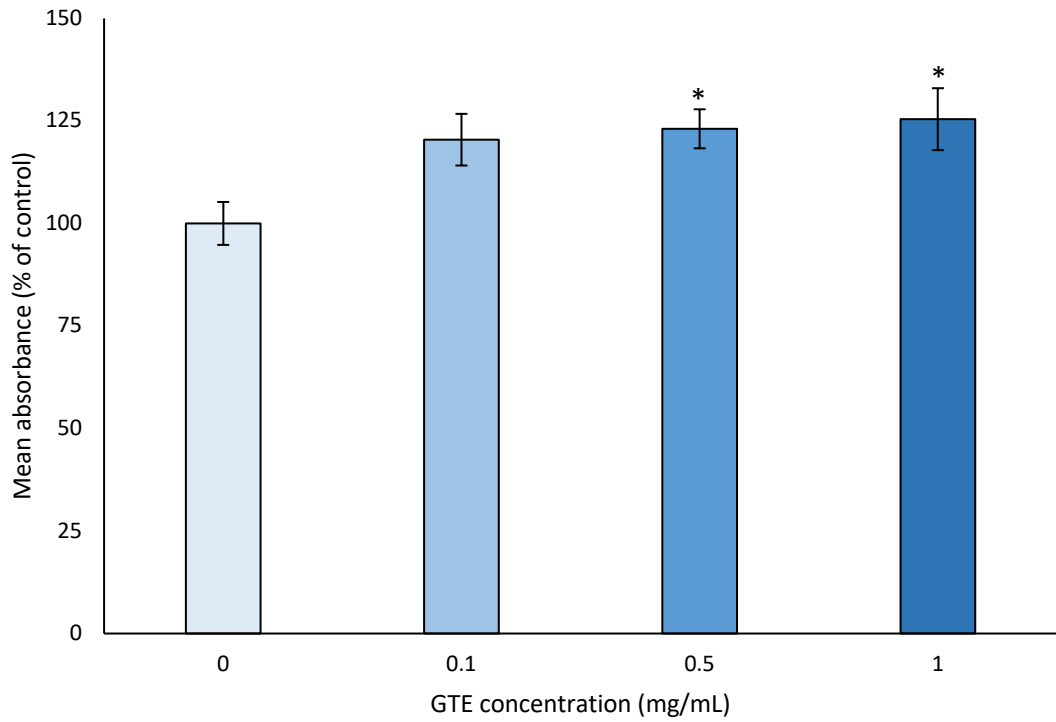


Figure 3.4. Change in HepG2 cell viability measured by MTT assay following exposure to 0, 0.1, 0.5 and 1.0 mg/mL GTE with spent medium replaced prior to addition of MTT dye solution (n = 12 for each concentration). Error bars indicate relative standard deviation. \*Mean absorbance differed significantly compared to that recorded for the same treatment concentration in the first GTE MTT assay, as determined by the Mann-Whitney U test ( $p < .05$ ).

Further development of this assay is required, and absorbance should be read from a set of control wells prepared at the same GTE concentrations, with the addition of solubilisation solution/stop mix but without the addition of dye solution. The purpose of including the solubilisation solution/stop mix is to retain the lysis and solubilisation step so the absorbance of the dark pigment may be properly measured. The mean of the absorbance values obtained from these controls could then be calculated and subtracted from the mean absorbance values obtained from sample plates that have been treated with dye solution. This would reduce interference from the brown pigmentation observed in HepG2 cells, providing more accurate measurements and potentially demonstrating the expected decrease in cell viability with increasing GTE concentration.

## 3.2 Hepatotoxicity of GTE and its metabolites

### 3.2.1 Cell density

Microscopic examination of the cells post-exposure showed approximately 80% confluence across the bottom of the wells in the control samples (Figure 3.5). In comparison, approximately 50-60% confluence was observed in the wells containing the GTE- and GTE metabolite (GTEM)-treated samples. It was difficult to distinguish any difference between the cell number and viability of GTE- and GTEM-treated cells by microscopy alone. In both treatments the medium changed from pink to brown and the cells also took on a darker appearance, as observed in section 3.1.

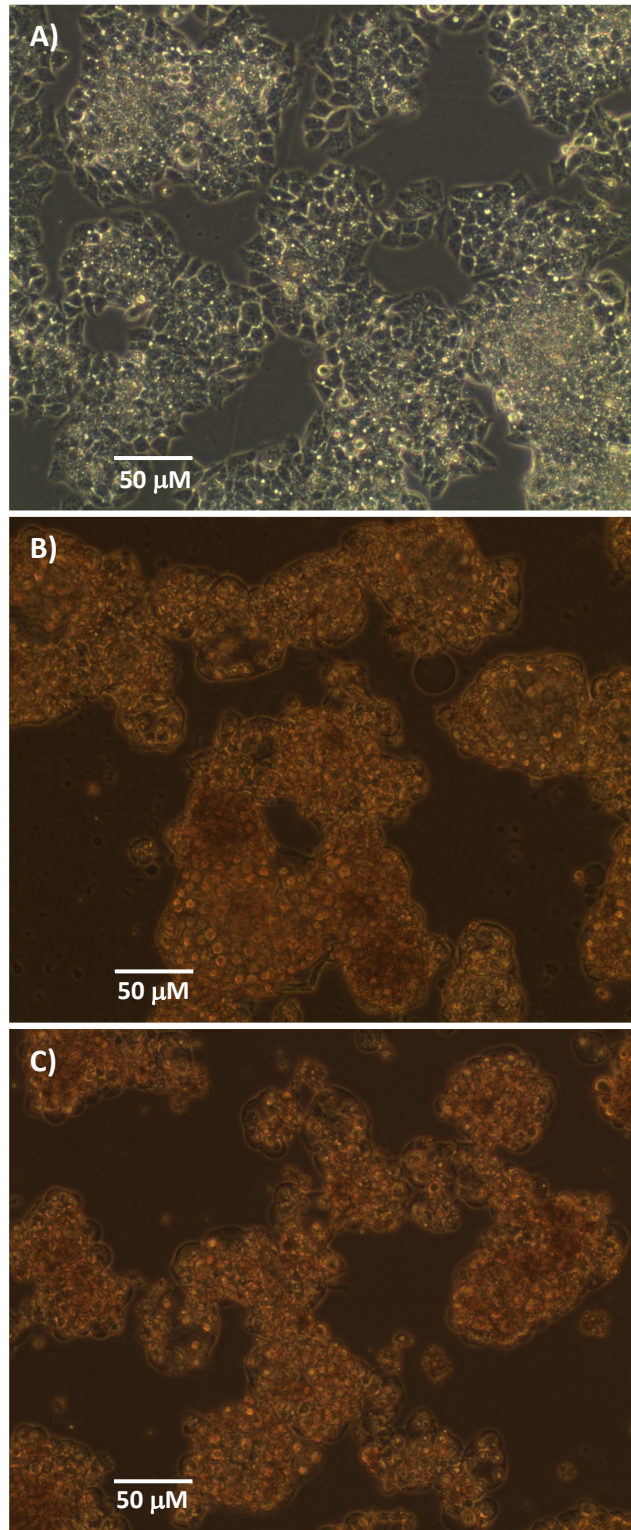


Figure 3.5. Light microscope images at 100x magnification comparing untreated HepG2 cells (A) with those exposed to 1 mg/mL GTE (B) or 1 mg/mL GTEM (C) for 24 h.

The mean HepG2 cell concentration in untreated controls was  $1.06 \times 10^6$  cells/mL ( $\pm 4.77 \times 10^5$ ), more than twice that observed in the treatment groups (Figure 3.6). Untreated cells had an RSD of 44.92%; this variation is likely explained by the loss of a large number of cells from one well during the PBS wash step, thus, the concentration of control cells is expected to have been higher than the mean described here. Given that only two wells were used for determining post-exposure cell concentration, with two cell counts from each, a higher number of wells should be used in future in order to more accurately determine a concentration of untreated cells. At the conclusion of the 24-h incubation period, GTE-treated samples had the lowest mean cell concentration at  $3.75 \times 10^5$  cells/mL ( $\pm 7.07 \times 10^4$ ), whilst a mean of  $4.40 \times 10^5$  cells/mL ( $\pm 1.34 \times 10^5$ ) was observed in the GTEM-treated samples. Greater variation was observed in the GTEM treatment group, which had an RSD of 30.53%, compared to GTE-treated cells (18.86% RSD). Given that the GTEM-treated cells had an RSD >20%, the mean cell concentration determined for this treatment group is potentially unreliable. As with the untreated controls, it is possible that increasing the number of wells used for cell counts may aid in the reduction of variation within the GTEM treatment group.

The decrease in mean cell concentration observed in the treatment groups may be indicative of hepatotoxicity, as these results are consistent with previous findings that high-doses of GTE elicit cytotoxicity in hepatocytes.<sup>95</sup> Given that the degree of GTE metabolism was not determined prior to treating cells with GTEM, it is difficult to establish whether it was the metabolites or unaltered GTE constituents responsible for the cytotoxicity observed in GTEM-treated cells. Given that Phase II metabolism tends to render compounds relatively inert for excretion, the reduced

toxicity observed in GTEM-treated cells in comparison to the GTE treatment group may be due to a decreased concentration of toxic precursors.<sup>18, 19</sup>

HepG2 cells were difficult to trypsinise post-exposure to GTE and GTEM, potentially due to a reaction between the GTE and the well coating. This resulted in only 80-90% of the cells being successfully resuspended, thus the cell concentrations determined for these treatments may be underestimated.

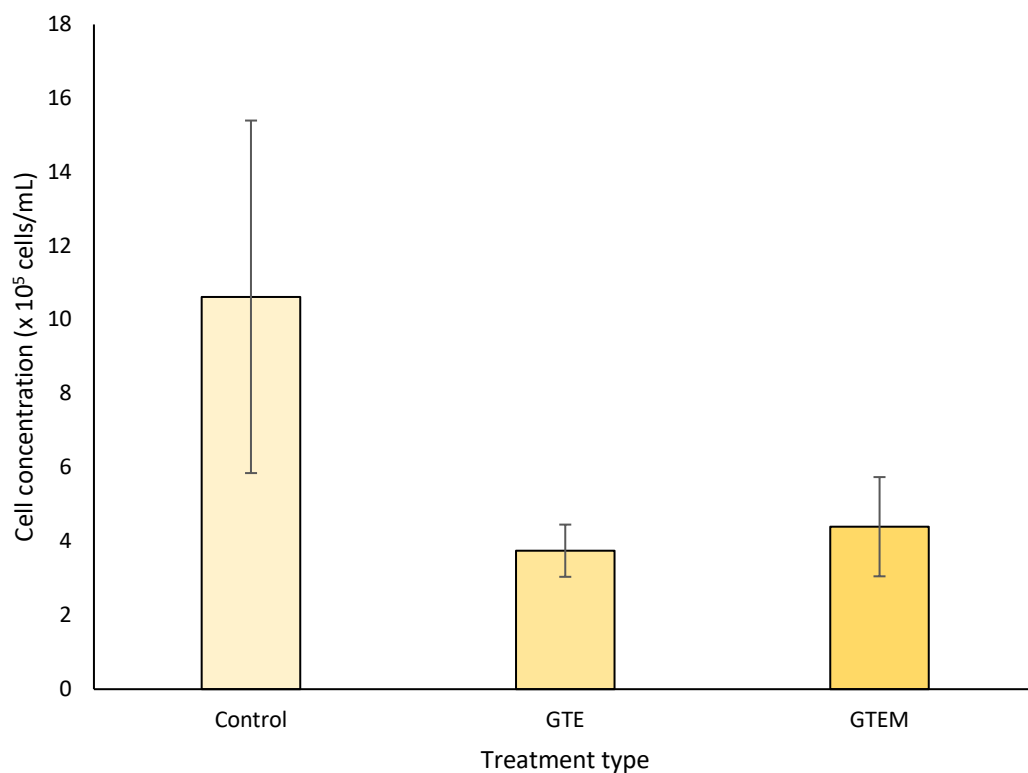


Figure 3.6. HepG2 cell concentration following exposure to 1 mg/mL GTE or 1 mg/mL GTEM for 24 h compared to untreated controls (n = 2 for each sample group). Error bars indicate standard deviation.

### 3.2.2 Metabolomic analysis

The PCA scores plot generated to compare the three sample groups demonstrated a difference between GTE and GTEM-treated samples compared to untreated controls (Figure 3.7a). Principal component 1 (PC-1) explained 19% of the observed variance, whilst 17% was explained by principal component 2 (PC-2). Variance between the GTE- and GTEM-treated cells was unable to be determined from the PCA scores plots comparing these two sample groups (3.7b).

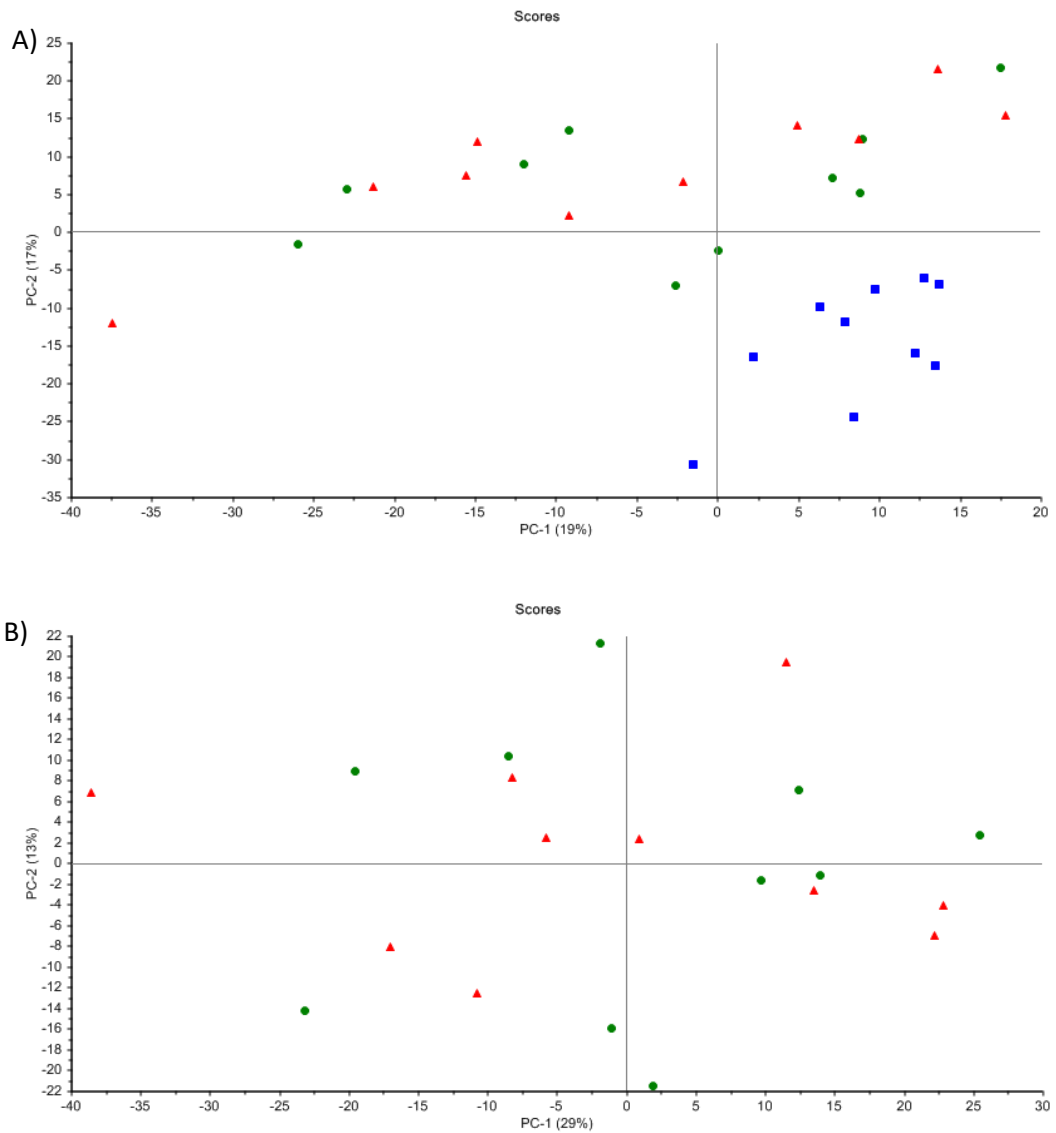


Figure 3.7. PCA scores plots using the first two principal components for comparisons of HepG2 cell metabolite profiles following treatment with serum-free DMEM containing 1 mg/mL GTE (green) or 1 mg/mL GTEM (red) and untreated controls (blue), as measured by GC-MS analysis (n = 10 for each sample group). A difference in metabolite profile was observed between untreated cells compared to both treatment groups (A). A difference between GTE-treated cells and the GTEM treatment groups was unable to be determined via PCA (B).



A difference in metabolite profile was observed in the PLS-DA scores plot comparing the GTE and GTEM treatment groups (Figure 3.8). This difference was primarily explained by factor-1, with 10% and 71% of the observed variance explained.

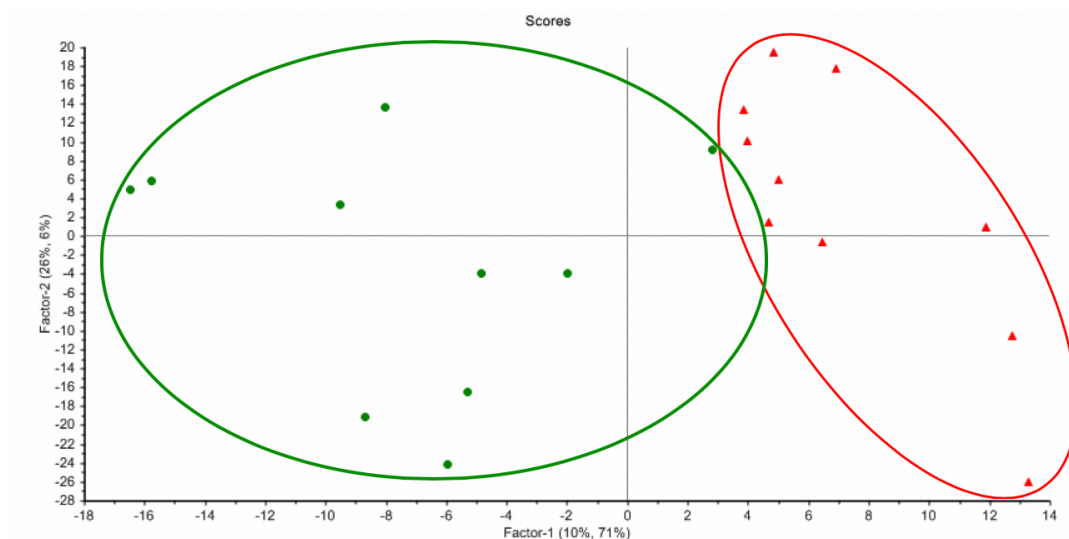


Figure 3.8. PLS-DA scores plot using the first two principal components (factors) for comparison of HepG2 cell metabolite profiles following exposure to 1 mg/mL GTE (green) or 1 mg/mL GTEM (red) for 24 h, as measured by GC-MS analysis (n = 10 for each sample group). Using PLS-DA, a difference was distinguished between the metabolite profiles of GTE-treated cells compared to the GTEM treatment group.

Using PLS-DA X-loadings and a threshold of  $\pm 0.05$ , 42 compounds contributing most to the variance observed between sample groups were identified (Figure S1). 22 of these were putatively identified after meeting at least 2 of the 3 match criteria outlined in section 2.4.4.3 when compared to the NIST library. Following the removal of compounds deemed likely to be solvent-derived, 18 metabolites remained. Comparing these 18 metabolites, a significant difference was observed between the

profiles of untreated controls compared to GTE-treated cells ( $p < .001$ ), and also between the controls and GTEM treatment group ( $p = .001$ ) (Figure S2). The metabolite profile of GTE-treated cells was not found to significantly differ from that of the GTEM treatment group ( $p = .446$ ). Of the 18 metabolites, 15 demonstrated a positive fold-change ( $>1.0$ ) in mean peak area size in both treatment types compared to those derived from control samples (Table 3.1). A negative fold-change ( $<1.0$ ) was observed in the remaining 3. All metabolites were found to differ significantly between sample groups, with the exception of D-phenylalanine, serine and L-glutamine.

Gallic acid, 9-octadecanoic acid, an unidentified short-chain fatty acid, palmitic acid, citric acid and 5,8,11-eicosatrienoic acid demonstrated changes  $>10$ -fold in both treatment types, listed here in decreasing magnitude of change observed in GTE-treated cells. Palmitelaidic acid and an unidentified piperidine derivative had a change  $>10$ -fold in GTE-treated samples only; neither of these metabolites were identified as contributing substantially to the variance observed between GTEM samples and untreated controls. L-5-oxoproline had a change  $>10$ -fold in GTEM-treated samples and also contributed to the difference in metabolite profile observed between GTE-treated cells and controls. Only 3 metabolites demonstrated a negative fold-change, all of which were amino acids: L-glutamine (GTEM: 0.93), L-glutamic acid (GTE: 0.52) and glycine (GTE: 0.40, GTEM: 0.47). Of the amino acids, carbohydrates and fatty acids, the greatest fold-changes were observed in L-5-oxoproline (GTE: 8.47, GTEM: 10.38), myo-inositol (GTE: 5.35, GTEM: 7.91) and 9-octadecanoic acid (GTE: 32.05, GTEM: 21.30), respectively.

Table 3.1. Fold change observed in metabolites of HepG2 cells post-exposure to 1 mg/mL GTE or 1 mg/mL GTEM compared to untreated controls, as measured by GC-MS analysis (n = 10 for each sample group). Changes were primarily observed in amino acids and fatty acids. Green arrows indicate a positive-fold change compared to untreated controls and red arrows indicate a negative fold-change. \*Metabolite differed significantly between sample groups, as determined by the Kruskal-Wallis test ( $p < .05$ ).

Metabolite	GTE	GTEM
<b>Amino acids</b>		
L-5-Oxoproline*	↑ 8.47	↑ 10.38
L-Isoleucine*	↑ 4.95	↑ 5.03
DL-Phenylalanine	↑ 2.96	↑ 3.93
Serine	-	↑ 1.14
L-Glutamine	-	↓ 0.93
L-Glutamic acid*	↓ 0.52	-
Glycine*	↓ 0.40	↓ 0.47
<b>Carbohydrates</b>		
Myo-Inositol*	↑ 5.35	↑ 7.91
Unidentified carbohydrate*	-	↑ 3.58
<b>Fatty acids</b>		
9-Octadecanoic acid*	↑ 32.05	↑ 21.30
Unidentified short-chain fatty acid*	↑ 27.57	↑ 28.72
Palmitic acid*	↑ 23.02	↑ 18.70
5,8,11-Eicosatrienoic acid*	↑ 16.65	↑ 15.23
Palmitelaidic acid*	↑ 15.75	-
<b>Other metabolites</b>		
Gallic acid*	↑ 52.58	↑ 54.88
Citric acid*	↑ 16.76	↑ 26.22
Unidentified piperidine derivative*	↑ 12.30	-
Uracil*	↑ 6.25	-

L-5-oxoproline, a cyclised L-glutamic acid derivative also known as pyroglutamic acid, is an intermediate in the  $\gamma$ -glutamyl cycle, the pathway in which glutathione is biosynthesised and metabolised.<sup>122, 124</sup> Glutathione is a non-enzymatic free radical scavenger which can become depleted during oxidative stress; this may result in the accumulation of intermediates of the  $\gamma$ -glutamyl cycle, including L-5-oxoproline.<sup>126</sup> Additionally, L-5-oxoproline can induce acidosis and other adverse health effects at sufficiently high concentrations.<sup>121</sup> It is possible that the observed positive fold-change in L-5-oxoproline is an indication that cells from both treatment groups were under oxidative stress.

A negative fold-change was observed in glutamine, glutamic acid and glycine; this may indicate their consumption as an alternative energy source, potentially due to a fault in the glycolytic pathway.<sup>122</sup> Conversely, the amino acids isoleucine, phenylalanine and glycine demonstrated a positive fold-change. This could be indicative of protein degradation or a malfunction in protein synthesis, either of which could cause an elevation of free amino acids within the cells. GTEM-treated cells demonstrated a positive fold-change in serine; it has previously been found that serine has an antioxidant function, therefore a positive fold-change in this amino acid could be due to its mobilisation in response to a pro-oxidant state within the cells.<sup>127</sup>

An unidentified carbohydrate demonstrated a positive fold-change, which may be indicative of a malfunction in the glycolytic pathway that has potentially reduced cellular ability to use carbohydrates as an energy source.<sup>122</sup> Alternatively, it could indicate that treated cells lost their capacity to convert non-glucose carbohydrates into glycolysis-compatible compounds. Either of these suggestions could explain the

requirement for alternative energy sources, such as amino acids, in order for cells to continue generating energy whilst bypassing glycolysis.

A positive fold-change was also observed in myo-inositol, a key structural component of the inositol phosphate secondary messengers which are involved in a variety of cell signalling pathways.<sup>128, 129</sup> Of note, inositol phosphate controls intracellular calcium ion ( $\text{Ca}^{2+}$ ) concentration; in hepatocytes, type I inositol 1,4,5-triphosphate receptor (InsP3 R-I)-mediated  $\text{Ca}^{2+}$  signalling is involved in triggering the early phase of liver regeneration.<sup>128</sup> Additionally, it has been suggested that inositol-requiring enzyme-1 $\alpha$  (IRE1 $\alpha$ ), an endoplasmic reticulum transmembrane protein, may also promote liver regeneration via regulation of the signal transducer and activator of transcription 3 (STAT3) pathway, which has a role in hepatocyte proliferation during the regenerative response.<sup>129</sup> It is therefore possible that the positive fold-change observed in myo-inositol in cells treated with GTE or GTEM may be due to increased inositol requirement within the cells in an attempt to initiate regeneration in response to GTE- or GTEM-induced damage.

Citric acid also demonstrated a positive fold-change in both treatment groups. Citrate, the species of citric acid present at a biological pH, is the first intermediate of the tricarboxylic acid (TCA) cycle; thus, an accumulation of citric acid may result from inadequate conversion of citrate to isocitrate in this pathway.<sup>121, 122, 124</sup> Aside from a breakdown at this point potentially causing the build-up of citrate, it may also contribute to the energy demand driving the use of amino acids as an energy source. It is also worth noting that in healthy cells an excess of citrate can lead to the inhibition of phosphofructokinase, the enzyme which catalyses the rate-limiting

conversion of fructose-6-phosphate to fructose-1,6-bisphosphate in glycolysis.<sup>122</sup> An accumulation of citric acid, therefore, may also be contributing to the shutdown of glycolysis, thus adding to the suspected cellular demand for non-carbohydrate energy sources that can bypass the glycolytic pathway.

Another key observation was the positive fold-change in 9-octadecanoic acid, palmitic acid, 5,8,11-eicosatrienoic acid and an unidentified short-chain fatty acid in both treatment groups, as well as palmitelaidic acid in GTE-treated cells. Fatty acids are primary targets for free radical and singlet oxygen oxidations, which may result in the release of fatty acids into the cell and ultimately the disruption of cell membranes.<sup>130</sup> It is therefore possible that the positive fold-change in fatty acids observed here may be due to membrane degradation as a result of oxidative stress.

A positive fold-change was observed in the nucleobase uracil, which may be indicative of reduced RNA synthesis or increased pyrimidine degradation.<sup>122, 124</sup> A reduction in RNA could lead to a decrease in protein synthesis, thus contributing to the positive fold-change observed in some amino acids. Alternatively, pyrimidine metabolism could indicate the degradation of DNA and RNA, which can also occur as a result of oxidative stress.<sup>122, 124</sup>

Gallic acid demonstrated a large positive fold-change in both treatment types (>50), however given that this is not an endogenous compound, its contribution to the difference between treated cells and the controls is likely only due to cellular uptake of catechin gallates from the medium.<sup>121</sup> The presence of gallic acid as its own entity could indicate its cleavage from catechin gallates within the cells although, given that HepG2 cells have little metabolic function, the extent to which this may have

occurred is questionable.<sup>5</sup> At the very least, the positive fold-change in gallic acid within both treatment groups likely indicates that catechin gallates were being taken up by the cells.

### 3.3 Identification of GTE metabolites

620 compounds were identified following GC-MS analysis of the metabolised GTE samples. After removing the alkanes and components present in the S9 controls and unmetabolised GTE, 521 compounds remained. 17 of these were present in  $\geq 70\%$  of the metabolised GTE samples; therefore, these were regarded as having the highest probability of being GTE metabolites (Table 3.2). 10 of the 17 suspected GTE metabolites were also detected in the metabolised catechin samples (Table S1-S4).

One compound found in the unmetabolised GTE was also found in 100% of the metabolised GTE samples (RT: 31.1217, base peak: 281). This compound was putatively identified as gallic acid after exceeding all 3 match criteria outlined in section 2.4.4.3 when compared to the NIST library, thus it was retained in the list of suspected GTE metabolites due to it being a known component of catechins such as EGCG and ECG.<sup>51</sup> The remaining 17 compounds suspected to be GTE metabolites were unable to be positively identified without further experimentation and analysis.

Table 3.2. Suspected metabolites of GTE following metabolism with S9 human liver fraction and frequency of detection using GC-MS analysis. GTE was metabolised at two concentrations: 1 mg/mL and 5 mg/mL (n = 10 for each concentration) \*Components also detected in metabolised standards of CH, EC, EGC and/or EGCG.

Compound	RT (min)	Base Peak	Detected in samples (%)
17	11.6083	116	85
28*	16.2233	116	80
116	17.2000	117	75
126*	18.3283	99	95
182*	21.4600	71	70
184*	21.8900	75	90
192*	22.8067	174	90
217*	27.5300	299	95
220	27.9300	174	90
257*	31.1217	281	100
258*	31.2017	72	75
261	31.7450	147	75
312*	33.2900	217	100
318	34.5083	299	90
337*	36.5400	147	90
339	37.8117	299	95
353	41.2500	361	95

### 3.4 The effect of GTE on paracetamol-induced hepatotoxicity

#### 3.4.1 Cell density

HepG2 cells from control samples reached approximately 80% confluence by the conclusion of the exposure period and the cells appeared to be healthy (Figure 3.9).



Confluence of cells exposed to APAP was estimated to be 70-75% and the cells again had a healthy appearance, although were aggregated in smaller clusters than those observed in the controls. Confluence of both the GTE- and APAP/GTE-treated samples was approximately 50-60% and it was difficult to distinguish any obvious difference between these treatment groups via microscopy. Cells in the GTE and APAP/GTE sample groups also formed smaller aggregates, similar to those observed in the APAP-treated cells. Cells exposed to GTE or the combined treatment had a darker appearance than the untreated controls and APAP-treated cells, and a colour change in the medium from pink to brown was observed.

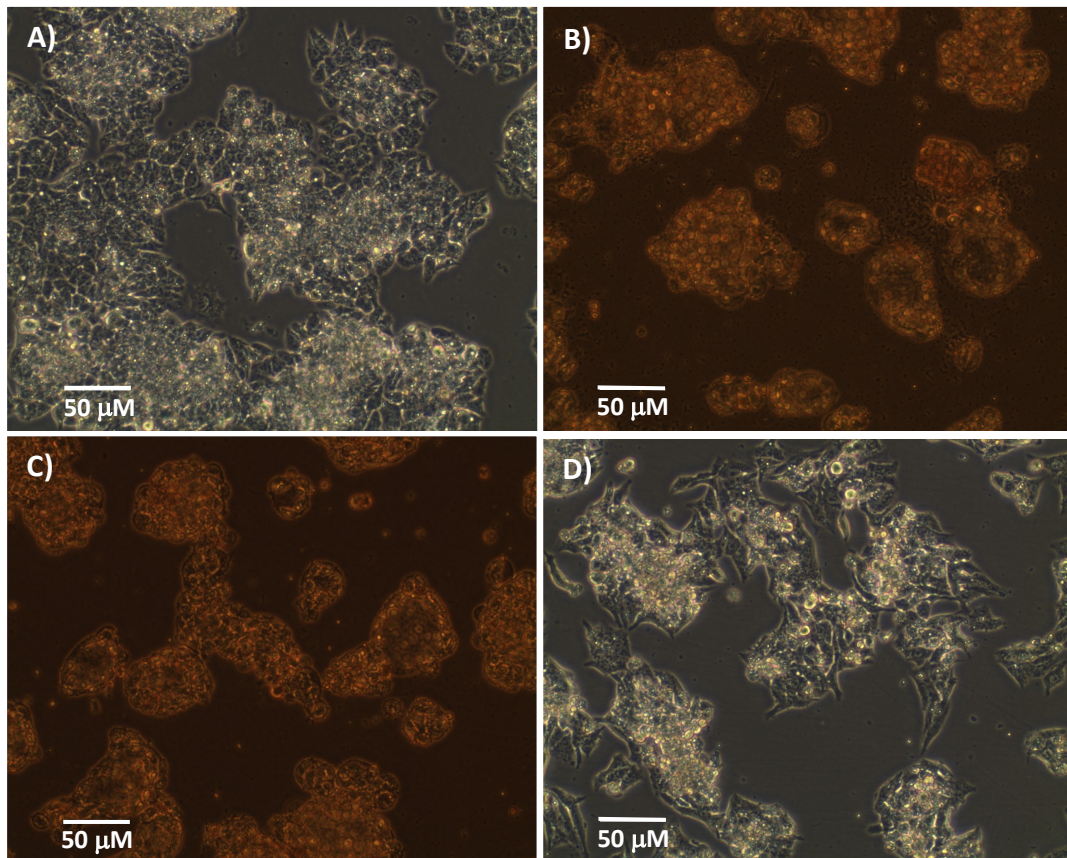


Figure 3.9. Light microscope images at 100x magnification comparing untreated HepG2 cells (A) with those exposed to 1 mg/mL GTE (B), 15 mM APAP and 1 mg/mL GTE (C) or 15 mM APAP (D) for 24 h.

In the untreated controls, the mean HepG2 cell concentration was  $1.13 \times 10^6$  cells/mL ( $\pm 6.68 \times 10^5$ ) (Figure 3.10). The RSD determined from the concentration of untreated cells was 59.27%, which may be due to loss of cells during the removal of spent medium or the PBS wash step prior to trypsinising; therefore, untreated cell concentration was likely to be higher than described here. As outlined in section 3.2.1, only two wells were used for performing cell counts; future studies should include at least three wells in order to provide a more accurate estimate of untreated cell concentration. Of the sample groups, the APAP-treated cells appeared to retain the greatest viability with a mean cell concentration of  $6.80 \times 10^5$  cells/mL ( $\pm 1.13 \times 10^5$ ).

Little difference was demonstrated between the GTE-treated cells and those exposed to a combination of APAP and GTE, with mean cell concentrations found to be  $3.45 \times 10^5$  ( $\pm 7.07 \times 10^3$ ) and  $3.55 \times 10^5$  cells/mL ( $\pm 7.78 \times 10^4$ ), respectively. This may be due to the GTE concentration of 1 mg/mL being too high, thus resulting in the effects of high-dose GTE masking the effects of APAP and GTE in combination. Based on the cell counts, it was not possible to determine whether the effects observed in the APAP/GTE treatment group were from the combined treatment or predominantly due to the high GTE dose. If this test were to be repeated, a lower GTE concentration should be used in order to better elucidate whether GTE aids or exacerbates APAP-induced hepatotoxicity. All treatment groups demonstrated relatively low variation,

with the lowest RSD observed in GTE-treated cells (2.05%), followed by the APAP (16.64%) and APAP/GTE (21.91%) treatment groups

As was observed in section 3.2.1, HepG2 cells were difficult to trypsinise post-exposure to GTE and the combined APAP/GTE treatment, believed to be due to the GTE reacting with the well coating. As a result, approximately 80-90% of the cells resuspended successfully, therefore the actual cell concentrations for these treatment groups were slightly higher than described here.

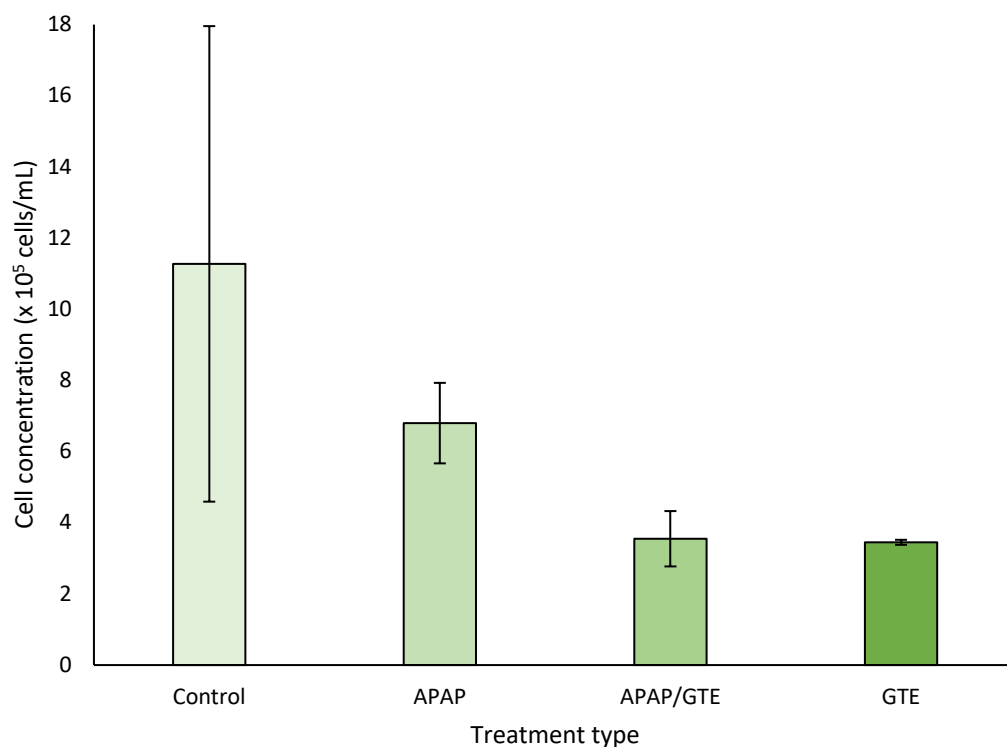


Figure 3.10. HepG2 cell concentration following exposure to 15 mM APAP, a combination of 15 mM APAP and 1 mg/mL GTE or 1 mg/mL GTE for 24 h compared to untreated controls (n = 2 for each sample group). Error bars indicate standard deviation.

### 3.4.2 Metabolomic analysis

PCA was used to compare the three treatment groups with untreated controls (Figure 3.11). Controls and APAP-treated cells demonstrated a difference in metabolite profile compared to the GTE- and APAP/GTE-treated cells, with 22% of the observed variance explained by PC-1 and 16% by PC-2. No variance between the GTE and APAP/GTE treatment groups was able to be determined from the PCA plots, nor between the controls and APAP-treated samples.

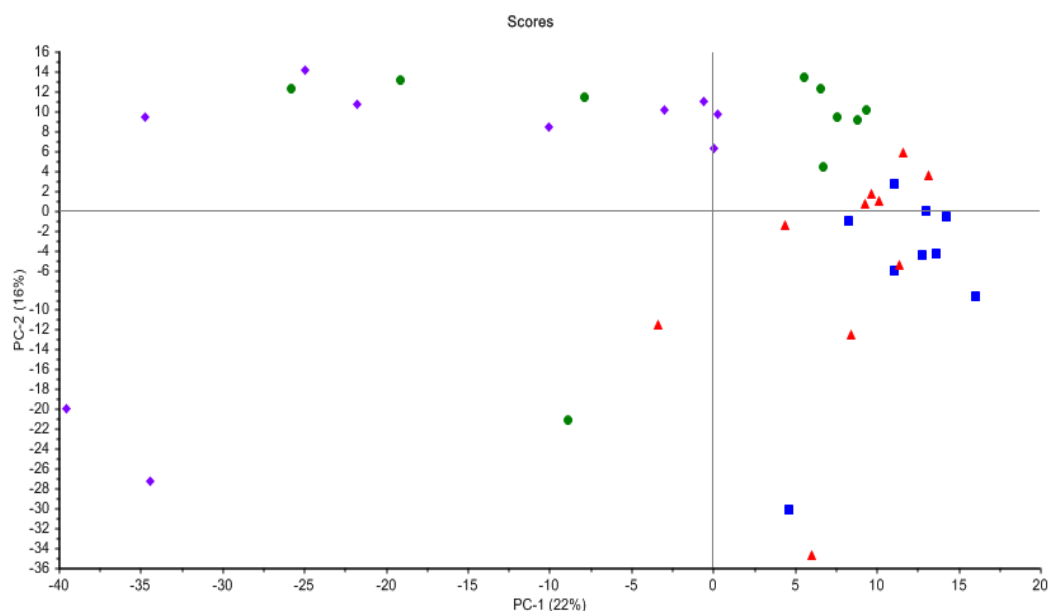


Figure 3.11. PCA scores plot using the first two principal components for comparison of HepG2 cell metabolite profile of untreated controls (blue) to cells exposed to 1 mg/mL GTE (green), 15 mM APAP/1 mg/mL GTE (purple) or 15 mM APAP (red) for 24 h, as measured by GC-MS analysis (n = 10 for each sample group). A difference was observed between the metabolite profiles of untreated controls and APAP-treated cells compared to GTE and the combined APAP/GTE treatment groups. No difference was observed in the metabolite profile of untreated cells compared to APAP-treated cells via PCA, nor between the GTE-treated cells compared to the combined treatment group.

The PLS-DA scores plot comparing the GTE-treatment group with untreated cells showed a difference in metabolite profile, 24% and 75% of which was explained by factor-1 (Figure 3.12a). Additionally, a difference was observed between untreated cells and the combined treatment group across factor-1, with 15% and 71% of the variance explained (Figure 3.12b). Most notably, a difference in metabolite profile was observed when the untreated cells were compared with the APAP treatment group, which had been difficult to distinguish in the PCA scores plot (Figure 3.12c). The variance observed here was explained 15% and 71% by factor-1.

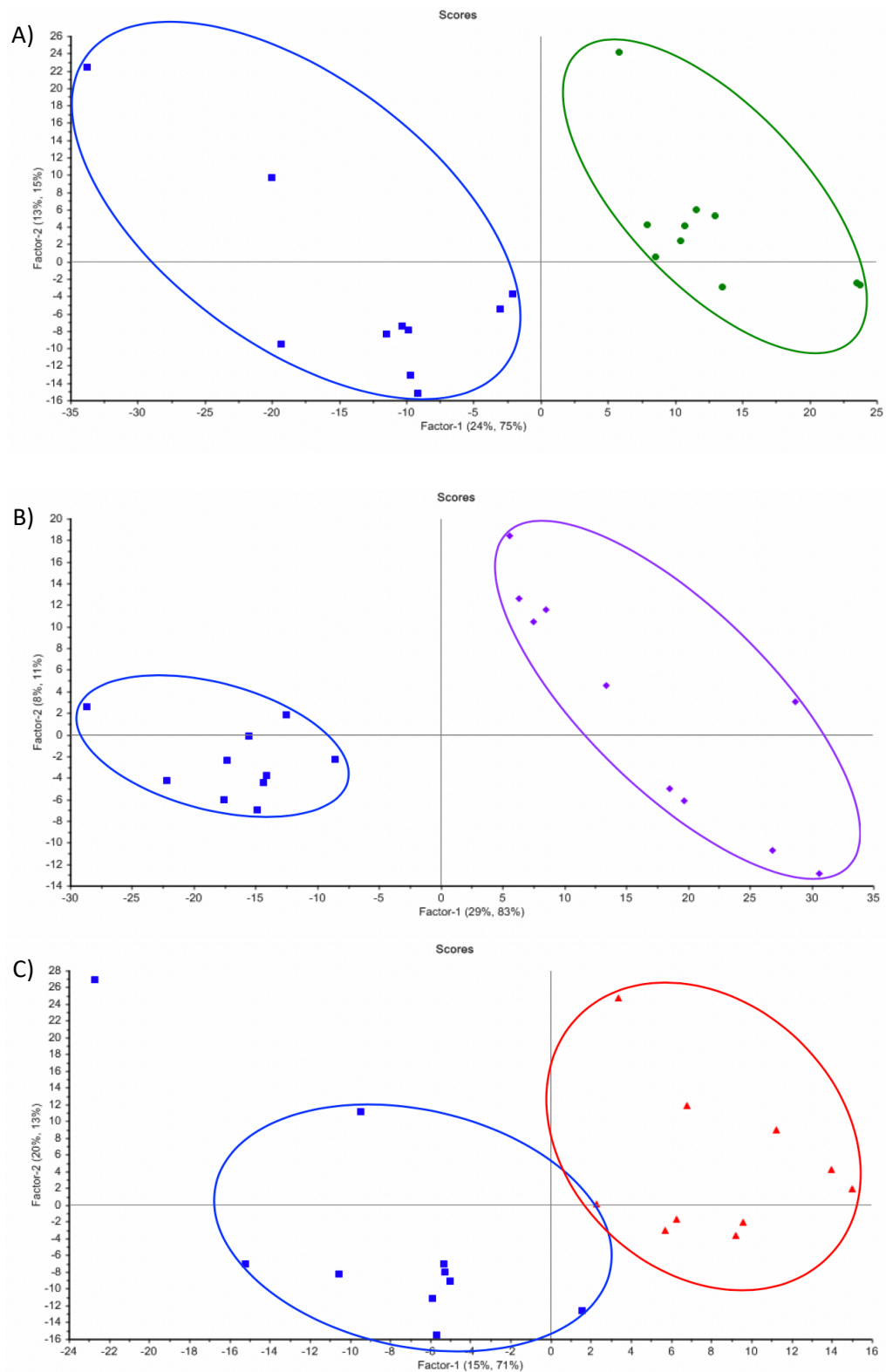


Figure 3.12. PLS-DA scores plots using the first two principal components (factors) for comparison of HepG2 cell metabolite profile in untreated controls (blue) to cells treated with: A) 1 mg/mL GTE (green), B) 15 mM APAP/1 mg/mL GTE (purple), and C) 15 mM APAP (red), as measured by GC-MS analysis (n = 10 for each sample group).

Two PLS-DA scores plots were produced comparing GTE-treated cells with the APAP and APAP/GTE treatment groups, with a difference in metabolite profile being observed in both. The difference observed between the GTE-treatment group and APAP-treated cells was 20% and 59% explained by factor-1 (Figure 3.13a). When comparing the GTE-treated cells with the combined treatment group, the difference observed was primarily across factor-1, with 26% and 46% of the variance explained (Figure 3.13b).

Finally, an additional PLS-DA scores plot was constructed to compare APAP-treated cells with the combined treatment group. A difference in metabolite profile was again observed across factor-1, with 27% and 74% of the variance explained (Figure 3.13c).

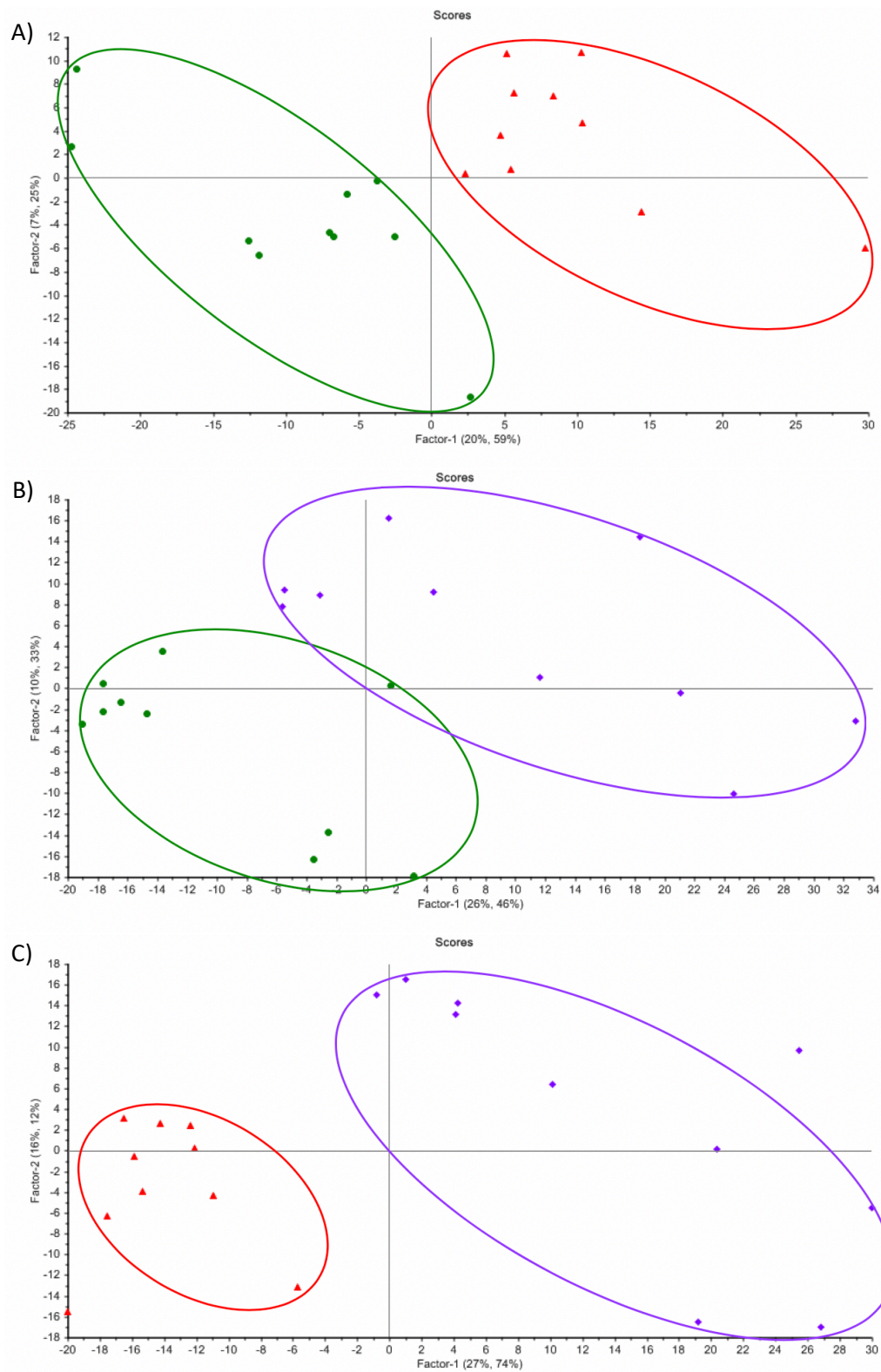


Figure 3.13. PLS-DA scores plots using the first two principal components (factors) for comparison of HepG2 cell metabolite profiles following treatment with: A) 1 mg/mL GTE (green) vs. 15 mM APAP (red), B) 1 mg/mL GTE vs. 15 mM APAP/1 mg/mL GTE (purple), and C) 15 mM APAP vs. 15 mM APAP/1 mg/mL GTE, as measured by GC-MS analysis (n = 10 for each sample group).



The PLS-DA X-loadings were used with a threshold of +/- 0.05 to identify the 34 compounds contributing most to the variance between the sample groups (Figure S3, S4). When compared to the NIST library, 22 of these compounds met at least 2 of the 3 criteria defined in section 2.3.4.3 and thus were putatively deemed a match. After removing the compounds that were likely to be solvent-derived, 17 metabolites remained.

Based on these 17 metabolites, a significant difference was observed between the profiles of untreated controls compared to GTE-treated cells ( $p=.001$ ), and also between the controls and combined treatment group ( $p<.001$ ) (Figure S5). Additionally, the metabolite profile of APAP-treated cells differed significantly from the GTE and combined treatment groups ( $p=.006$  and  $<.001$ , respectively). No significant difference was observed between the controls and APAP-treated cells ( $p=.540$ ), nor between the GTE and APAP/GTE treatment groups ( $p=.117$ ).

Of these 17 metabolites, 10 demonstrated a positive fold-change in comparison to the same compounds from control samples and 5 had a negative fold-change (Table 3.3). The remaining 2 metabolites had mixed fold-changes across the treatment groups, however both of these were positive in the GTE-treated cells. Alanine demonstrated a negative fold-change in the APAP/GTE and APAP treatment groups, whilst myo-inositol had a negative fold-change in the APAP/GTE-treated cells and a positive fold-change in the APAP sample group. Of the amino acids, carbohydrates and fatty acids, the largest fold-changes were observed in  $\beta$ -alanine (GTE: 21.97, GTE/APAP: 21.23, APAP: 9.32), D-mannose (GTE: 2.64) and stearic acid (GTE: 5.51,

GTE/APAP: 6.98), respectively. All metabolites were found to differ significantly between sample groups, with the exception of alanine.

Table 3.3. Fold change observed in metabolites of HepG2 cells post-exposure to 1 mg/mL GTE, a combination of 15 mM APAP/1 mg/mL GTE or 15 mM APAP compared to untreated controls (n = 10 for each sample group). Changes were primarily observed in amino acids and fatty acids. Green arrows indicate a positive-fold change compared to untreated controls and red arrows indicate a negative fold-change. \*Metabolite differed significantly between sample groups, as determined by the Kruskal-Wallis test ( $p < .05$ ). †NIST match only met 2 of 3 match criteria outlined in section 2.4.4.3.

Metabolite	GTE	APAP/GTE	APAP
<b>Amino acids</b>			
β-Alanine*	↑ 21.97	↑ 21.23	↑ 9.32
Alanine†	↑ 1.14	↓ 0.60	↓ 0.86
L-Threonine*	↓ 0.67	↓ 0.19	-
Serine*	↓ 0.61	↓ 0.30	-
L-Glutamic acid*	↓ 0.47	↓ 0.08	-
L-Lysine*	-	↓ 0.41	-
L-Isoleucine*	↓ 0.30	↓ 0.12	-
<b>Carbohydrates</b>			
D-Mannose*†	↑ 2.64	-	-
Myo-inositol*	↑ 1.06	↓ 0.53	↑ 6.39
<b>Fatty acids</b>			
Unidentified short-chain fatty acid*†	↑ 9.60	↑ 10.48	↑ 1.74
Stearic acid*	↑ 5.51	↑ 6.98	-
Oleic acid*	↑ 5.10	↑ 7.13	-
Palmitic acid*	↑ 4.84	↑ 7.02	-
Arachidonic acid*	↑ 4.12	↑ 3.53	↑ 1.54
<b>Other</b>			
Unidentified piperidine derivative*	↑ 9.16	↑ 8.64	↑ 2.04
Pipecolic acid*	↑ 5.02	↑ 3.43	↑ 2.19
Cholesterol*	↑ 3.39	↑ 3.03	↑ 1.62

A large positive fold-change was observed in  $\beta$ -alanine across all three treatment groups, most notably in the GTE- and APAP/GTE-treated cells (>20-fold).  $\beta$ -alanine is a non-proteinogenic amino acid that is commonly metabolised to aspartic acid under normal conditions.<sup>122</sup> In circumstances of increased energy demand,  $\beta$ -alanine can be converted into alanine and malonate semialdehyde: alanine can then be converted into pyruvate and fed into the TCA cycle; malonate semialdehyde can be converted to malonate, followed by malonyl CoA which then contributes to fatty acid synthesis.<sup>122, 124</sup>  $\beta$ -alanine is also the rate-limiting precursor to the reactive oxygen species (ROS) scavenger carnosine, and it can be produced as a result of catabolism of pyrimidine nucleotides such as cytosine and uracil, which may occur as a result of DNA or RNA degradation.<sup>122, 124, 131</sup> The positive fold-change observed here most likely reflects  $\beta$ -alanine production via pyrimidine catabolism in response to increased cellular demand for carnosine or as a result of DNA and RNA degradation, either of which could be due to oxidative stress. Some  $\beta$ -alanine present in the cells may have undergone conversion to alanine and malonate semialdehyde, which may explain the positive fold-change in alanine observed in the GTE-treated cells.

The amino acids L-threonine, serine, L-glutamic acid and L-isoleucine demonstrated a negative fold-change in GTE- and APAP/GTE-treated cells, and alanine demonstrated a negative fold-change in the APAP/GTE- and APAP-treated cells. This negative fold-change in amino acids could reflect a demand for alternative energy sources within the cells due to carbohydrate depletion or malfunction of the glycolytic pathway.<sup>122</sup> Alanine, threonine, serine, glutamine and glutamic acid can all be converted into pyruvate and fed directly into the TCA cycle, allowing oxidative

phosphorylation to continue whilst bypassing glycolysis.<sup>122, 124</sup> Additionally, isoleucine can be converted into acetyl CoA and fed directly into the TCA cycle.<sup>122, 124</sup> Thus, a reduction in these amino acids likely indicates a cellular demand for non-carbohydrate energy sources in order to continue producing ATP whilst bypassing glycolysis. A positive fold-change was observed in the carbohydrates D-mannose and myo-inositol, contributing to the theory that treated cells may have lost the ability to use carbohydrates as an energy source. Aside from its use as an energy source, serine has been demonstrated to have an antioxidant role, thus it is possible that a negative fold-change in this amino acid could be due to its consumption as a free radical scavenger.<sup>127</sup>

A negative fold-change in L-lysine was observed in the combined treatment group, which can be converted into acetyl CoA via the saccharopine pathway to be utilised in the TCA cycle.<sup>122, 124</sup> Thus, as with the other amino acids found to have a negative fold-change in treated cells, it is possible that L-lysine was being used as an alternative energy source by the cells. All three treatment groups demonstrated a positive fold-change in pipercolic acid, a metabolite of lysine, supporting the theory that lysine was being degraded in the cells.<sup>122</sup>

As outlined previously, myo-inositol is an integral component of inositol phosphates, secondary messengers involved in cellular signal transduction.<sup>128, 129</sup> For example, InsP3 RI-dependent  $Ca^{2+}$  signalling has been found to play a role in the early stages of liver regeneration and the IRE1 $\alpha$  regulation of hepatocyte proliferation via control of STAT3; therefore, it is possible that the positive fold-change observed in the GTE and APAP treatment groups reflects hepatocyte regeneration in response to GTE-

induced hepatotoxicity.<sup>128, 129</sup> The APAP/GTE treatment group demonstrated a negative fold-change in this compound, which may indicate consumption or depletion of inositol within the cells due to increased cytotoxicity.

A positive fold-change was observed in stearic acid, oleic acid and palmitic acid in GTE- and APAP/GTE-treated cells, along with arachidonic acid and an unidentified short-chain fatty acid in all treatment groups. Cholesterol also demonstrated a positive fold-change in cells from all treatment groups. As outlined previously, lipid peroxidation resulting in disruption to cell membranes can occur during oxidative stress, thus the positive fold-changes observed in cholesterol and fatty acids may be a result of membrane degradation.<sup>130</sup> Additionally, it is possible that the positive fold-change in arachidonic acid may in part be due to an inflammatory response occurring within the cells.<sup>121</sup>

## 4. General discussion

### 4.1. GTE-induced oxidative stress

This study has demonstrated that GTE induces hepatotoxicity in HepG2 cells, inducing a wide range of biochemical changes which ultimately led to a decrease in cell concentration. Cells treated with GTE, GTE metabolites (GTEM) or a combination of APAP and GTE all demonstrated a loss in cell viability and changes in key cellular components, such as amino acids, fatty acids and carbohydrates. Given that the rise in herbal complementary and alternative medicine (HCAM) usage is showing no signs of slowing and that GTE is already very popular, the findings are particularly concerning and further contribute to the growing body of research suggesting that GTE is capable of causing herb-induced liver injury (HILI).<sup>1, 81, 95, 98</sup>

The biochemical changes observed in this study were suggestive of lipid peroxidation and membrane damage, pyrimidine and protein degradation, increased cellular requirement for non-carbohydrate energy sources and disruption to glycolysis and potentially the TCA cycle, of which the latter may have occurred as a result of mitochondrial dysfunction.<sup>121, 122, 124</sup> The changes observed in  $\beta$ -alanine may also reflect an increase in demand for the ROS scavenger carnosine.<sup>122, 124, 131</sup> Additionally, the changes observed in myo-inositol suggests that an increase in inositol signalling was occurring, potentially in an attempt to carry out cellular repair and regeneration.<sup>128, 129</sup> These biochemical pathways are commonly disrupted during oxidative stress, suggesting that the hepatocytes entered a pro-oxidant state.<sup>132, 133</sup> These findings are consistent with previous studies which have implicated oxidative stress in GTE-induced hepatotoxicity.<sup>40, 46, 95, 98, 99</sup>

Oxidative stress is characterised by an imbalance between free radicals and the antioxidants within the cell, and is commonly implicated in cytotoxicity and other disease processes.<sup>133, 134</sup> Free radicals, such as ROS and reactive nitrogen species (RNS), are pro-oxidant molecules which are highly reactive due to the presence of at least one unpaired electron.<sup>134</sup> In healthy cells, free radicals can be produced endogenously as by-products of processes such as aerobic respiration and at low concentrations have a number of beneficial physiological roles.<sup>134</sup> Antioxidants protect the cells by preventing or repairing free radical damage.<sup>133, 134</sup> During oxidative stress there is an overproduction of ROS and RNS or a deficiency in cellular antioxidants (or both), resulting in the inability to sufficiently neutralise free radicals and ultimately leading to the oxidation of important cellular molecules, such as lipids, proteins and nucleic acids, as observed in this study.<sup>132-134</sup> Eventually, when cellular damage is beyond repair, oxidative stress leads to cell death; this may explain the significant decrease in cell concentration observed in the GTE, GTEM and APAP/GTE treatment groups. Future studies should measure oxidative stress in GTE-treated HepG2 cells in order to confirm that this process was occurring in the cells analysed in this study.

To further investigate the role of oxidative stress in GTE-induced hepatotoxicity, direct or indirect approaches could be used to measure oxidative stress *in vitro* using markers such as ROS, lipid peroxidation, antioxidants, damage to DNA or RNA and oxidation or nitration of proteins.<sup>132</sup> An example of a direct method commonly used to assess oxidative stress is the dichlorodihydrofluorescein diacetate (DCFDA) assay, which can be used to measure ROS, such as hydrogen peroxide, in cells.<sup>133, 135</sup> DCFDA passively diffuses into cells and is subsequently hydrolysed to DCFH, which then



reacts with ROS to produce DCF as a fluorescent product.<sup>133, 135</sup> This can be measured using flow cytometry or a microplate reader, with the intensity of fluorescence giving an indication of ROS levels, and therefore oxidative stress, within cells.<sup>133, 135</sup> The major limitation of using ROS as a measure of oxidative stress is their transient nature, which may hinder the accuracy and precision of the results; this can be overcome by analysing oxidative damage, such as protein carbonyl content or lipid peroxidation, as an indirect measure of oxidative stress.<sup>132, 133</sup>

A wide range of assays have been developed for the analysis of oxidative damage; for example, the thiobarbituric acid-reactive substances (TBARS) assay is a popular approach used to measure lipid peroxidation via the use of malondialdehyde (MDA) as a marker.<sup>132, 133, 136</sup> In this assay, a conjugate is formed between thiobarbituric acid and MDA, which can be separated from other thiobarbituric acid conjugates using techniques such as high performance liquid chromatography (HPLC) and measured using fluorescence with the result giving an indication of lipid peroxidation within the cell.<sup>133, 136</sup> The positive fold-change in fatty acids observed in this study possibly indicates lipid peroxidation, thus it may be useful to couple the TBARS assay with the DCFDA assay to confirm that GTE, GTEM and APAP/GTE treatments induce oxidative stress in HepG2 cells, an approach that has previously been used to assess this mechanism in this cell line.<sup>137, 138</sup>

The observed changes in amino acids and carbohydrates in the GTEM, APAP/GTE and both GTE treatment groups may also be indicative of a disruption in cellular respiration. Disruption to glycolysis in response to GTE has previously been described in the literature, with a 2016 paper suggesting that epigallocatechin-3-gallate (EGCG)

directly inhibits phosphofructokinase.<sup>100, 101</sup> The change in citric acid, or citrate at biological pH, observed in the GTEM and first GTE treatment groups suggests a possible disruption in the TCA cycle, leading to the accumulation of this intermediate.<sup>121</sup> This suggests that the mitochondria may have been affected in GTE- and GTEM-treated cells. Mitochondrial dysfunction is commonly implicated in oxidative stress, and it has previously been found that the mitochondria may be a target for GTE constituents such as EGCG, with the resulting mitochondrial dysfunction and elevated antioxidant response being suggested as possible contributors to GTE-induced hepatotoxicity.<sup>40</sup>

To confirm whether mitochondrial damage occurred, an assay such as the cellular ATP glucose-galactose shift assay may be used.<sup>139</sup> Despite the reported reduced galactose metabolism in HepG2 cells, recent modifications to this assay have enhanced its sensitivity and specificity, thus enhancing the reliability of its results.<sup>139</sup> Whilst assays tend to be the most commonly adopted approach to measuring oxidative stress and mitochondrial dysfunction, metabolomic analysis has demonstrated promise in recent years with the potential to provide more sensitive and specific results via the use of HPLC, LC-MS/MS and GC-MS.<sup>136, 140</sup> The cellular disturbances suspected to occur in HepG2 cells following exposure to various treatments of GTE are summarised in Figure 4.1.

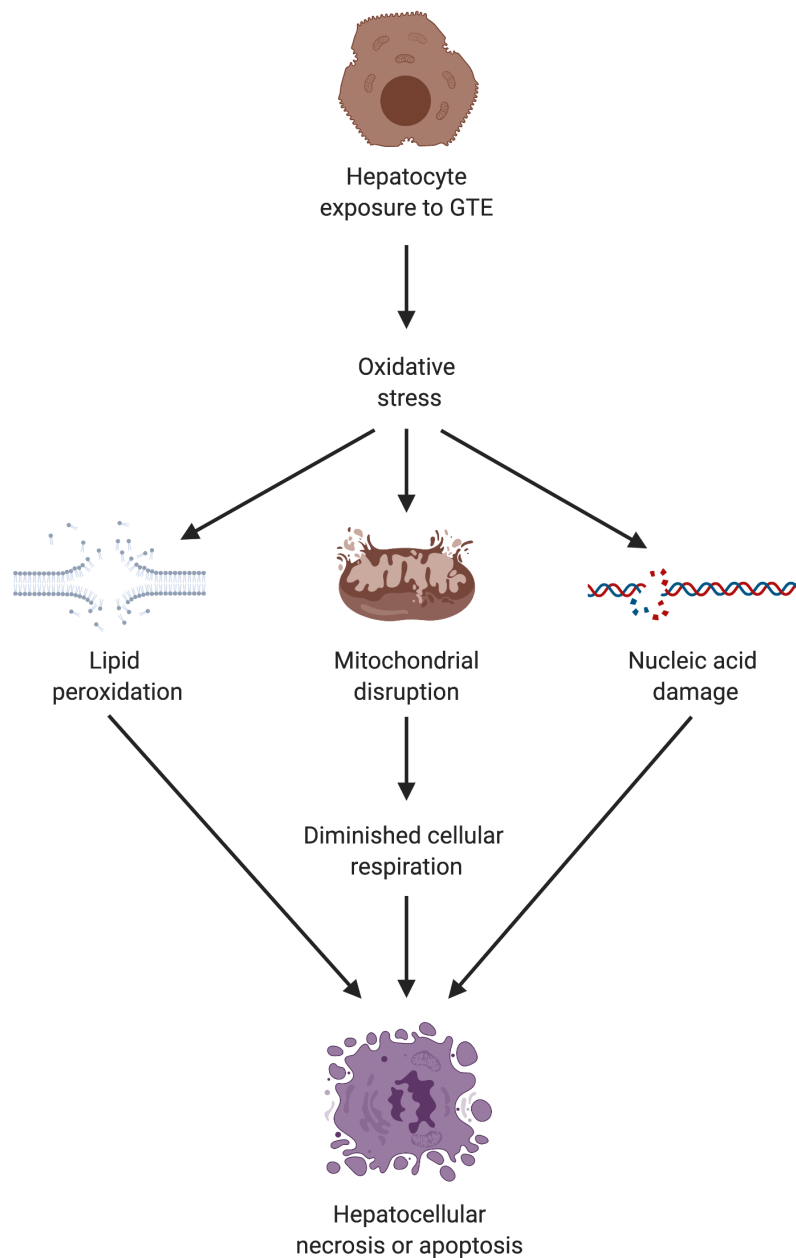


Figure 4.1. Summary of cellular disturbances suspected to occur during GTE-induced hepatotoxicity based on the data from this study. Created with BioRender.com.

## 4.2 GTE metabolites

Given that, aside from gallic acid, the suspected GTE metabolites were unable to be putatively identified in the timeframe of this study, further analysis is required to determine the identity of these compounds. A 2019 paper described the use of LC-

MS and nuclear magnetic resonance (NMR) spectroscopy to characterise variations in metabolite profile amongst cranberry supplements, thus a method similar to this would be ideal for the isolation and identification of the compounds in metabolised GTE samples.<sup>141, 142</sup> The extent to which GTE was metabolised by S9 human liver fraction in the 1-h reaction period used in this study was not determined. Given that NMR signal intensity is directly proportional to the concentration of a given metabolite, it is inherently quantitative and so could also be used to determine the extent of GTE metabolism based on concentration of unmetabolised GTE constituents prior to commencing the reaction compared to the amount remaining at its conclusion.<sup>142</sup> The information obtained from these metabolomic analyses could subsequently be used to determine the likelihood of a given compound being a GTE metabolite.

The upper  $m/z$  limit of 1000 of the instrument used in this study may have inhibited the detection of larger GTE metabolites. For example, EGCG has a  $m/z$  of 648, making it possible that conjugated metabolites of EGCG may have been too large to be detected, thus reducing the number of compounds identified in the metabolised GTE samples.<sup>143</sup> If the GTE metabolites produced in this study were to be characterised using LC-MS and NMR, the potential for large EGCG metabolites should be considered and modifications made in order to obtain the most comprehensive results.

Another limitation to this section of the study was that it is possible that the metabolism carried out using S9 human liver fraction was not a complete representation of the metabolic processes normally carried out in hepatocytes *in*

*vivo*. Additionally, GTE constituents such as catechins have been shown to undergo extensive microbial metabolism in the intestine prior to absorption.<sup>61</sup> It has also been found that catechins may be metabolised via methylation and sulfation in enterocytes prior to being absorbed into the portal vein.<sup>59, 62</sup> These microbial and intestinal GTE metabolites are inevitably different to those produced by hepatocytes, thus it is possible that these conjugations may have a different level of toxicity to those observed in this study.<sup>59, 61, 62</sup> It is also possible that hepatocytes are predominantly exposed to microbial and intestinal metabolites of GTE, and not the unmetabolised constituents analysed in this study, therefore further analysis is required to examine the toxicity of these metabolites in an effort to more comprehensively understand the compounds to which hepatocytes are exposed *in vivo* following ingestion of GTE.

### 4.3 Future considerations

This project had a number of limitations that may have impacted the *in vivo* relevance of the results obtained and which should be considered in future studies. The doses used in this study were chosen after having been demonstrated to induce cytotoxicity and were therefore not necessarily pharmacologically relevant.<sup>26, 117</sup> Whilst this allowed for the assessment of which biochemical pathways may have been affected in hepatocytes during GTE-induced hepatotoxicity, it may not be completely demonstrative of what occurs in individuals who develop liver damage in response to this HCAM. The length of treatment must also be taken into account when considering dosage; due to the limited timeframe, this study focused on acute, high doses in order to elicit a timely toxic response. Future studies should use

pharmacological doses and chronic exposure periods in order to better represent the conditions under which cases of GTE-induced liver damage have manifested.<sup>3, 4</sup>

Bioavailability must also be taken into consideration, given the low oral bioavailability previously demonstrated in GTE components such as catechins, particularly when consumed in a fed state.<sup>33</sup> Additionally, microbial metabolism of catechins results in a variety of conjugations and thus may impact their overall bioavailability.<sup>61</sup> It is therefore likely that the GTE components and metabolites to which cells were exposed in this study were not a complete representation of what they may come into contact with *in vivo*.

Whilst analysing hepatocyte metabolism *in vitro* is achievable, it is not possible to completely assess the pharmacokinetics of GTE using this model. Understanding the absorption, distribution and excretion of GTE constituents and metabolites in addition to their metabolism will be paramount to understanding and predicting the risk of toxicity induced by GTE, or other herbal medicines, in certain individuals.

In addition to the pharmacology of GTE and its constituents, there are other factors which may contribute to the toxicity observed in certain individuals which could not be sufficiently examined in the timeframe of this study. For example, it has been demonstrated that the contamination and adulteration of herbal supplements is not only possible, but rife among these products.<sup>12, 144</sup> Given that in many instances of liver damage the GTE product consumed has not been available for testing, it is difficult to rule out contamination or adulteration of these products leading to the liver damage reported. Given that this study did not characterise the composition of

the GTE product prior to cell exposures, contamination or adulteration cannot be ruled out as a possible contributor to the cytotoxicity observed.

Genetic variation may also play a role in determining which individuals may be more predisposed to developing a liver injury when consuming GTE.<sup>34, 35, 86</sup> For example, polymorphisms resulting in altered function or abundance of the enzymes responsible for the biotransformation of catechins may increase the likelihood of hepatotoxicity due to the potentially toxic accumulation of these compounds or the increased production of toxic metabolites.<sup>34</sup> Additionally, changes in the proteins involved in Phase III detoxification could limit the clearance of catechins and metabolites from the liver, causing them to build up, potentially resulting in hepatotoxicity.<sup>24, 25</sup> Future studies should examine whether any common genetic abnormalities are able to be identified amongst individuals who develop liver injury following supplementation with this HCAM.

Co-medication with other herbal supplements or drugs could result in herb-herb or herb-drug interactions, which may contribute to certain individuals being more susceptible to developing GTE-induced liver damage.<sup>16, 17</sup> In fact, a number of cases of liver damage in which GTE was identified as the most likely culprit have been in individuals using a supplement which contained GTE as one of many ingredients.<sup>4</sup> It is possible that GTE could interact with other components present in these products to cause liver injury, and may not be as damaging when consumed in isolation at a safe dosage. Further research should be conducted in order to determine the composition of these products and whether the hepatotoxicity of these substances can really be narrowed down to a single component.

If this study were to be repeated, it may also be beneficial to use a different hepatocyte cell line, such as HepaRG. It is well established that HepG2 cell responses are not completely comparable to *in vivo* hepatocyte responses; for example, the diminished function of the CYP450 enzymes is a particular setback when assessing toxicity with this cell line.<sup>5</sup> HepaRG cells are an immortalised cell line which have retained metabolic function, therefore these may be a better choice in future.<sup>5</sup> Additionally, using 3D cultures that include non-parenchymal liver cells may produce results more comparable to *in vivo* responses than the traditional 2D culture used in this study, given that they allow more complex cell-cell interactions.<sup>145</sup> Of course, the gold standard would be to obtain primary human hepatocyte cultures, however this is unlikely to be an option until further evidence is gathered.<sup>5, 145</sup>

A major challenge with GC-MS analysis is the formation of multiple derivatisation products. This makes it challenging to gain a complete understanding of a given metabolic profile due to the production of multiple results for the same compound. In this study, the method of overcoming this without further analysis was to select the result that appeared to contribute most to the variation between samples, and disregard the others. This is flawed and thus it would be more suitable to conduct further analysis using other forms of metabolomic analysis such as LC-MS and NMR spectroscopy, the complementarity of which was discussed in a 2018 systematic review.<sup>5</sup>

#### 4.4 Conclusion

This study used *in vitro* techniques to analyse the hepatotoxicity of GTE and has demonstrated that this supplement is capable of causing HILI. Whilst this study only



analysed one GTE product available on the Australian market, it has highlighted the potential risk this supplement poses to consumer health. The results indicated that disruption to cellular respiration, proteins, nucleic acids and lipids were likely to have occurred in HepG2 cells following exposure to a range of GTE treatments, contributing to the growing body of evidence which suggests that GTE-induced hepatotoxicity occurs as a result of oxidative stress.<sup>40, 98, 99</sup> Cells treated with metabolised GTE appeared to be less affected than those exposed to unmetabolised GTE, suggesting that the metabolism of GTE renders toxic parent compounds inert.

In addition to determining the biochemical changes induced by GTE and the extent to which this is mediated by GTE metabolites, this study has also demonstrated that metabolomics is an effective and comprehensive tool for toxicological analysis. Using the method described in this study, it was possible to not only determine the end-point toxicity but also provide insight into the mechanisms most likely driving the loss of cell viability observed in response to treatment with this herbal supplement. Metabolomics is therefore a valuable technique which should be incorporated into future studies investigating *in vitro* toxicology.

This study focused on GTE, one of a number of HCAMs implicated in increasing cases of liver damage worldwide; particularly concerning given that consumers often purchase these herbal medicines in the belief that their natural origin is synonymous with them being safe. It is therefore imperative that appropriate steps are taken to ensure that the right measures are in place to prevent adverse reactions to HCAMs, such as the GTE-induced hepatotoxicity observed in this study, from continuing to contribute to morbidity and mortality in the Australian community.

## 5. References

1. Australian National Audit Office. Therapeutic Goods Administration: complementary medicines [document on the Internet]. 2011 [cited 2019 Mar 4]. Available from: <https://www.anao.gov.au/sites/default/files/201112%20Audit%20Report%20No%2003.pdf>.
2. National Institutes of Health. LiverTox [document on the Internet]. 2018 [cited 2019 Mar 22]. Available from: <https://livertox.nih.gov>.
3. Mazzanti G, Menniti-Ippolito F, Moro PA, et al. Hepatotoxicity from green tea: a review of the literature and two unpublished cases. *Eur J Clin Pharmacol*. 2009;65(4):331-41. doi:10.1007/s00228-008-0610-7
4. Mazzanti G, Di Sotto A and Vitalone A. Hepatotoxicity of green tea: an update. *Arch Toxicol*. 2015;89(8):1175-91. doi:10.1007/s00204-015-1521-x
5. Cuykx M, Rodrigues RM, Laukens K, Vanhaecke T and Covaci A. In vitro assessment of hepatotoxicity by metabolomics: a review. *Arch Toxicol*. 2018;92(10):3007-29. doi:10.1007/s00204-018-2286-9
6. Australian Medical Association. AMA position statement - complementary medicine - 2018 [document on the Internet]. 2018 [cited 2019 Feb 25]. Available from: <https://ama.com.au/position-statement/ama-position-statement-complementary-medicine-2018>.
7. World Health Organization. WHO guidelines for assessing quality of herbal medicines with reference to contaminants and residues [document on the Internet]. 2007 [cited 2019 Feb 27]. Available from:

[https://apps.who.int/iris/bitstream/handle/10665/43510/9789241594448\\_eng.pdf?sequence=1&isAllowed=y](https://apps.who.int/iris/bitstream/handle/10665/43510/9789241594448_eng.pdf?sequence=1&isAllowed=y).

8. Complementary Medicines Australia. Annual Report 2017-2018 [document on the Internet]. 2018 [cited 2019 Mar 2]. Available from: <http://cmaustralia.org.au/resources/Documents/Annual%20Report/Final%20CMA%20Annual%20Report%202018v1.pdf>.

9. Therapeutic Goods Administration. Australian regulatory guidelines for complementary medicines [document on the Internet]. 2018 [cited 2019 Feb 25]. Available from: <https://www.tga.gov.au/publication/australian-regulatory-guidelines-complementary-medicines-argcm>.

10. Therapeutic Goods Administration. Equivalence of herbal extracts in complementary medicines [document on the Internet]. 2011 [cited 2019 Feb 26]. Available from: <https://www.tga.gov.au/equivalence-herbal-extracts-complementary-medicines>.

11. Therapeutic Goods Administration. Half yearly performance snapshot: July to December 2017 [document on the Internet]. 2017 [cited 2019 Mar 2]. Available from: <https://www.tga.gov.au/half-yearly-performance-snapshot-july-december-2017>.

12. Coghlan ML, Maker G, Crighton E, et al. Combined DNA, toxicological and heavy metal analyses provides an auditing toolkit to improve pharmacovigilance of traditional Chinese medicine (TCM). *Sci Rep*. 2015;5:17475. doi:10.1038/srep17475

13. Booker A, Agapouda A, Frommenwiler DA, Scotti F, Reich E and Heinrich M. St John's wort (*Hypericum perforatum*) products – an assessment of their authenticity and quality. *Phytomedicine*. 2018;40:158-64. doi:10.1016/j.phymed.2017.12.012

14. Huo H, Liu Y, Liu W, et al. A full solution for multi-component quantification-oriented quality assessment of herbal medicines, Chinese agarwood as a case. *J Chromatogr A*. 2018;1558:37-49. doi:10.1016/j.chroma.2018.05.018
15. Liu J, Zhang Q, Liu M, Ma L, Shi Y and Ruan J. Metabolomic analyses reveal distinct change of metabolites and quality of green tea during the short duration of a single spring season. *J Agric Food Chem*. 2016;64(16):3302-9. doi:10.1021/acs.jafc.6b00404
16. Ben-Arye E, Attias S, Levy I, Goldstein L and Schiff E. Mind the gap: disclosure of dietary supplement use to hospital and family physicians. *Patient Educ Couns*. 2017;100(1):98-103. doi:10.1016/j.pec.2016.07.037
17. Levy I, Attias S, Ben-Arye E, Goldstein L and Schiff E. Adverse events associated with interactions with dietary and herbal supplements among inpatients. *Br J Clin Pharmacol*. 2017;83(4):836-45. doi:10.1111/bcp.13158
18. Benedetti MS, Whomsley R, Poggesi I, et al. Drug metabolism and pharmacokinetics. *Drug Metab Rev*. 2009;41(3):344-90. doi:10.1080/10837450902891295
19. Almazroo OA, Miah MK and Venkataramanan R. Drug metabolism in the liver. *Clin Liver Dis*. 2017;21(1):1-20. doi:10.1016/j.cld.2016.08.001
20. Melchart D, Hager S, Albrecht S, Dai J, Weidenhammer W and Teschke R. Herbal Traditional Chinese Medicine and suspected liver injury: a prospective study. *World J Hepatol*. 2017;9(29):1141-57. doi:10.4254/wjh.v9.i29.1141
21. Wong LL, Lacar L, Roytman M and Orloff SL. Urgent liver transplantation for dietary supplements: an under-recognized problem. *Transplant Proc*. 2017;49(2):322-5. doi:10.1016/j.transproceed.2016.11.041

22. Byeon J-H, Kil J-H, Ahn Y-C and Son C-G. Systematic review of published data on herb induced liver injury. *J Ethnopharmacol.* 2019;233:190-6. doi:10.1016/j.jep.2019.01.006
23. Ishikawa T. The ATP-dependent glutathione S-conjugate export pump. *Trends Biochem Sci.* 1992;17(11):463-8. doi:10.1016/0968-0004(92)90489-V
24. Choi JH, Ahn BM, Yi J, et al. MRP2 haplotypes confer differential susceptibility to toxic liver injury. *Pharmacogenet Genomics.* 2007;17(6). doi:10.1097/01.fpc.0000236337.41799.b3
25. Dawson S, Stahl S, Paul N, Barber J and Kenna JG. In vitro inhibition of the bile salt export pump correlates with risk of cholestatic drug-induced liver injury in humans. *Drug Metab Dispos.* 2012;40(1):130. doi:10.1124/dmd.111.040758
26. Behrends V, Giskeødegård GF, Bravo-Santano N, Letek M and Keun HC. Acetaminophen cytotoxicity in HepG2 cells is associated with a decoupling of glycolysis from the TCA cycle, loss of NADPH production, and suppression of anabolism. *Archives of Toxicology.* 2019;93(2):341-53. doi:10.1007/s00204-018-2371-0
27. Ostapowicz G, Fontana RJ, Schiødt FV, et al. Results of a prospective study of acute liver failure at 17 tertiary care centers in the United States. *Ann Intern Med.* 2002;137(12):947-54. doi:10.7326/0003-4819-137-12-200212170-00007
28. Dag MS, Aydinli M Fau - Ozturk ZA, Ozturk Za Fau - Turkbeyler IH, et al. Drug- and herb-induced liver injury: a case series from a single center. *Turk J Gastroenterol.* 2014;25:41-5. doi:10.5152/tjg.2014.4486
29. Shehu AI, Ma X and Venkataramanan R. Mechanisms of drug-induced hepatotoxicity. *Clin Liver Dis.* 2017;21(1):35-54. doi:10.1016/j.cld.2016.08.002

30. Mosedale M and Watkins PB. Drug-induced liver injury: Advances in mechanistic understanding that will inform risk management. *Clin Pharmacol Ther.* 2017;101(4):469-80. doi:10.1002/cpt.564
31. Wang R, Qi X, Yoshida EM, et al. Clinical characteristics and outcomes of traditional Chinese medicine-induced liver injury: a systematic review. *Expert Rev Gastroenterol Hepatol.* 2018;12(4):425-34. doi:10.1080/17474124.2018.1427581
32. Lammers LA, Achterbergh R, van Schaik RHN, Romijn JA and Mathôt RAA. Effect of short-term fasting on systemic cytochrome P450-mediated drug metabolism in healthy subjects: a randomized, controlled, crossover study using a cocktail approach. *Clin pharmacokinet.* 2017;56(10):1231-44. doi:10.1007/s40262-017-0515-7
33. Chow HHS, Hakim IA, Vining DR, et al. Effects of dosing condition on the oral bioavailability of green tea catechins after single-dose administration of polyphenon E in healthy individuals. *Clin Cancer Res.* 2005;11(12):4627. doi:10.1158/1078-0432.CCR-04-2549
34. Nicoletti P, Aithal GP, Bjornsson ES, et al. Association of liver injury from specific drugs, or groups of drugs, with polymorphisms in HLA and other genes in a Genome-Wide Association Study. *Gastroenterology.* 2017;152(5):1078-89. doi:10.1053/j.gastro.2016.12.016
35. Polimanti R, Piacentini S, Manfellotto D and Fuciarelli M. Human genetic variation of CYP450 superfamily: analysis of functional diversity in worldwide populations. *Pharmacogenomics.* 2012;13(16):1951-60. doi:10.2217/pgs.12.163
36. Ariyoshi N, Iga Y, Hirata K, et al. Enhanced susceptibility of HLA-mediated Ticlopidine-induced idiosyncratic hepatotoxicity by CYP2B6 polymorphism in

- Japanese. *Drug Metab Pharmacokinet.* 2010;25(3):298-306.  
doi:10.2133/dmpk.25.298
37. Chalasani N, Bonkovsky HL, Fontana R, et al. Features and outcomes of 899 patients with drug-induced liver injury: the DILIN prospective study. *Gastroenterology.* 2015;148(7):1340-52.e7. doi:10.1053/j.gastro.2015.03.006
38. Hadi A, Pourmasoumi M, Kafeshani M, Karimian J, Maracy MR and Entezari MH. The effect of green tea and sour tea (*Hibiscus sabdariffa* L.) supplementation on oxidative stress and muscle damage in athletes. *J Diet Suppl.* 2017;14(3):346-57. doi:10.1080/19390211.2016.1237400
39. Jówko E, Długolecka B, Makaruk B and Cieśliński I. The effect of green tea extract supplementation on exercise-induced oxidative stress parameters in male sprinters. *Eu J Nutr.* 2015;54(5):783-91. doi:10.1007/s00394-014-0757-1
40. James KD, Kennett MJ and Lambert JD. Potential role of the mitochondria as a target for the hepatotoxic effects of (-)-epigallocatechin-3-gallate in mice. *Food Chem Toxicol.* 2018;111:302-9. doi:10.1016/j.fct.2017.11.029
41. Choi EJ, Chee K-M and Lee BH. Anti- and prooxidant effects of chronic quercetin administration in rats. *Eur J Pharmacol.* 2003;482(1):281-5. doi:10.1016/j.ejphar.2003.09.067
42. Hong M, Li S, Tan HY, et al. A network-based pharmacology study of the herb-induced liver injury potential of traditional hepatoprotective Chinese herbal medicines. *Molecules.* 2017;22(4):632. doi:10.3390/molecules22040632
43. Sakata R, Nakamura T, Torimura T, Ueno T and Sata M. Green tea with high-density catechins improves liver function and fat infiltration in non-alcoholic fatty

liver disease (NAFLD) patients: a double-blind placebo-controlled study. Intern J Mol Med. 2013;32:989-94. doi:10.3892/ijmm.2013.1503

44. Therapeutic Goods Administration. *Camellia sinensis* (green tea) extract: safety advisory - potential risk of harm to the liver [document on the Internet]. 2018 [cited Available from: <https://www.tga.gov.au/alert/camellia-sinensis-green-tea-extract>].

45. Smith RJ, Bertilone C and Robertson AG. Fulminant liver failure and transplantation after use of dietary supplements. Med J Aust. 2016;204(1):30-2. doi:10.5694/mja15.00816

46. El-Bakry HA, El-Sherif G and Rostom RM. Therapeutic dose of green tea extract provokes liver damage and exacerbates paracetamol-induced hepatotoxicity in rats through oxidative stress and caspase 3-dependent apoptosis. Biomed Pharmacother. 2017;96:798-811. doi:10.1016/j.biopha.2017.10.055

47. Lu Y, Sun J, Petrova K, et al. Metabolomics evaluation of the effects of green tea extract on acetaminophen-induced hepatotoxicity in mice. Food and Chemical Toxicology. 2013;62:707-21. doi:10.1016/j.fct.2013.09.025

48. Salminen WF, Yang X, Shi Q, Greenhaw J, Davis K and Ali AA. Green tea extract can potentiate acetaminophen-induced hepatotoxicity in mice. Food and Chemical Toxicology. 2012;50(5):1439-46. doi:10.1016/j.fct.2012.01.027

49. Hayat K, Iqbal H, Malik U, Bilal U and Mushtaq S. Tea and its consumption: benefits and risks. Crit Rev Food Sci Nutr. 2015;55(7):939-54. doi:10.1080/10408398.2012.678949

50. Koch W, Kukula-Koch W, Komsta Ł, Marzec Z, Szwerca W and Głowniak K. Green tea quality evaluation based on its catechins and metals composition in



combination with chemometric analysis. *Molecules*. 2018;23(7):1689.  
doi:10.3390/molecules23071689

51. Graham HN. Green tea composition, consumption, and polyphenol chemistry. *Prev Med*. 1992;21(3):334-50. doi:10.1016/0091-7435(92)90041-F

52. Dostal AM, Samavat H, Espejo L, Arikawa AY, Stendell-Hollis NR and Kurzer MS. Green tea extract and catechol-O-methyltransferase genotype modify fasting serum insulin and plasma adiponectin concentrations in a randomized controlled trial of overweight and obese postmenopausal women. *J Nutr*. 2016;146(1):38-45. doi:10.3945/jn.115.222414

53. Zheng Y, Toborek M and Hennig B. Epigallocatechin gallate-mediated protection against tumor necrosis factor- $\alpha$ -induced monocyte chemoattractant protein-1 expression is heme oxygenase-1 dependent. *Metabolism*. 2010;59(10):1528-35. doi:10.1016/j.metabol.2010.01.018

54. Stalmach A, Troufflard S, Serafini M and Crozier A. Absorption, metabolism and excretion of Choladi green tea flavan-3-ols by humans. *Mol Nutr Food Res*. 2009;53(S1):S44-S53. doi:10.1002/mnfr.200800169

55. Schröder L, Marahrens P, Koch JG, et al. Effects of green tea, matcha tea and their components epigallocatechin gallate and quercetin on MCF-7 and MDA-MB-231 breast carcinoma cells. *Oncol Rep*. 2019;41(1):387-96. doi:10.3892/or.2018.6789

56. Lambert JD, Sang S and Yang CS. Biotransformation of green tea polyphenols and the biological activities of those metabolites. *Mol Pharm*. 2007;4(6):819-25. doi:10.1021/mp700075m

57. Lu H, Meng X and Yang CS. Enzymology of methylation of tea catechins and inhibition of catechol-O-methyltransferase by (-)-epigallocatechin gallate. *Drug Metab Dispos.* 2003;31(5):572. doi:10.1124/dmd.31.5.572
58. Lu H, Meng X, Li C, et al. Glucuronides of tea catechins: enzymology of biosynthesis and biological activities. *Drug Metab Dispos.* 2003;31(4):452. doi:10.1124/dmd.31.4.452
59. Vaidyanathan JB and Walle T. Glucuronidation and sulfation of the tea flavonoid (-)-epicatechin by the human and rat enzymes. *Drug Metab Dispos.* 2002;30(8):897. doi:10.1124/dmd.30.8.897
60. Misaka S, Kawabe K, Onoue S, et al. Effects of green tea catechins on cytochrome P450 2B6, 2C8, 2C19, 2D6 and 3A activities in human liver and intestinal microsomes. *Drug Metab Pharmacokinet.* 2013;28(3):244-9. doi:10.2133/dmpk.DMPK-12-RG-101
61. Feng WY. Metabolism of green tea catechins: an overview. *Curr Drug Metab.* 2006;7(7):755-809. doi:10.2174/138920006778520552
62. Kuhnle G, Spencer JPE, Schroeter H, et al. Epicatechin and catechin are O-methylated and glucuronidated in the small intestine. *Biochem Biophys Res Commun.* 2000;277(2):507-12. doi:10.1006/bbrc.2000.3701
63. Ramadan G, El-Beih NM, Talaat RM and Abd El-Ghffar EA. Anti-inflammatory activity of green versus black tea aqueous extract in a rat model of human rheumatoid arthritis. *Int J Rheum Dis.* 2017;20(2):203-13. doi:10.1111/1756-185X.12666

64. Pang J, Zhang Z, Zheng T-z, et al. Green tea consumption and risk of cardiovascular and ischemic related diseases: a meta-analysis. *Int J Cardiol.* 2016;202:967-74. doi:10.1016/j.ijcard.2014.12.176
65. Akie H, Keizo O, Naotaka T, et al. Effect modification of green tea on the association between rice intake and the risk of diabetes mellitus: a prospective study in Japanese men and women. *Asia Pac J Clin Nutr.* 2017;26(3):545-55. doi:10.6133/apjcn.042016.04
66. Schimidt HL, Garcia A, Martins A, Mello-Carpes PB and Carpes FP. Green tea supplementation produces better neuroprotective effects than red and black tea in Alzheimer-like rat model. *Food Res Int.* 2017;100:442-8. doi:10.1016/j.foodres.2017.07.026
67. Yu J, Song P, Perry R, Penfold C and Cooper AR. The effectiveness of green tea or green tea extract on insulin resistance and glycemic control in type 2 diabetes mellitus: a meta-analysis. *Diabetes Metab J.* 2017;41(4):251-62. doi:10.4093/dmj.2017.41.4.251
68. Fritz H, Seely D, Kennedy DA, Fernandes R, Cooley K and Fergusson D. Green tea and lung cancer: a systematic review. *Integr Cancer Ther.* 2012;12(1):7-24. doi:10.1177/1534735412442378
69. Xu Y, Zhang M, Wu T, Dai S, Xu J and Zhou Z. The anti-obesity effect of green tea polysaccharides, polyphenols and caffeine in rats fed with a high-fat diet. *Food Funct.* 2015;6(1):296-303. doi:10.1039/C4FO00970C
70. Cunha CA, Lira FS, Rosa Neto JC, et al. Green tea extract supplementation induces the lipolytic pathway, attenuates obesity, and reduces low-grade

inflammation in mice fed a high-fat diet. *Mediators Inflamm.* 2013;2013:635470-  
doi:10.1155/2013/635470

71. Dulloo AG, Duret C, Rohrer D, et al. Efficacy of a green tea extract rich in catechin polyphenols and caffeine in increasing 24-h energy expenditure and fat oxidation in humans. *Am J Clin Nutr.* 1999;70(6):1040-5. doi:10.1093/ajcn/70.6.1040

72. Chen IJ, Liu C-Y, Chiu J-P and Hsu C-H. Therapeutic effect of high-dose green tea extract on weight reduction: a randomized, double-blind, placebo-controlled clinical trial. *Clin Nutr.* 2016;35(3):592-9. doi:10.1016/j.clnu.2015.05.003

73. Hursel R, Viechtbauer W, Dulloo AG, et al. The effects of catechin rich teas and caffeine on energy expenditure and fat oxidation: a meta-analysis. *Obes Rev.* 2011;12(7):e573-e81. doi:10.1111/j.1467-789X.2011.00862.x

74. Jurgens TM, Whelan AM, Killian L, Doucette S, Kirk S and Foy E. Green tea for weight loss and weight maintenance in overweight or obese adults. *Cochrane Database Syst Rev.* 2012(12). doi:10.1002/14651858.CD008650.pub2

75. Arzenton E ML, Paon V, Capra F, Apostoli P, Guzzo F, Conforti A, Leone R. Acute hepatitis caused by green tea infusion: a case report. *Adv Pharmacoepidemiol Drug Saf.* 2014;3(4):1-5. doi:10.4172/2167-1052.1000170

76. Bergman J and Schjøtt J. Hepatitis caused by Lotus-f3? *Basic Clin Pharmacol Toxicol.* 2009;104(5):414-6. doi:10.1111/j.1742-7843.2009.00385.x

77. Fong T-L, Klontz KC, Canas-Coto A, et al. Hepatotoxicity due to hydroxycut: a case series. *Am J Gastroenterol.* 2010;105(7):1561-6. doi:10.1038/ajg.2010.5

78. Weinstein DH, Twaddell WS, Raufman J-P, Philosophe B and Mindikoglu AL. SlimQuick™ - associated hepatotoxicity in a woman with alpha-1 antitrypsin heterozygosity. *World J Hepatol.* 2012;4(4):154-7. doi:10.4254/wjh.v4.i4.154

79. Whitsett M, Marzio DH-D and Rossi S. SlimQuick™-associated hepatotoxicity resulting in fulminant liver failure and orthotopic liver transplantation. *ACG Case Rep J.* 2014;1(4):220-2. doi:10.14309/crj.2014.59
80. Yellapu RK, Mittal V, Grewal P, Fiel M and Schiano T. Acute liver failure caused by 'fat burners' and dietary supplements: a case report and literature review. *Can J Gastroenterol.* 2011;25(3):157-60.
81. Patel SS, Beer S, Kearney DL, Phillips G and Carter BA. Green tea extract: a potential cause of acute liver failure. *World J Gastroenterol.* 2013;19(31):5174-7. doi:10.3748/wjg.v19.i31.5174
82. Surapaneni BK, Le M, Jakobovits J, Vinayek R and Dutta S. A case of acute severe hepatotoxicity and mild constriction of common bile duct associated with ingestion of green tea extract: a clinical challenge. *Clin Med Insights Gastroenterol.* 2018;11. doi:10.1177/1179552218779970
83. Fernández J and Navascués. Three cases of liver toxicity with a dietary supplement intended to stop hair loss. *Rev Esp Enferm Dig.* 2014;106(8).
84. Jiménez-Encarnación E, Ríos G, Muñoz-Mirabal A and Vilá LM. Euforia-induced acute hepatitis in a patient with scleroderma. *BMJ Case Rep.* 2012;2012:bcr2012006907. doi:10.1136/bcr-2012-006907
85. Pillukat MH, Bester C, Hensel A, et al. Concentrated green tea extract induces severe acute hepatitis in a 63-year-old woman – a case report with pharmaceutical analysis. *J Ethnopharmacol.* 2014;155(1):165-70. doi:10.1016/j.jep.2014.05.015
86. Urban TJ, Daly AK and Aithal GP. Genetic basis of drug-induced liver injury: present and future. *Semin Liver Dis.* 2014;34(02):123-33. doi:10.1055/s-0034-1375954

87. Kaswala D, Shah S, Patel N, Raisoni S and Swaminathan S. Hydroxycut-induced Liver Toxicity. *Ann Med Health Sci Res.* 2014;4(1):143-5. doi:10.4103/2141-9248.126627
88. Sarma DN, Barrett ML, Chavez ML, et al. Safety of Green Tea Extracts. *Drug Saf.* 2008;31(6):469-84. doi:10.2165/00002018-200831060-00003
89. Zheng EX, Rossi S, Fontana RJ, et al. Risk of liver injury associated with green tea extract in SLIMQUICK<sup>®</sup> weight loss products: results from the DILIN prospective study. *Drug Saf.* 2016;39(8):749-54. doi:10.1007/s40264-016-0428-7
90. Lugg ST, Braganza Menezes D and Gompertz S. Chinese green tea and acute hepatitis: a rare yet recurring theme. *BMJ Case Rep.* 2015;2015:bcr2014208534. doi:10.1136/bcr-2014-208534
91. Federico A, Tiso A and Loguercio C. A case of hepatotoxicity caused by green tea. *Free Radic Biol Med.* 2007;43(3):474. doi:10.1016/j.freeradbiomed.2007.05.010
92. ABC News. Man given two weeks to live after taking popular weight-loss product purchased online [document on the Internet]. 2016 [cited 2019 Apr 22]. Available from: <https://www.abc.net.au/news/2016-02-14/man-faced-death-after-taking-popular-weight-loss-product/7162378>.
93. BBC News. The food supplement that ruined my liver [document on the Internet]. 2018 [cited 2019 Apr 24]. Available from: <https://www.bbc.com/news/stories-45971416>.
94. Bun SS, Bun H, Guédon D, Rosier C and Ollivier E. Effect of green tea extracts on liver functions in Wistar rats. *Food Chem Toxicol.* 2006;44(7):1108-13. doi:10.1016/j.fct.2006.01.006

95. Lambert JD, Kennett MJ, Sang S, Reuhl KR, Ju J and Yang CS. Hepatotoxicity of high oral dose (-)-epigallocatechin-3-gallate in mice. *Food Chem Toxicol.* 2010;48(1):409-16. doi:10.1016/j.fct.2009.10.030
96. Wang D, Wang Y, Wan X, Yang CS and Zhang J. Green tea polyphenol (-)-epigallocatechin-3-gallate triggered hepatotoxicity in mice: responses of major antioxidant enzymes and the Nrf2 rescue pathway. *Toxicol Appl Pharmacol.* 2015;283(1):65-74. doi:10.1016/j.taap.2014.12.018
97. Sang S, Lambert JD, Hong J, et al. Synthesis and structure identification of thiol conjugates of (-)-epigallocatechin gallate and their urinary levels in mice. *Chem Res Toxicol.* 2005;18(11):1762-9. doi:10.1021/tx050151l
98. Galati G, Lin A, Sultan AM and O'Brien PJ. Cellular and in vivo hepatotoxicity caused by green tea phenolic acids and catechins. *Free Radic Biol Med.* 2006;40(4):570-80. doi:10.1016/j.freeradbiomed.2005.09.014
99. Schmidt M, Schmitz HJ, Baumgart A, et al. Toxicity of green tea extracts and their constituents in rat hepatocytes in primary culture. *Food Chem Toxicol.* 2005;43(2):307-14. doi:10.1016/j.fct.2004.11.001
100. Lu Q-Y, Zhang L, Yee JK, Go V-LW and Lee W-N. Metabolic Consequences of LDHA inhibition by Epigallocatechin Gallate and Oxamate in MIA PaCa-2 Pancreatic Cancer Cells. *Metabolomics.* 2015;11(1):71-80. doi:10.1007/s11306-014-0672-8
101. Li S, Wu L, Feng J, et al. In vitro and in vivo study of epigallocatechin-3-gallate-induced apoptosis in aerobic glycolytic hepatocellular carcinoma cells involving inhibition of phosphofructokinase activity. *Sci Rep.* 2016;6:28479. doi:10.1038/srep28479

102. Chan PC, Ramot Y, Malarkey DE, et al. Fourteen-week toxicity study of green tea extract in rats and mice. *Toxicol Pathol.* 2010;38(7):1070-84. doi:10.1177/0192623310382437
103. Ishiyama M, Miyazono Y, Sasamoto K, Ohkura Y and Ueno K. A highly water-soluble disulfonated tetrazolium salt as a chromogenic indicator for NADH as well as cell viability. *Talanta.* 1997;44(7):1299-305. doi:10.1016/S0039-9140(97)00017-9
104. Mosmann T. Rapid colorimetric assay for cellular growth and survival: Application to proliferation and cytotoxicity assays. *Journal of Immunological Methods.* 1983;65(1):55-63. doi:10.1016/0022-1759(83)90303-4
105. Ramirez T, Daneshian M, Kamp H, et al. Metabolomics in toxicology and preclinical research. *ALTEX.* 2013;30(2):209-25. doi:10.14573/altex.2013.2.209
106. Hyver KJ, Gearhart RC, Goodley P, et al. High resolution gas chromatography. 3rd ed. ed. California, U.S.A: Hewlett-Packard Co., 1989.
107. Sparkman OD, Penton ZE and Kitson FG. Gas chromatography and mass spectrometry: a practical guide. 2nd ed. ed. California, U.S.A: Academic Press, 2011.
108. Deda O, Gika H, Raikos N and Theodoridis G. Chapter 4 - GC-MS-Based Metabolic Phenotyping. In: Lindon JC, Nicholson JK and Holmes E, (eds.). *The Handbook of Metabolic Phenotyping.* Elsevier, 2019, p. 137-69.
109. McMaster MC. LC/MS: a practical user's guide. New Jersey, U.S.A: John Wiley & Sons, Inc., 2005.
110. Knapp DR. Handbook of analytical derivatization reactions. New York, U.S.A: Wiley & Sons, Inc., 1979.



111. Watson JT and OD. S. Introduction to mass spectrometry: instrumentation, applications and strategies for data interpretation. 4th ed. ed. Chichester, England: John Wiley & Sons, Ltd., 2007.
112. Wanner KT, Höfner G and editors. Mass spectrometry in medicinal chemistry: applications in drug discovery. Weinheim, Germany: Wiley-VCH, 2007.
113. Siuzdak G. The expanding role of mass spectrometry in biotechnology. 2nd ed. ed. San Diego, U.S.A: MCC Press, 2006.
114. Tennant JR. EVALUATION OF THE TRYPAN BLUE TECHNIQUE FOR DETERMINATION OF CELL VIABILITY. *Transplantation*. 1964;2(6).
115. Richardson SJ, Bai A, Kulkarni AA and Moghaddam MF. Efficiency in Drug Discovery: Liver S9 Fraction Assay As a Screen for Metabolic Stability. *Drug metabolism letters*. 2016;10(2):83-90. doi:10.2174/1872312810666160223121836
116. Richter LHJ, Flockerzi V, Maurer HH and Meyer MR. Pooled human liver preparations, HepaRG, or HepG2 cell lines for metabolism studies of new psychoactive substances? A study using MDMA, MDBD, butylone, MDPPP, MDPV, MDPB, 5-MAPB, and 5-API as examples. *Journal of Pharmaceutical and Biomedical Analysis*. 2017;143:32-42. doi:10.1016/j.jpba.2017.05.028
117. Farrington R. Herbal medicine toxicity: the role of adulterants, contaminants and pharmacokinetic interactions. PhD [thesis]. Adelaide (SA): University of Adelaide; 2019.
118. Hayton S, Maker GL, Mullaney I and Trengove RD. Untargeted metabolomics of neuronal cell culture: A model system for the toxicity testing of insecticide chemical exposure. *Journal of Applied Toxicology*. 2017;37(12):1481-92. doi:10.1002/jat.3498

119. Abbiss H, Rawlinson C, Maker GL and Trengove R. Assessment of automated trimethylsilyl derivatization protocols for GC–MS-based untargeted metabolomic analysis of urine. *Metabolomics*. 2015;11(6):1908-21. doi:10.1007/s11306-015-0839-y
120. Abbiss H, Maker GL and Trengove RD. Metabolomics Approaches for the Diagnosis and Understanding of Kidney Diseases. *Metabolites*. 2019;9(2):34. doi:10.3390/metabo9020034
121. Wishart DS, Feunang YD, Marcu A, et al. HMDB 4.0: the human metabolome database for 2018. *Nucleic Acids Res*. 2018;46(D1):D608-D17. doi:10.1093/nar/gkx1089
122. Jewison T, Su Y, Disfany FM, et al. SMPDB 2.0: big improvements to the Small Molecule Pathway Database. *Nucleic Acids Res*. 2014;42(Database issue):D478-D84. doi:10.1093/nar/gkt1067
123. Chong J, Soufan O, Li C, et al. MetaboAnalyst 4.0: towards more transparent and integrative metabolomics analysis. *Nucleic Acids Res*. 2018;46(W1):W486-W94. doi:10.1093/nar/gky310
124. Kanehisa M, Furumichi M, Tanabe M, Sato Y and Morishima K. KEGG: new perspectives on genomes, pathways, diseases and drugs. *Nucleic Acids Res*. 2017;45(D1):D353-D61. doi:10.1093/nar/gkw1092
125. Usui T, Saitoh Y and Komada F. Induction of CYP3As in HepG2 Cells by Several Drugs.&mdash;Association between Induction of CYP3A4 and Expression of Glucocorticoid Receptor&mdash. *Biological and Pharmaceutical Bulletin*. 2003;26(4):510-7. doi:10.1248/bpb.26.510

126. Hulbert AJ, Pamplona R, Buffenstein R and Buttemer WA. Life and Death: Metabolic Rate, Membrane Composition, and Life Span of Animals. *Physiological Reviews*. 2007;87(4):1175-213. doi:10.1152/physrev.00047.2006
127. Maralani MN, Movahedian A and Javanmard SH. Antioxidant and cytoprotective effects of L-Serine on human endothelial cells. *Res Pharm Sci*. 2012;7(4):209-15.
128. Oliveira AG, Andrade VA, Guimarães ES, et al. Calcium signalling from the type I inositol 1,4,5-trisphosphate receptor is required at early phase of liver regeneration. *Liver International*. 2015;35(4):1162-71. doi:10.1111/liv.12587
129. Liu Y, Shao M, Wu Y, et al. Role for the endoplasmic reticulum stress sensor IRE1a in liver regenerative responses. *Journal of Hepatology*. 2015;62(3):590-8. doi:10.1016/j.jhep.2014.10.022
130. Assies J, Mocking RJT, Lok A, Ruhé HG, Pouwer F and Schene AH. Effects of oxidative stress on fatty acid- and one-carbon-metabolism in psychiatric and cardiovascular disease comorbidity. *Acta Psychiatr Scand*. 2014;130(3):163-80. doi:10.1111/acps.12265
131. Blancquaert L, Everaert I, Missinne M, et al. Effects of Histidine and  $\beta$ -alanine Supplementation on Human Muscle Carnosine Storage. *Medicine & Science in Sports & Exercise*. 2017;49(3).
132. Ho E, Karimi Galougahi K, Liu C-C, Bhindi R and Figtree GA. Biological markers of oxidative stress: Applications to cardiovascular research and practice. *Redox Biology*. 2013;1(1):483-91. doi:10.1016/j.redox.2013.07.006
133. Katerji M, Filippova M and Duerksen-Hughes P. Approaches and Methods to Measure Oxidative Stress in Clinical Samples: Research Applications in the Cancer

- Field. *Oxidative Medicine and Cellular Longevity*. 2019;2019:29.  
doi:10.1155/2019/1279250
134. Poprac P, Jomova K, Simunkova M, Kollar V, Rhodes CJ and Valko M. Targeting Free Radicals in Oxidative Stress-Related Human Diseases. *Trends in Pharmacological Sciences*. 2017;38(7):592-607. doi:10.1016/j.tips.2017.04.005
135. Ubezio P and Civoli F. Flow cytometric detection of hydrogen peroxide production induced by doxorubicin in cancer cells. *Free Radical Biology and Medicine*. 1994;16(4):509-16. doi:10.1016/0891-5849(94)90129-5
136. Tsikas D. Assessment of lipid peroxidation by measuring malondialdehyde (MDA) and relatives in biological samples: Analytical and biological challenges. *Analytical Biochemistry*. 2017;524:13-30. doi:10.1016/j.ab.2016.10.021
137. Wu D and Cederbaum AI. Inhibition of autophagy promotes CYP2E1-dependent toxicity in HepG2 cells via elevated oxidative stress, mitochondria dysfunction and activation of p38 and JNK MAPK. *Redox Biology*. 2013;1(1):552-65. doi:10.1016/j.redox.2013.10.008
138. Sohn S-H, Kim S-K, Kim Y-O, et al. A comparison of antioxidant activity of Korean White and Red Ginsengs on H<sub>2</sub>O<sub>2</sub>-induced oxidative stress in HepG2 hepatoma cells. *Journal of ginseng research*. 2013;37(4):442-50. doi:10.5142/jgr.2013.37.442
139. Xu Q, Liu L, Vu H, et al. Can Galactose Be Converted to Glucose in HepG2 Cells? Improving the in Vitro Mitochondrial Toxicity Assay for the Assessment of Drug Induced Liver Injury. *Chemical Research in Toxicology*. 2019;32(8):1528-44. doi:10.1021/acs.chemrestox.9b00033

140. Balcke GU, Kolle SN, Kamp H, et al. Linking energy metabolism to dysfunctions in mitochondrial respiration – A metabolomics in vitro approach. *Toxicology Letters*. 2011;203(3):200-9. doi:10.1016/j.toxlet.2011.03.013
141. Turbitt JR, Colson KL, Killday KB, Milstead A and Neto CC. Application of 1H-NMR-based metabolomics to the analysis of cranberry (*Vaccinium macrocarpon*) supplements. *Phytochemical Analysis*. 2019;0(0). doi:10.1002/pca.2867
142. Emwas A-H, Roy R, McKay RT, et al. NMR Spectroscopy for Metabolomics Research. *Metabolites*. 2019;9(7):123. doi:10.3390/metabo9070123
143. Kurata S and Sakurai T. Simultaneous Analysis of Eight Catechins in Tea Drinks by Gas Chromatography/Mass Spectrometry. *BUNSEKI KAGAKU*. 2012;61:63-8. doi:10.2116/bunsekikagaku.61.63
144. Crighton E, Coghlan ML, Farrington R, et al. Toxicological screening and DNA sequencing detects contamination and adulteration in regulated herbal medicines and supplements for diet, weight loss and cardiovascular health. *Journal of Pharmaceutical and Biomedical Analysis*. 2019;176:112834. doi:10.1016/j.jpba.2019.112834
145. Zeilinger K, Freyer N, Damm G, Seehofer D and Knöspel F. Cell sources for in vitro human liver cell culture models. *Exp Biol Med (Maywood)*. 2016;241(15):1684-98. doi:10.1177/1535370216657448

## 6. Supplementary information

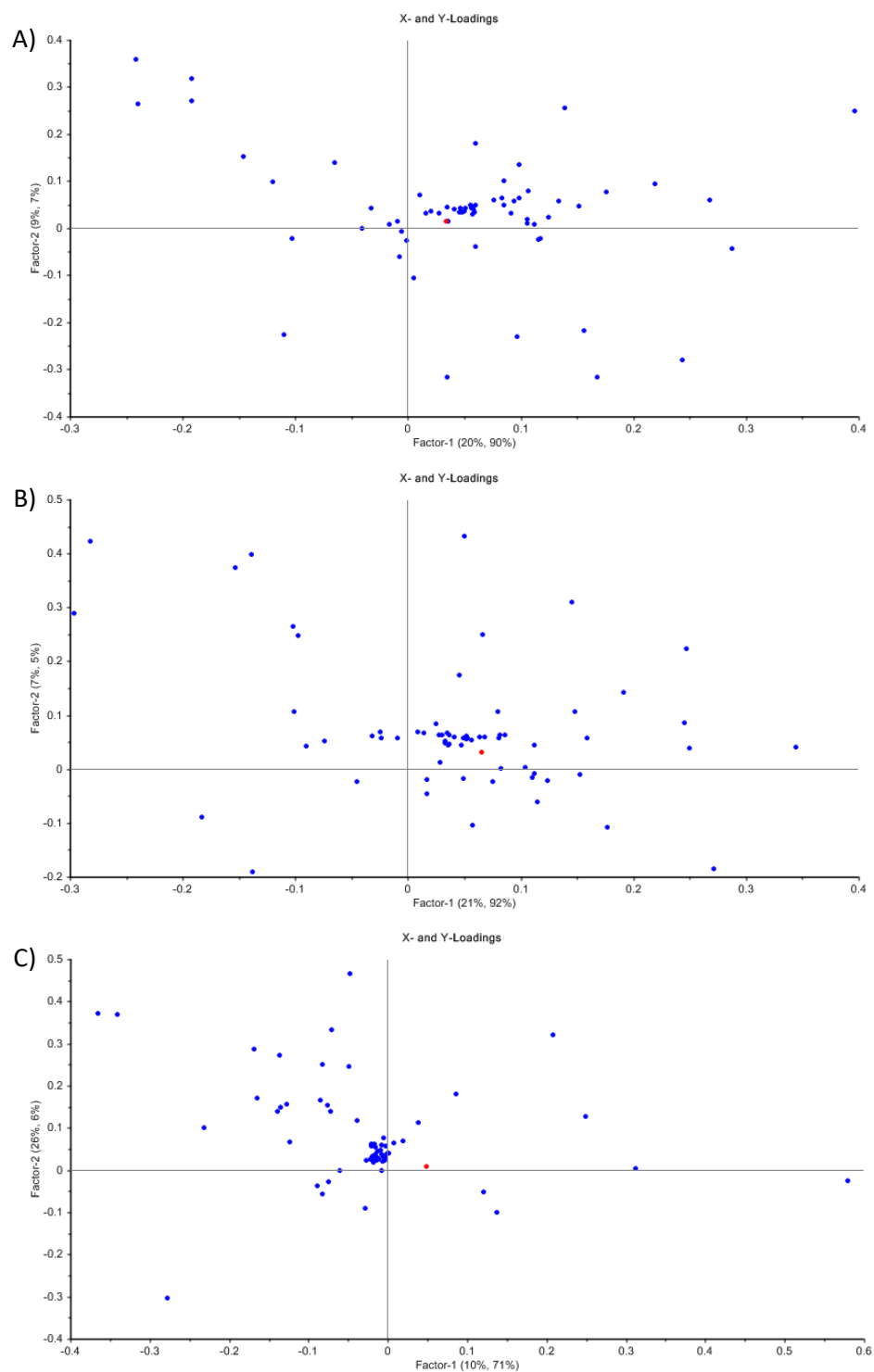
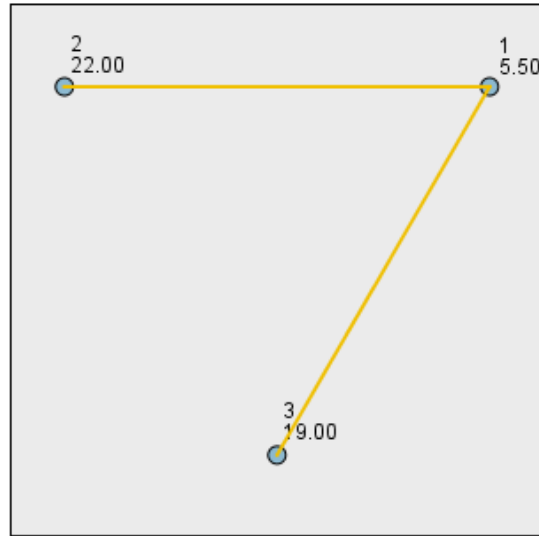


Figure S1. X- and Y-loadings plot from which X-loadings were derived for analysis of metabolites contributing most to variance between untreated controls and GTE-treated cells (A), untreated controls and GTEM-treated cells (B), and GTE-treated and GTEM-treated cells (C), measured by GC-MS.

### Pairwise Comparisons of Sample Groups



Each node shows the sample average rank of Sample Groups.

Sample 1-Sam...	Test Statistic	Std. Error	Std. Test Statistic	Sig.	Adj.Sig.
1-3	-13.500	3.937	-3.429	.001	.002
1-2	-16.500	3.937	-4.191	.000	.000
3-2	3.000	3.937	.762	.446	1.000

Each row tests the null hypothesis that the Sample 1 and Sample 2 distributions are the same. Asymptotic significances (2-sided tests) are displayed. The significance level is .05. Significance values have been adjusted by the Bonferroni correction for multiple tests.

Figure S2. Kruskal-Wallis pairwise comparisons of sample groups: 1) untreated controls, 2) 1 mg/mL GTE treatment group, and 3) 1 mg/mL GTEM treatment group. All sample groups were prepared in 10 replicates. A significance difference was observed between the metabolite profile of untreated cells compared to GTE-treated cells, and also between the controls and GTEM treatment group ( $p < .05$ ). The metabolite profile of GTE-treated cells was not found to differ significantly from that of the GTEM treatment group.

Table S1. Unidentified metabolites of purified catechin hydrate (CH) following metabolism with S9 human liver fraction and GC-MS analysis (n = 3). CH concentration prior to initiation of metabolism was 1 mg/mL. \*Components also detected in metabolised green tea extract.

<b>Compound</b>	<b>RT (min)</b>	<b>Base Peak</b>	<b>Detected in samples (%)</b>
3*	16.2233	116	100
4	16.3883	174	66.66667
6	16.5867	299	33.33333
7	16.6250	205	33.33333
9	17.4483	174	66.66667
11	18.1433	184	33.33333
12*	18.3283	99	100
16	20.0817	74	66.66667
17	20.0883	234	33.33333
18	20.5533	217	100
19*	21.4600	71	100
20*	21.8900	75	33.33333
22	22.3300	102	100
24	22.6917	156	33.33333
25*	22.8067	174	33.33333
26	22.9350	84	100
28	23.3650	220	33.33333
29	24.7500	246	66.66667
30	24.9850	127	100
31	25.5600	86	100
33	25.8867	260	66.66667
34	27.0767	272	100



35	27.1850	217	100
37*	27.5300	299	100
38*	29.3017	174	100
39	29.5017	103	33.33333
41	29.7600	147	100
43	29.9700	205	100
45	30.3067	147	66.66667
47	30.5050	147	100
48*	31.1217	281	33.33333
49*	31.2017	72	100
50	31.4733	204	100
53	32.3000	204	33.33333
54	32.7633	117	100
55	33.1600	217	100
56*	33.2900	217	33.33333
57	33.6017	315	100
59	34.7783	213	33.33333
60	34.7867	213	33.33333
62	35.4400	75	100
63	35.5317	75	100
66	38.9583	217	33.33333
67	38.9667	217	66.66667
69	43.0033	204	100
71	43.6683	204	100
76	44.6267	169	33.33333

80	49.9000	361	100
81	51.5033	204	66.66667

Table S2. Unidentified metabolites of purified epicatechin (EC) following metabolism with S9 human liver fraction and GC-MS analysis (n = 3). EC concentration prior to initiation of metabolism was 1 mg/mL. \*Components also detected in metabolised green tea extract.

<b>Compound</b>	<b>RT (min)</b>	<b>Base Peak</b>	<b>Detected in samples (%)</b>
3*	16.2233	116	33.33333
4	16.3883	174	66.66667
5	16.5783	299	66.66667
8	16.6400	299	66.66667
9	17.4483	174	66.66667
10	17.7583	147	33.33333
11	18.1433	184	33.33333
12*	18.3283	99	66.66667
13	20.0233	127	33.33333
17	20.0883	234	66.66667
18	20.5533	217	100
19*	21.4600	71	33.33333
20*	21.8900	75	33.33333
22	22.3300	102	66.66667
26	22.9350	84	33.33333
27	22.9833	239	33.33333
29	24.7500	246	66.66667
30	24.9850	127	66.66667

31	25.5600	86	66.66667
33	25.8867	260	66.66667
34	27.0767	272	66.66667
35	27.1850	217	100
36	27.3767	174	33.33333
37*	27.5300	299	66.66667
38*	29.3017	174	33.33333
39	29.5017	103	66.66667
41	29.7600	147	66.66667
43	29.9700	205	100
45	30.3067	147	100
47	30.5050	147	100
48*	31.1217	281	100
49*	31.2017	72	66.66667
50	31.4733	204	100
52	32.1933	297	33.33333
54	32.7633	117	100
55	33.1600	217	66.66667
56*	33.2900	217	33.33333
57	33.6017	315	100
58	33.6750	315	33.33333
60	34.7867	213	33.33333
62	35.4400	75	100
63	35.5317	75	100
64	35.9400	117	33.33333

65*	36.5400	147	33.33333
66	38.9583	217	33.33333
67	38.9667	217	33.33333
69	43.0033	204	100
70	43.0817	280	33.33333
71	43.6683	204	100
75	44.5950	169	33.33333
80	49.9000	361	100
81	51.5033	204	66.66667

Table S3. Unidentified metabolites of purified epigallocatechin (EGC) following metabolism with S9 human liver fraction and GC-MS analysis (n = 3). EGC concentration prior to initiation of metabolism was 1 mg/mL. \*Components also detected in metabolised green tea extract.

<b>Compound</b>	<b>RT (min)</b>	<b>Base Peak</b>	<b>Detected in samples (%)</b>
3*	16.2233	116	66.66667
4	16.3883	174	66.66667
6	16.5867	299	100
9	17.4483	174	100
12*	18.3283	99	66.66667
14	20.0383	72	33.33333
17	20.0883	234	66.66667
18	20.5533	217	100
19*	21.4600	71	100
22	22.3300	102	100
24	22.6917	156	33.33333

25*	22.8067	174	66.66667
26	22.9350	84	66.66667
28	23.3650	220	33.33333
29	24.7500	246	100
30	24.9850	127	100
31	25.5600	86	100
33	25.8867	260	100
34	27.0767	272	100
35	27.1850	217	100
37*	27.5300	299	100
38*	29.3017	174	33.33333
39	29.5017	103	66.66667
40	29.6867	103	33.33333
41	29.7600	147	66.66667
43	29.9700	205	100
45	30.3067	147	66.66667
47	30.5050	147	100
48*	31.1217	281	66.66667
49*	31.2017	72	100
50	31.4733	204	100
51	32.1900	297	33.33333
54	32.7633	117	100
55	33.1600	217	66.66667
57	33.6017	315	100
59	34.7783	213	33.33333

62	35.4400	75	66.66667
63	35.5317	75	100
66	38.9583	217	33.33333
67	38.9667	217	33.33333
68	40.6250	217	33.33333
69	43.0033	204	100
71	43.6683	204	100
80	49.9000	361	100
81	51.5033	204	100

Table S4. Unidentified metabolites of purified epigallocatechin-3-gallate (EGCG) following metabolism with S9 human liver fraction and GC-MS analysis (n = 3). EGCG concentration prior to initiation of metabolism was 1 mg/mL. \*Components also detected in metabolised green tea extract.

<b>Compound</b>	<b>RT (min)</b>	<b>Base Peak</b>	<b>Detected in samples (%)</b>
3*	16.2233	116	66.66667
4	16.3883	174	66.66667
6	16.5867	299	33.33333
8	16.6400	299	33.33333
9	17.4483	174	66.66667
12*	18.3283	99	33.33333
15	20.0533	234	33.33333
16	20.0817	74	33.33333
17	20.0883	234	33.33333
18	20.5533	217	100
19*	21.4600	71	66.66667

20*	21.8900	75	33.33333
22	22.3300	102	66.66667
23	22.3533	84	33.33333
24	22.6917	156	33.33333
26	22.9350	84	33.33333
27	22.9833	239	33.33333
29	24.7500	246	66.66667
30	24.9850	127	66.66667
31	25.5600	86	66.66667
32	25.8317	103	33.33333
34	27.0767	272	66.66667
35	27.1850	217	66.66667
37*	27.5300	299	66.66667
38*	29.3017	174	33.33333
39	29.5017	103	66.66667
41	29.7600	147	66.66667
42	29.9050	204	33.33333
43	29.9700	205	66.66667
45	30.3067	147	66.66667
46	30.3783	205	33.33333
47	30.5050	147	66.66667
48*	31.1217	281	66.66667
49*	31.2017	72	66.66667
50	31.4733	204	66.66667
53	32.3000	204	33.33333

54	32.7633	117	66.66667
55	33.1600	217	33.33333
57	33.6017	315	66.66667
59	34.7783	213	33.33333
62	35.4400	75	33.33333
63	35.5317	75	66.66667
66	38.9583	217	66.66667
69	43.0033	204	66.66667
71	43.6683	204	66.66667
80	49.9000	361	66.66667
81	51.5033	204	33.33333
83	54.6150	560	66.66667
84	54.6417	560	33.33333



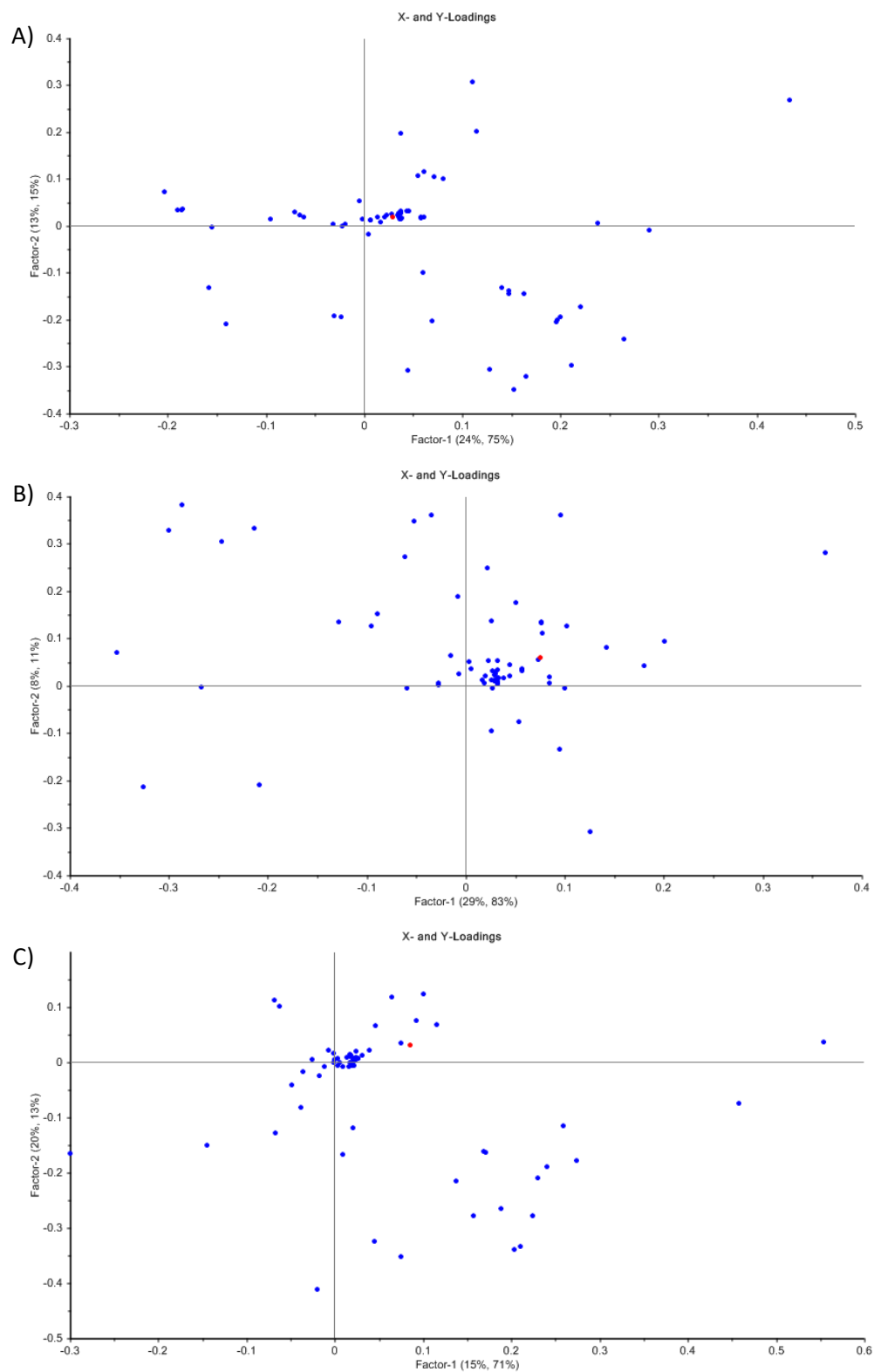


Figure S3. X- and Y-loadings plot from which X-loadings were derived for analysis of metabolites contributing most to variance between untreated HepG2 cells and A) GTE-treated cells, B) APAP/GTE-treated cells, and C) APAP -treated cells, measured by GC-MS.

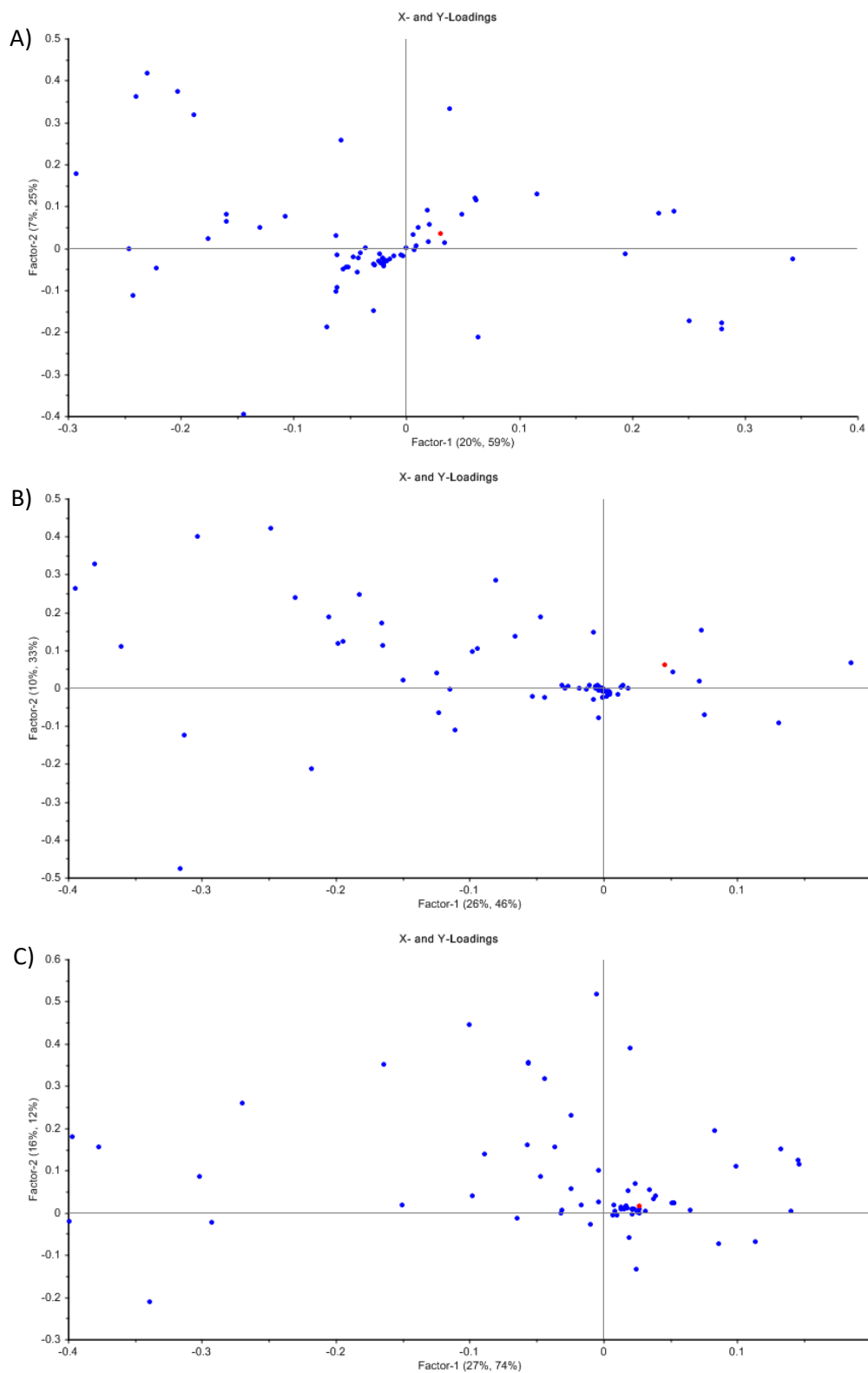
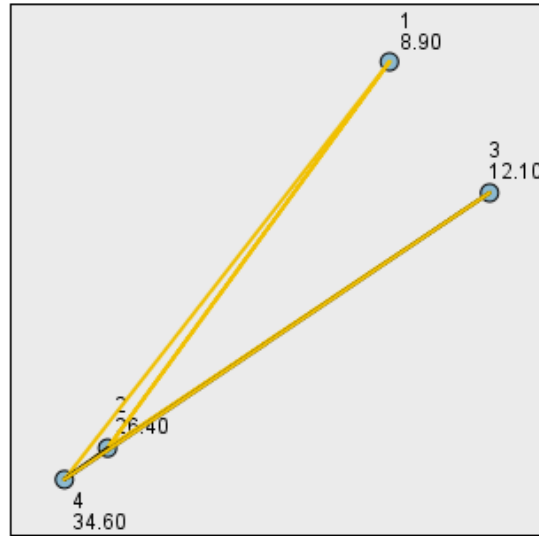


Figure S4. X- and Y-loadings plot from which X-loadings were derived for analysis of metabolites contributing most to variance between HepG2 cells treated with GTE vs APAP (A), GTE vs APAP/GTE (B), and APAP vs APAP/GTE (C), measured by GC-MS.

### Pairwise Comparisons of Sample Groups



Each node shows the sample average rank of Sample Groups.

Sample 1-Sam...	Test Statistic	Std. Error	Std. Test Statistic	Sig.	Adj.Sig.
1-3	-3.200	5.228	-.612	.540	1.000
1-2	-17.500	5.228	-3.347	.001	.005
1-4	-25.700	5.228	-4.916	.000	.000
3-2	14.300	5.228	2.735	.006	.037
3-4	-22.500	5.228	-4.304	.000	.000
2-4	-8.200	5.228	-1.568	.117	.701

Each row tests the null hypothesis that the Sample 1 and Sample 2 distributions are the same. Asymptotic significances (2-sided tests) are displayed. The significance level is .05. Significance values have been adjusted by the Bonferroni correction for multiple tests.

Figure S5. Kruskal-Wallis pairwise comparisons of sample groups: 1) untreated controls, 2) 1 mg/mL GTE-treated cells, 3) 15 mM APAP-treated cells, and 4) 15 mM APAP/1 mg/mL GTE combined treatment group. All sample groups were prepared in 10 replicates. A significant difference was observed between the metabolite profiles of untreated controls compared to both the GTE-treated cells and the combined treatment group ( $p < .05$ ). The metabolite profile of APAP-treated cells differed significantly from the GTE and combined treatment groups. No significant difference was observed between the controls and APAP-treated cells, nor between the GTE and APAP/GTE treatment groups.